UNIVERSITA' DEGLI STUDI DI PADOVA

Dipartimento di Ingegneria Industriale DII

Corso di Laurea Magistrale in Energy Engineering

Ventilation effectiveness of a decentralized mechanical ventilation system: on-site measurements and CFD analysis

Supervisor:

Prof. Michele De Carli

Student:

Alessandro Salmaso

2088648

Academic Year 2024/2025

Abstract

The evolution of the building sector, with increased airtightness and reduced leakage in building envelopes, has meant that the presence of mechanical ventilation systems in interior spaces is becoming increasingly important and essential to meet indoor air quality requirements. The advent of decentralized ventilation systems, which have recently emerged on the market, represents a significant development in this field. These systems offer a cost-effective solution by ensuring compactness and reducing installation costs. Therefore, they can be a good solution in both renovations and new constructions. The concept of these systems concerns the air exchange in the room where they are installed, with the air intake and outlet close to each other without the presence of ducts, unlike traditional centralized systems in which the air supply and extraction vents are located in different rooms to favour a uniform air exchange within the building. The present thesis explores the topic of ventilation effectiveness. An analysis of the existing literature on the subject is conducted, and its results are used to study the effectiveness of a decentralized ventilation system. Evaluations are carried out through an experimental approach, involving the generation and measurement of CO_2 concentration at different room positions and CFD simulations.

Index

1. INTRODUCTION

The term *ventilation* means the process of supplying outdoor air to or removing indoor air from a building, in order to control the pollutant levels, humidity or temperature [1].

The purpose of a ventilation system is to provide acceptable air quality in the space being ventilated. In the modern society, people spend most of their time in internal environments (e.g. houses, offices, cars), so the importance of the air quality is growing. In particular, since the pandemic of the 2020, the need for a healthy indoor air quality has become a crucial aspect that can no longer be neglected. Poor indoor air quality affects comfort of people, it's directly linked to the productivity and can cause effects on health like headache or irritated eyes [2]. Another aspect that highlights the importance of the ventilation is the increase in new buildings of insulation and airtightness, leading to a lower infiltration rate. Therefore, to ensure an appropriate quality of the air, a ventilation system is needed.

1.1 Thermal comfort

Thermal comfort is the condition of mind that express subjective satisfaction with the thermal environment. [3]

The thermal state of a person is determined by six parameters, four are related to the environment:

- Air temperature;
- Air velocity;
- Mean radiant temperature;
- Relative humidity;

and two are related to the person himself:

- Activity performed;
- Clothing thermal resistance.

The thermal comfort is a concept that describes the satisfaction of the people with the environment, from a thermal point of view. Since the comfort is a personal parameter, to obtain a more objective analysis Fanger introduced his own model, with two key parameters: PMV (Predicted Mean Vote) and PPD (Predicted Percentage of Dissatisfied).

PMV is expressed by a number between -3 to +3, it's a thermal sensation scale (named ASHRAE scale) useful to define the situation of an environment:

ASHRAE scale	
+3	Hot
+2	Warm
+1	Slightly warm
0	Neutral
-1	Slightly cool
-2	Cool
-3	Cold

Table 1.2 – Comfort levels [5]

Thermal neutrality is characterized by PMV = 0, and average comfortable conditions are reached with -0.5 < PMV < 0.5, as explained in the Standard EN ISO 7730 [4].

PPD (or simply PD in the following for simplicity, although PPD refers to global discomfort and PD to local one) is an index that represents the percentage of people expected to be dissatisfied in the environment, ideally a PPD equal to 0% means that everyone in the environment is expected to be satisfied: the higher is the PPD the higher is the number of people dissatisfied. As it's mentioned in the Standard [4], thermally dissatisfied people are those who votes *hot, warm, cool* or *cold* on the 7-point thermal sensation scale presented before. A PMV = 0 corresponds to a PPD = 5% and this is because, due to individual preferences, it is impossible to achieve a single environment condition that satisfies all the people inside. When the PMV is known, the PPD can be obtained using the following equation:

$$PPD = 100 - 95 * \exp\left(-0.03353 * PMV^4 - 0.2179 * PMV^2\right) \quad (1)$$

See Figure 1 to understand the relationship between these two parameters, the figure is taken from the Standard EN ISO 7730:2005.

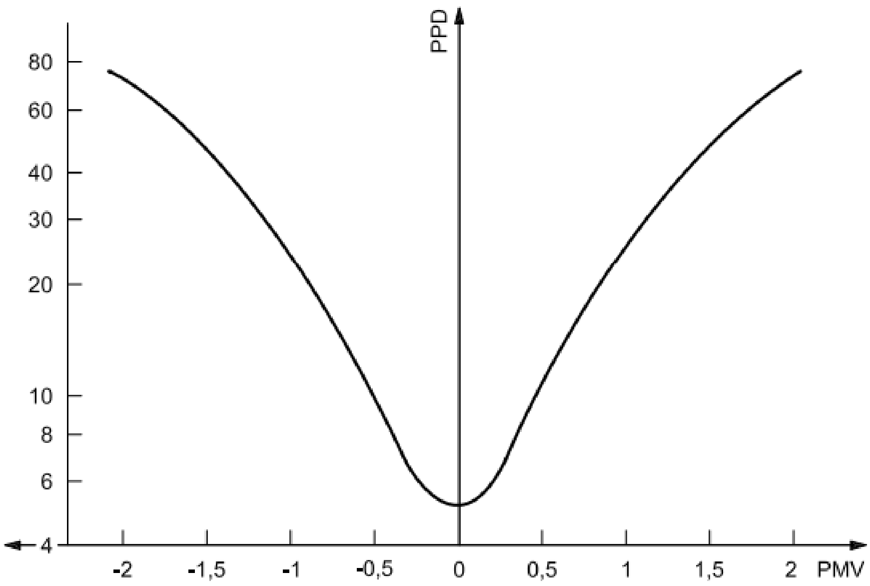

Figure 1.1 – PPD as a function of PMV [4]

Recommended criteria for thermal environment are illustrated in the Standard EN 16798-1-2019 (Appendix A) [5] and are reported in the Table 1.2, where it's possible to see which PPD and PMV threshold values delimit the different categories:

Category	Thermal state of the body as a whole	
	PPD %	PMV
I	< 6	- 0.2 < PMV < + 0.2
II	< 10	- 0.5 < PMV < + 0.5
III	< 15	- 0.7 < PMV < + 0.7

Table 1.2 – Comfort levels [5]

1.1.1 Local thermal discomfort

The local thermal discomfort, instead, refers to a condition where there is an uneven temperature distribution on the body, and this situation have to be avoided to guarantee a satisfactory environment.

The most important sources of local discomfort are [6]:

- Draught;
- Vertical air temperature difference;
- Warm and cool floors;
- Radiant asymmetry.

The draught is the most common cause of complaint, it refers to the movement of cold air through the body and to avoid it, air velocity must be kept under control.

The vertical air temperature difference is evaluated between head and ankles, a high temperature difference can cause discomfort, therefore with the increasing of the Δt, the percentage of people dissatisfied increases (see Figure 1.2).

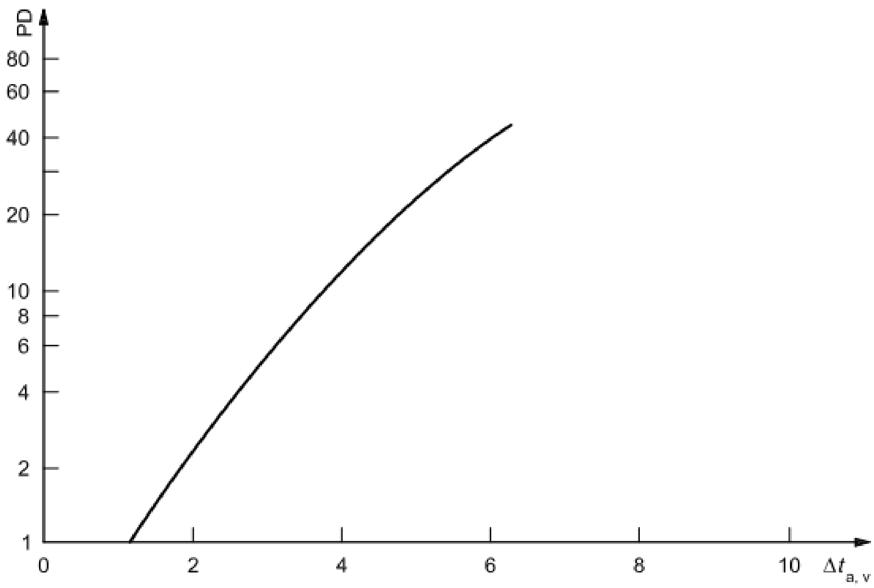

Figure 1.2 – Local discomfort due to vertical temperature difference [4]

If the surface temperature of the floor is either too low or too high, the occupants may experience discomfort in their lower limbs. The optimal temperature range is between 19 and 29 °C, with a temperature higher or lower the probability to have someone experiencing discomfort is higher (see Figure 1.3).

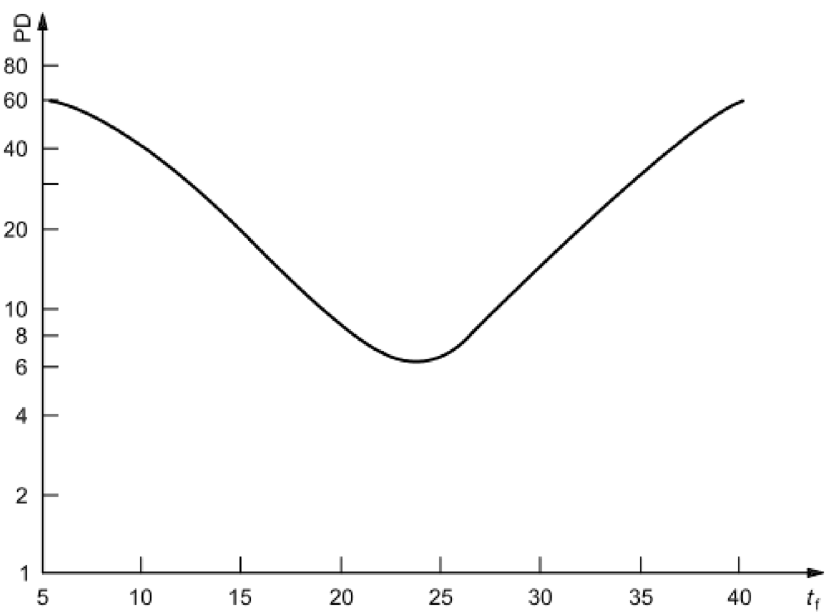

Figure 1.3 – Local discomfort due to warm and cool floors [4]

The worst cases for the radiant asymmetry are with a warm ceiling (line 1 in the Figure 1.4) and with a cold wall (in general due to a window, line 2). Cool ceiling (line 3) and warm wall (line 4) are less problematic.

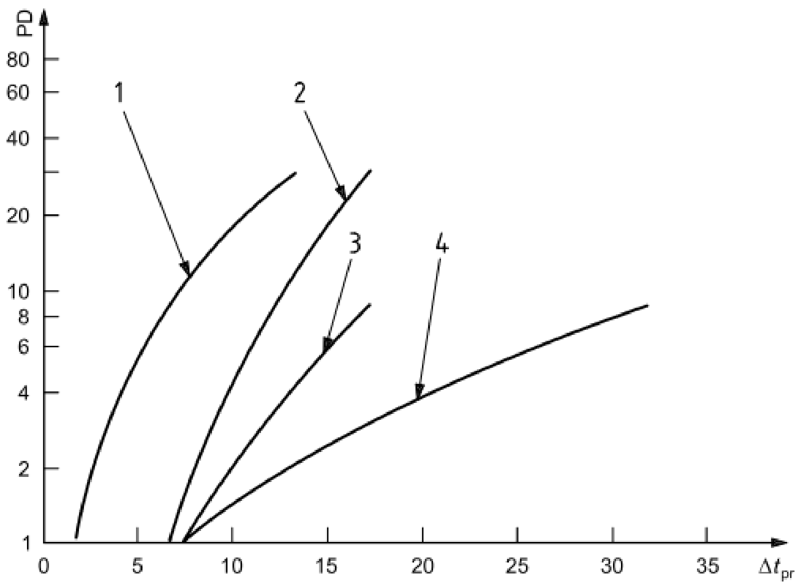

Figure 1.4 – Local discomfort due to radiant temperature asymmetry [4]

In the Table 1.3 there is a recap to link the different categories and the PD with the local thermal discomfort.

	Draught			Vertical air temperature difference (head – ankle)		Range of floor surface temperature	
	DR (Draught Rate)	Maximum air velocity [a)]		PD	Temperature difference [b)]	PD	Floor surface temperature range
		Winter	Summer				
	[%]	[m/s]	[m/s]	[%]	[K]	[%]	[°C]
Category I	10	0.10	0.12 [c)]	3	2	10	19 to 29
Category II	20	0.16	0.19 [c)]	5	3	10	19 to 29
Category III	30	0.21	0.24 [c)]	10	4	15	17 to 31
	Radiant temperature asymmetry						
	PD		Warm ceiling		Cool wall	Cool ceiling	Warm wall
	[%]		[K]		[K]	[K]	[K]
Category I	5		< 5		< 10	< 14	< 23
Category II	5		< 5		< 10	< 14	< 23
Category III	10		< 7		< 13	< 18	< 35
Notes: a) Assuming an activity level of 1.2 met, a turbulence intensity of 40% and an air temperature equal to the operative temperature of around 20 °C in winter and 23 °C in summer. b) Difference between 1.1 and 0.1 m above the floor. c) When the air temperature is above 25 °C higher maximum air speeds are allowed and often even preferred (draught becomes pleasurable breeze); but only under the condition that occupants have direct control over the air speed.							

Table 1.3 – Local thermal discomfort design criteria [5]

1.2 Indoor Air Quality and indoor pollutants

The definition of *acceptable indoor air quality* given by the ASHRAE 62.1 is the following: “air in which there are no known contaminants at harmful concentrations as determined by cognizant authorities and with which a substantial majority (80% or more) of the people exposed do not express dissatisfaction”.

The most common pollutants emitted by persons are CO_2 (usually used as a marker to check the air quality in office buildings), bio effluents and H_2O, but the list of possible contaminant sources is longer. The most frequent from the building structure, from the environment and from the machines are [5]:

- VOC (Volatile Organic Compounds);
- Formaldehyde;
- Microorganisms;
- Combustion products;
- Radon.

Water vapour is not directly a problem for the human health, but if the concentration increases or decreases too much, the relative humidity can become higher or lower than threshold limits. A too high relative humidity can lead to the formation of mould and presence of bacteria, while too low humidity can cause, for example, dry and irritated skin and throat.

The improvement of indoor air quality in buildings can be achieved by 2 ways:

- control and reduction of pollutant sources;
- removal and dilution of contaminants from the environment through ventilation.

The Sick Building Syndrome (SBS) refers to generic health problems (e.g. headaches) resulting from being in a poorly ventilated environment with a high presence of pollutants. The discomfort conditions are reached not only due to the presence of people (i.e. production of CO_2), but also due to the use of specific devices and construction materials (e.g. an appropriate choice of the materials can be crucial).

In the following section the most important pollutants are briefly discussed, defining the limits that must be respected, with particular attention to CO_2.

1.2.1 CO_2

Carbon dioxide is an inert, odourless and colourless gas. In addition to being a product of combustion, in buildings it's mainly generated by the breathing process and human metabolic activities. The CO_2 level is a crucial parameter in the evaluation of the indoor air quality, in particular too high concentration can lead to headaches and similar symptoms.

The amount of CO_2 produced by a person depends on the type of activity performed, e.g. working in an office has a different impact than working in a factory, in particular the different production of CO_2 is linked with the different metabolic rate. An interesting study of the 2017 made by the NIST [7] describes which is the CO_2 generation rate referring to different ages and different physical activities (expressed in met). For example, considering a male figure (in the graph below all the values refer to male people) in the range between 20 and

50 years old, the CO_2 generation rate referred to office activities is 0.0056 l/s. In the Figure 1.5 different CO_2 generation rates referred to different conditions are reported.

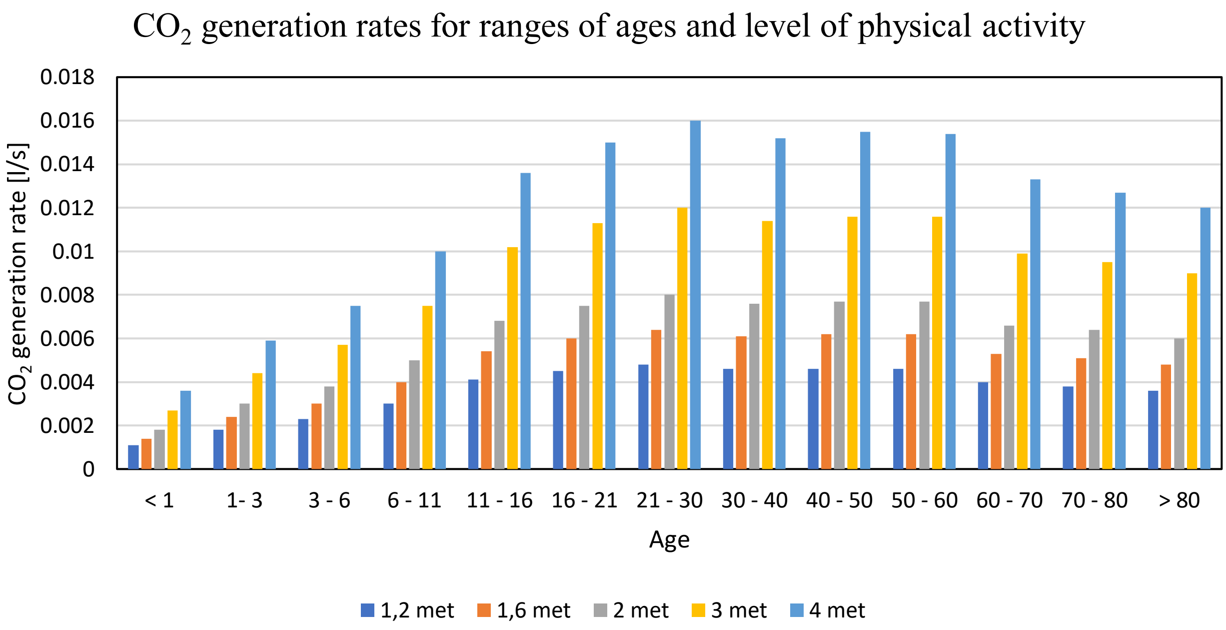

Figure 1.5 – CO_2 generation rates for ranges of ages and level of physical activity

The different classes of IAQ can be defined also trough the CO_2 concentration in the room, in particular it should be noted that the values used to define these ranges must be considered as values above the external concentration (the average value of which is approximately 450 ppm). For example, category I is up to 550 ppm above the external concentration, i.e. up to around 1000 ppm total. For each category, a reference value is also given for the flow rate to be supplied, expressed in l/s per person: e.g. with a flow rate of 10 l/s per person, the corresponding IAQ class is the I. For health reasons, the minimum flow rate in occupied rooms should never go below 4 l/s per person.

Category	CO_2 concentration in ppm above outdoors level	Corresponding air flow in l/s per person
I	550	10
II	800	7
III	1350	4

Table 1.4 – CO_2 values for different classes [5]

1.2.2 Volatile Organic Compounds

Volatile Organic Compounds (VOC) are a group of substances that contribute to the air pollution, the most common of these are formaldehyde and benzene. VOCs are present in a wide range of products: primary sources are, for example, paints, cleaning products and building materials. A significant exposure to VOCs may evolve into effects for human health (e.g. headaches, eyes irritation, nausea), so it’s crucial to minimize both the emission sources (using specific products and materials) and the lifetime of these substances in the indoor environments (improving ventilation).

1.2.3 Radon

Radon [8] is a radioactive and inert gas that is produced as a result of the uranium decay. Radon is odorless, colorless and tasteless, so it’s not perceptible to our senses, it can be detected only through specific tests and sensors. If this gas is inhaled, the danger for human health can be very high, particularly the most serious consequence can be lung cancer. For this reason, the WHO (World Health Organization) has included Radon in group 1 of the carcinogenic substances for human health. This gas is present in the ground and can enter inside buildings through walls and foundations, it's a pollutant that must be controlled and appropriate ventilation is necessary to prevent health problems.

As it was previously noted, the carbon dioxide is not the only pollutant, however it’s the mostly used as reference for the IAQ for several reasons: it’s easy to measure, it’s not toxic at low concentrations and it’s related to human breathing, so it’s related to the occupancy, therefore it's appropriate to indicate whether ventilation is adequate. The Table 1.5 presents the permissible limits for the most frequently occurring pollutants in addition to CO_2, these values shall be checked to avoid healthy issues and to guarantee a safe environment. They are indicated by the WHO as air quality guideline levels (AQG) and represent the final result that must be achieved.

Pollutant	Unit	Time	Value
PM2.5	$\mu g\ m^{-3}$	Year	5
		24 hours	15
PM10	$\mu g\ m^{-3}$	Year	15
		24 hours	45
Ozone	$\mu g\ m^{-3}$	8 hours	100
NO2	$\mu g\ m^{-3}$	Year	10
		24 hours	25
SO2	$\mu g\ m^{-3}$	24 hours	40
CO	$mg\ m^{-3}$	24 hours	4
		8 hours	10
Radon	$Bq\ m^{-3}$	Year	300 [9]

Table 1.5 – Recommended values for indoor pollutants [10]

1.3 Types of ventilation

There are different solutions to ventilate a building, and all these possibilities can be divided in 3 categories:

- Natural ventilation;
- Mechanical ventilation;
- Hybrid ventilation (combination of natural and mechanical solutions).

Natural ventilation

Natural ventilation is the result of natural forces, such as wind and buoyancy, which drive the exchange of air between indoor and outdoor environments. The intake of fresh air can help in reducing indoor air pollutants. The natural ventilation depends on many factors such as the climate of the location, the building design and the orientation of the dwelling. Warm air, being lighter than cold air, tends to rise; this difference of temperature creates a natural movement of the air that ventilate the building, in accordance with the chimney effect.

Mechanical ventilation

Mechanical ventilation involves the use of fans to facilitate the movement of air into and out of a building. Mechanical ventilation is a common and useful method to control air quality in all situations where natural ventilation is insufficient or not possible. With this solution, the flow rates can be controlled and modified in accordance with the specific circumstances, with the objective of saving energy and meet the ventilation requirements of the environment. It's possible to filter the air and, by installing a heat exchanger between the two air streams, it's possible to recover some heat and reduce the temperature difference between the fresh air and the air in the room.

A distinction can be made between dual-flow and single-flow systems. A dual-flow solution is more expensive but clearly more efficient: there are two different ducts for supply and exhaust, contamination is avoided, there is the possibility to have filtration and heat recovery. The main reason for choosing a single flow solution is the lower cost: if there is the desire to have some ventilation without the claim to have high performance this system allows a saving money.

Different types of mechanical ventilation are currently used, the most common are mixing ventilation, displacement ventilation and piston ventilation.

Mixing ventilation is the most widespread type of ventilation, and it's used to obtain homogeneous conditions throughout the entire room. It requires good mixing between supply air and room air that can be obtained through the actions of the induction effect, buoyancy and Coanda effect. In order to achieve optimal mixing, it is essential to avoid fresh air going directly to the extraction grilles (short circuit) and to avoid stagnation points where there is no air renewal.

In the displacement ventilation the fresh air enters at low velocities from the bottom, heat and pollutants are transferred from the breathing zone to the ceiling, where there is the outlet system. With this solution there is a stratification of both temperature and contaminants, the air enters colder than the average temperature and it's heated up taking heat and pollutants from the room, and thanks to the buoyancy forces it reaches the exit grills. The advantage is that the air quality in the occupied zone is higher than the ones obtained with the other types of ventilation, so it's possible to reduce the flow rate to obtain the same IAQ. This type of ventilation can be particularly effective if the occupied zone is relatively small compared to the total height of the room, as it provides energy savings by ensuring the correct IAQ only in the lower part of the environment. The disadvantage is that this solution is suited only for ventilation and cooling, in case of heating an additional system is required.

Piston ventilation is used in clean rooms and in all the applications where a low concentration of contaminants is required (e.g. operating theatres). The air enters from the top of the room through special panels that ensure laminar flow, to obtain this a large inlet area is required.

All these types of ventilation systems can follow a strategy named Demand Controlled Ventilation (DCV), which adjusts the flow rate of fresh air to the demand of the room. A traditional system works at a constant speed set by the user, independently from the quality of the air in the room. A DCV system, indeed, adjusts automatically the flow rate of the system by monitoring the level of some parameters used as indicators (e.g. CO_2, VOC): for example, if the system detects a concentration of CO_2 higher than a threshold value, the flow rate increases. In this way the system is self-regulating and can vary the amount of fresh air according to the needs of the environment. The DCV has some important advantages: by ensuring that ventilation is provided only when it's needed and with the appropriate flow rate, there are significant energy and cost savings.

1.3.1 Centralized vs decentralized solutions

The basic idea of centralized ventilation in a residential building is to introduce clean fresh air into the rooms of the house where people spend most of their time (living rooms and bedrooms), and extract "stale" air from the so-called "dirty" rooms (bathrooms and kitchens) where there is a considerable production of water vapour and CO_2. In non-residential buildings the concept is the same, the aim is to extract air from dirty rooms and introduce fresh air in clean rooms (e.g. offices). The building requires the installation of a network of ducts to connect the central unit with all the rooms that need ventilation. A significant benefit of a centralized system is linked to the noise of the machine: the machine is not placed directly in the room but is situated in a technical room, in this way it's easier to isolate acoustically the system. On the other side, a disadvantage is the necessity for cleaning and maintenance of the ducts, it's important to guarantee the correct conditions of the ducts, which represents an additional cost.

Unlike a centralized ventilation system, a decentralized one consists of smaller units installed directly in the environment requiring ventilation. It is simpler and more cost-effective to install as it does not require ductwork, making it an excellent choice for retrofit applications. It also allows local adjustment of operating conditions: by simply changing the fan speed, the airflow can be quickly adapted to the specific needs of each room. This feature also makes it easier to maintain different conditions in different rooms by setting individual units to different air flow rates, a feature that a centralized system can only achieve through a more complex design. However, one of the main drawbacks of decentralized systems, especially at high flow rates, is the noise generated by the units, which is a key area of study and research for manufacturers. The presence of an annoying noise level that can't be reduced through the ducts may ultimately lead some users to prefer a centralized solution. Another potential negative aspect of the decentralized system is the need to purchase multiple units, as each room requiring ventilation must be equipped with its own device.

The most basic solution is a decentralized single flow solution, which is the most cost-effective option but also the least efficient. The opposite end of the spectrum is represented by the centralized double-flow system, which is the most complex solution. It is characterized by an invasive installation process and the highest initial costs.

1.4 Parameters for evaluating system performance

1.4.1 Ventilation effectiveness

Ventilation effectiveness is a crucial concept upon the evaluation of the performance of a ventilation system. This parameter can be useful in providing several indications, including whether the mixing of fresh air is homogeneous, whether there are stagnation points, and whether pollutants are effectively diluted and removed.

One of the first general definitions of the ventilation effectiveness was given by Mats Sandberg, in his publication "*What is ventilation efficiency*" [11]:

$$\varepsilon_v = \frac{c_e - c_s}{c_i - c_s} \tag{2}$$

Where the different terms have the following meaning:

- c_e is the CO_2 concentration in the extract air [ppm];
- c_s is the CO_2 concentration in the supply air [ppm];
- c_i is the mean CO_2 concentration in the room, precisely in the occupied volume (height from 0.05 m to 1.8 m, distance of 0.5 m from internal walls and of 1 m from windows and external walls) [ppm] [12].

In order to better describe the performance of a system, some indices have been defined [13] to understand how the pollutants are distributed in the room and how efficient the air renewal is. These indices are divided in two main categories.

Indices representing the ability of a system to exchange the air in the room:

- Air change efficiency, ε^a;
- Local air change index, ε^a_p.

Indices representing the ability of a system to remove the air borne contaminants:

- Contaminant removal effectiveness (CRE), ε^c;
- Local air quality index, ε^c_p.

1.4.2 Air change efficiency

The air change efficiency [13], ε^a, is a measure of the rate at which the air, in a given space, is replaced in comparison to the theoretically fastest rate at which the same volume of air can be replaced with the same ventilation air flow. The shortest possible air change time for the air in the room, τ_n, which can only be achieved with piston flow, is always equal to the local mean age of the air (concept introduced by Sandberg, [11]) leaving the room. The actual air change time, $\bar{\tau}_r$, is linked to the room mean age of air, $\langle\bar{\tau}\rangle$, in particular:

$$\bar{\tau}_r = 2 * \langle\bar{\tau}\rangle \tag{3}$$

The air change efficiency, ε^a, is defined as the ratio between the shortest possible air change time for the air in the room, the nominal time constant τ_n, and the actual air change time $\bar{\tau}_r$. Alternatively, the definition of the air change efficiency can be expressed as the ratio between the lowest possible mean age of air $\tau_n/2$, and the room mean age of air $\langle\bar{\tau}\rangle$.

$$\varepsilon^a = \frac{\tau_n}{\bar{\tau}_r} * 100 = \frac{\tau_n}{2 * \langle\bar{\tau}\rangle} * 100 \tag{4}$$

The maximum achievable efficiency is 100%, which occurs for ideal piston flow. The Table 1.6 presents the air change efficiency for different flow conditions in a room, taken from the REHVA Guidebook:

Flow pattern	Air change efficiency ε^a
Ideal piston flow	100%
Displacement flow	$50\% \leq \varepsilon^a \leq 100\%$
Fully mixed flow	50%
Short-circuit flow	$\leq 50\%$

Table 1.6 – Air change efficiency

1.4.3 Local air change index

The local air change index [13], ε^a_p, is a metric that characterizes the conditions at a specific point. It is defined as the ratio between the nominal time constant τ_n and the local mean age of the air at point P, $\bar{\tau}_p$.

$$\varepsilon^a_p = \frac{\tau_n}{\bar{\tau}_p} * 100 \tag{5}$$

In the event of complete mixing, the local mean age of the air is identical throughout the entire room and equivalent to the nominal time constant. This results in a local air change index of 100% across the entire room.

1.4.4 Contaminant removal effectiveness

The contaminant removal effectiveness, CRE, ε^c, is a measure of the rate at which an airborne contaminant is removed from a given room [13]. It is defined as the ratio between the steady state concentration of contaminant in the exhaust air, c_e, and the steady state mean concentration of the room, $\langle c\rangle$.

$$\varepsilon^c = \frac{c_e}{\langle c\rangle} \tag{6}$$

It is important to note that the definitions of ventilation effectiveness and CRE are essentially the same, and it's clear that in a fully mixed situation, where the concentration in the exhaust is identical to that of the entire room, both ε_v and CRE are equal to 1. However, in other situations, CRE may differ from very small values to very large ones depending on the position of the contaminant source and the air flow in the room. When the contaminant source is not uniformly distributed, the position of the source highly influences the CRE value, for this reason a high value of CRE is not enough to show that the ventilation system works satisfactorily in ventilating the entire room. Two potential scenarios may be considered: firstly, a contaminant source near the exhaust, resulting in a mean concentration of the room that is lower than that of the exhaust; and secondly, a contaminant source situated in a stagnant zone, where $\langle c \rangle > c_e$. In displacement ventilation systems the ventilation effectiveness results in values higher than 1, because there is an important stratification of pollutants. By placing the exhaust grills in the upper part of the room, the concentration of contaminants is significantly higher in the exhaust air compared to the breathing level and the index is clearly greater than 1.

1.4.5 Local air quality index

The local air quality index, ε^c_p, is a measure of the local concentration at a given point [13]. It is defined as the ratio between the steady state concentration of contaminant at the exhaust air, c_e, and the steady state concentration of the same contaminant at the point P in the room, c_p:

$$\varepsilon_p^c = \frac{c_e}{c_p} \tag{7}$$

Similar air quality indices have been proposed: ε^c_{oz} is the index for the occupied zone and ε^c_b for the breathing zone:

$$\varepsilon_{oz}^c = \frac{c_e}{c_{oz}} \tag{8}$$

$$\varepsilon_b^c = \frac{c_e}{c_b} \tag{9}$$

The main purpose of using these indices is to describe the efficacy of a ventilation system, and a good indicator is the comparison between the concentration of pollutants at the extraction and the concentration in the occupied zone. In this way, it is possible to understand whether the pollutants are drawn towards the extraction or whether they stagnate in zones occupied by people. The most useful indices for this purpose are ventilation effectiveness and CRE: a result close to or greater than 1 means that the system succeeds in washing the room well from the pollutants in question. Air change efficiency, on the other hand, focuses more on the speed at which this removal of pollutants is carried out. To assess the efficacy of the decentralised ventilation unit in removing pollutants and ensuring satisfactory air quality in the occupied zone, ventilation effectiveness may be the most suitable parameter for analysis.

The ventilation effectiveness and all the indices related to it can be evaluated through on-field measurements by sensors or through computational fluid dynamics analysis. Using CFD software is possible to extend the results to all the room, while analysis based on on-field measurements are strictly linked to the position of the sensors.

1.5 How to perform analysis of CO_2 concentrations and ventilation effectiveness

The CO_2 is probably the most diffuse tracker gas, one of the most used in this type of analysis, because it's easy to measure through simple and widespread sensors and it's not problematic for the human health at low concentration. Another positive aspect of CO_2 lies in its correlation with human respiration, a phenomenon that has been extensively documented in the literature.

Several studies have been conducted with the goal of analysing the concentration of carbon dioxide in a given environment, e.g. the analysis of the spatial distribution of the CO_2 or the concentration decrease when people (i.e. the source of CO_2) leave the environment.

The primary methods identified in the literature for analysing CO_2 concentration are experimental analysis, which are conducted on-site with measuring instruments, and analytical analysis, which employ formulas and relationships to define CO_2 trends over time. An example is the study conducted by Monarkin [14], about a reversible decentralized ventilation system, a similar case to the one of this activity. If on-site measurements are carried out, it's essential that instruments are calibrated (in particular that CO_2 sensors are calibrated in the same conditions), that the boundary conditions remain unaltered throughout the test and that the tests are repeated several times to ensure their accuracy. The analytical analysis to measure and observe the pollutant concentration over time can be done using the following formula:

$$C(t) = C_e + 10^3 \frac{q_{gen}}{Q} + \left[C_0 - C_e - 10^3 \frac{q_{gen}}{Q}\right] e^{-(nt)} \tag{10}$$

Where the different terms have the following meaning:

- $C(t)$ is the concentration in the room at time t [ppm];
- C_e is the outdoor concentration [ppm];
- q_{gen} is the pollution rate in the room [l/h];
- Q is the amount of fresh supply air [m^3/h];
- n is the air change rate [1/h];
- t is the time [h].

The term between brackets, multiplied with the exponential term, is a dynamic term that increases when people enter in the room and decreases when people leave the room. In steady state condition, instead, the difference between the concentration at time *t* and the outdoor concentration it depends only on the ratio between the pollution rate in the room and the amount of fresh supply air.

The value obtained represents an average value after a certain period *t*, without considering the actual volume of the room and the spatial effects. However, experimental measurements frequently do not measure the average concentration over the entire volume of a room, but instead obtain a point measurement related to the position of the sensors. This is one of the limitations of comparing theoretical models with experimental measurements, and often the solution lies in the position in which the sensors are placed, which is linked to the objective of the individual case study. In scenarios where the objective is to measure the average concentration within a specific volume, it is possible to place sensors at various points within the environment, subsequently averaging the readings to compare with the theoretical value. Conversely, if the focus is on measuring the concentration in specific parts of the volume, the theoretical model can only provide a general indication, with experimental measurements being essential for detailed study of the particular case.

1.6 Overview of CFD applications

In recent years, the most common and widespread method to analyse the CO_2 concentration (and, therefore, the ventilation effectiveness) has become the use of CFD software, to simulate the entire domain of interest, obtaining a more complete result. Often the CFD analysis is coupled with a previous measurement, to obtain at the end a more comprehensive outcome. An interesting example is provided by the studies made by van Hooff and Blocken [15] [16], in which the behaviour of CO_2 and its decay within a semi-enclosed stadium was analysed. To verify the behaviour of CO_2, measurements were initially made using sensors, and subsequently, CFD simulations were carried out, a methodology that has also been employed in this thesis. In particular, in the works of van Hooff and Blocken, the CO_2 concentration decay was analysed using both measurements and simulations, with the measurements results employed as a reference to set the boundary conditions in the simulation. Once that the simulations were completed, a comparison of the concentration decay curves was done, with the goal to understand if the CFD model was able to represent accurately the CO_2 decay. Another study that demonstrates the importance of combining CFD and experimental analyses was conducted by the Technical University of Sofia [17] [18] [19], in which the distribution of CO_2 concentration within a ventilated classroom is analysed.

In contrast with the analysis of the CO_2 concentration, studies and publications concerning the ventilation effectiveness are considerably less frequent, but it’s still possible to find some analysis that can be used as a reference [13] [20]. One of the most common methods to analyse the air change efficiency is the use of a tracer gas concentration decay method: a certain amount of tracer gas is injected in the room and the variation of the concentration is analysed. It’s important to consider the following aspects when a tracer gas is used:

- During the measurements period there must be no reactions between the tracer gas and the room air;
- The tracer gas should be available at a low cost;
- It should be easily measured by common instruments;
- It should not be toxic or flammable.

The tracer gas that are used mostly are N_2O (nitrous oxide), SF_6 (sulphur hexafluoride) and CO_2.

A complete explanation, with useful examples, of how a tracer gas method to evaluate the efficiency must be done is given by REHVA [13], explaining all the different possibilities that can be considered (step up method, step down method, pulse method and passive methods).

Referring to the use of scFLOW, the CFD software used in this work (see section 3.3), the study conducted by Sheng, Yamanaka; Kobayashi and Chou [21] is an example of the tracer gas decay method, in which the gas used is a mixture of CO_2 and He. Also in the results of this study, there is a comparison between the results of measurements and those of simulations, a pattern that is common in the literature and was also followed in the implementation of this work.

2. CASE STUDY

2.1 Helty

Helty is a brand specialized in air treatment solutions, in particular in the design and production of decentralized ventilation systems. Helty is a relatively young company, born in 2018 from the Alpac Group and based in Schio, in the province of Vicenza. Alpac is a company that deals with window-hole insulation systems; in 2015 Alpac started manufacturing decentralized ventilation systems, in order to integrate them with the window openings already in production. In 2018 an important decision was taken to establish a separate brand for the production and marketing of ventilation machines. The idea behind Helty is to spread the culture of health in the indoor environment and improve the quality of life of those who spend the majority of their time indoors, such as at home or in the office.

Helty is part of a growing market for two main reasons:

- The increasing awareness of the importance of ensuring proper air quality, especially in this post-Covid era;
- A market that is still in its infancy but it's growing continuously. In fact, centralized solutions are much more common at the moment, while decentralized systems are a relatively young market, in which Helty is one of the leaders.

2.2 Research and Development office

The room designated for the case study, where measurements and simulations were carried out, is the R&D office. The office is rectangular in shape, with dimensions of 6.5 meters by 4.5 meters, and a height of 2.75 meters (a total of approximately 80 m^3). The office is oriented with one exterior wall and three interior walls, the exterior one faces southeast and contains two windows. The remaining interior walls border on other rooms within the company (two meeting rooms and the production facility). The office is equipped with a wall radiator for heating and an air conditioning unit for cooling. During the measurement period, covering the first half of October 2024, both heating and cooling systems were switched off. In the Figure 2.1 it's possible to see a picture of the office, to better understand the description of the room.

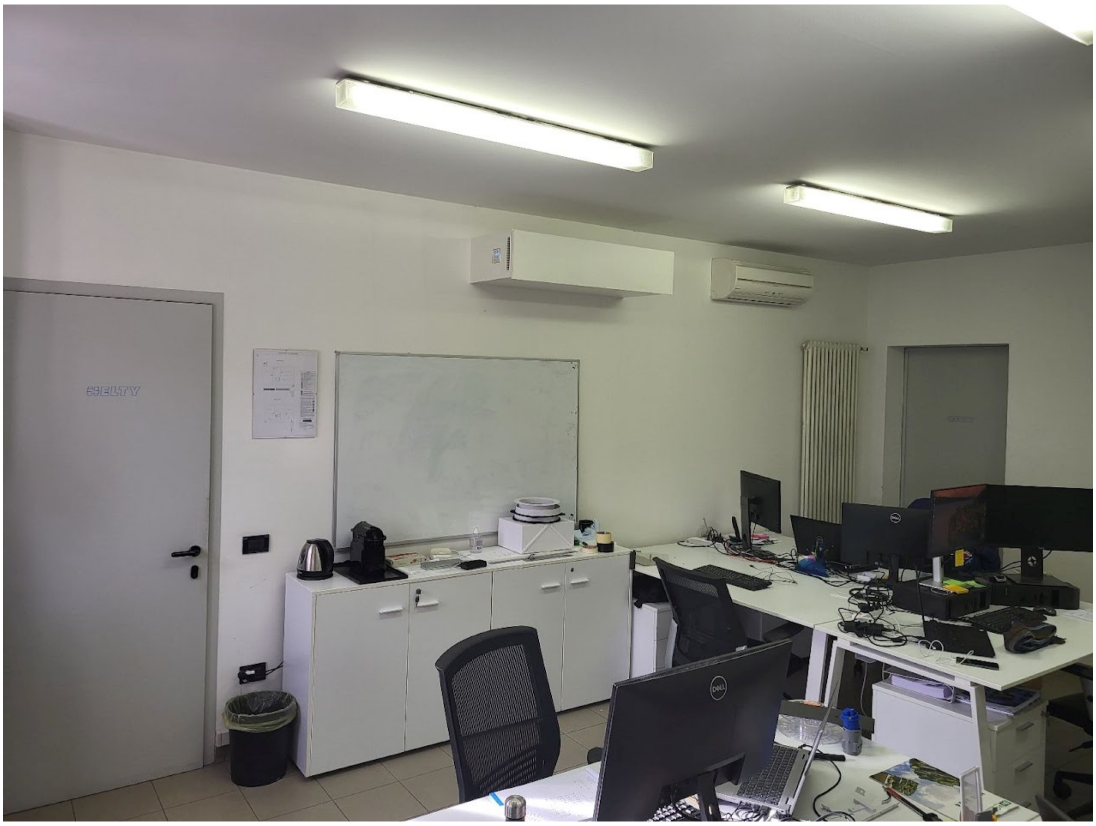

Figure 2.1 – Office

2.3 System description

In contrast to the majority of real installations, in this case the ventilation system does not draw clean air from the outside environment, but rather draws it from an indoor environment. This indoor environment corresponds to the company's production, which is a very large building (more than 1400 m^2 and 7 m high) where machine assembly takes place. It was neither heated nor cooled during the entire measurement period, maintaining a temperature in the range of 18-22 °C. The two holes in the wall, which correspond to the extraction of air from production and the reintroduction of air into production, are located at a height of approximately 6 meters.

The decentralized system installed in the room draws in fresh air from the production, that is an indoor environment with a CO_2 concentration similar to the outside one (ranging between 450 and 550 ppm). The machine analyzed has inlet and extraction on opposite sides, from the machine point of view it has air supply from the left and exhaust on the right. It's a dual flow system, so there are two through-holes in the wall that connect the machine to the production building, one hole for the fresh air intake and one for the discharge of the exhaust air. Inside of the machine there are two filters, an ePM1 80% (F9) filter in the supply to prevent the presence of impurities in the fresh air and an ISO Coarse 70% (G2) filter in the extraction side. The other main component is a counter-current heat exchanger, useful for bringing the supply air temperature closer to the room temperature. The supply and the exhaust openings are rectangular (170 x 35 mm), covered by a grid with horizontal holes (see Figure 2.2 and Figure 2.3 reported at the end of the chapter). The system can work at different velocities, the user can adjust the supply flow rate between six different options:

- Night operation mode;
- Velocity 1;
- Velocity 2;
- Velocity 3;
- Velocity 4;
- Hyperventilation mode.

The night operation mode is suitable for a bedroom application, but the flow rate is too low for an office application, for that reason this velocity was not considered in the analysis.

The system, thanks to sensors that control the presence of pollutants in the room, is able to manage the speed autonomously, varying it according to the measured concentration of CO_2 and VOC: when the value is higher than a threshold value, the flow rate is increased by one step. This option was switched off during the measurements.

Figure 2.2 – Supply of fresh air

Figure 2.3 – Extraction of exhaust air

3. WORKING METHODOLOGY

The analysis was initially conducted performing experimental measurements of the CO_2 concentration within the office environment. To achieve the goal of assessing ventilation efficiency, first the CO_2 concentration in the room was monitored, and then the different air flow rates provided by the machine were measured. From the measured concentration, it was possible to analyse the distribution of CO_2 and calculate the ventilation efficiency. The next step was to carry out CFD simulations, using scFLOW software, in order to represent the conditions that had been measured. A comparison was made between the outcomes of the simulations and the outcomes of the measurements.

This chapter will provide a complete explanation of the methodology employed in the experimental measurements, the calculation of the related parameters and the CFD simulations.

3.1 Experimental data collection

3.1.1 Measurements of CO_2 concentration

The study started with the acquisition of experimental data regarding the concentration of carbon dioxide within the office environment.

Before measurements could begin, it was essential to calibrate the measuring instruments and verify that they were accurately measuring the same CO_2 concentration value when placed next to each other. To complete the calibration procedure, all the sensors were placed outside during a sunny and slightly windy day. In these conditions it was possible to use the calibration mode of the instruments, obtaining a reliable result. Once this preliminary step was completed, the actual measurement phase could start.

A total of six sensors were utilised in this study, comprising three HOBO sensors (model: HOBO MX CO_2 logger), two Aranet sensors (model: Aranet4 HOME) and one PV28 sensor (model: PV28-AW). In addition to measuring CO_2 concentration in parts per million (ppm), the sensors in question are also capable of measuring air temperature and relative humidity. However, atmospheric pressure and dew point can only be measured by some of the sensors used. In particular, pressure can be measured by the Aranet sensors, while dew point can be measured by the HOBO sensors. In the remainder of the study, the sensors will be referred to simply as HOBO, Aranet and PV28, rather than by their full model's name, in order to avoid unnecessary complexity in the text. See Tables A.1, A.2 and A.3 in Appendix A for the technical datasheets of the sensors.

The two Aranet sensors were used to measure the CO_2 concentration at the air inlet and outlet, namely they were placed close to the supply and exhaust vents, at a height of about 2.5 m.

The three HOBO sensors were placed inside the office to measure the CO_2 concentration at three different points in the room. They were placed at a height of approximately 0.8 m from the ground, precisely above the desks, but at three different points in the room. The aim was to analyse the CO_2 distribution, with a focus on determining whether there was any point with stagnant CO_2 or whether there was good mixing when moving away from the supply.

The PV28 sensor was placed just outside the office, in the production hall, in order to detect the CO_2 concentration of the surrounding environment from which the fresh air was drawn. From now on, for the sake of simplicity, the adjacent production environment will be referred to as the outdoor environment (and consequently the terms outdoor air and outdoor concentration will be used).

In Figure 3.1 the positions of the sensors are represented by the red circles. In particular, the numbers here reported represent the sensor numbers in the figure (number 1 in the Figure 3.1 represents the position of the Aranet 1 etc.):

1. Aranet, supply of fresh air, will be referred to as Aranet 1;
2. Aranet, exhaust air, will be referred to as Aranet 2;
3. HOBO, will be referred to as HOBO 1;
4. HOBO, will be referred to as HOBO 2;
5. HOBO, will be referred to as HOBO 3;
6. PV28, outside air concentration, will be referred to as PV28.

The letters A, B, C and D represent the positions of the four people working in the office. The grey rectangle between the sensors 1 and 2 represents the decentralized ventilation system, while the two brown rectangles represent the desks and the two blue small rectangles in the top part are the two windows of the office.

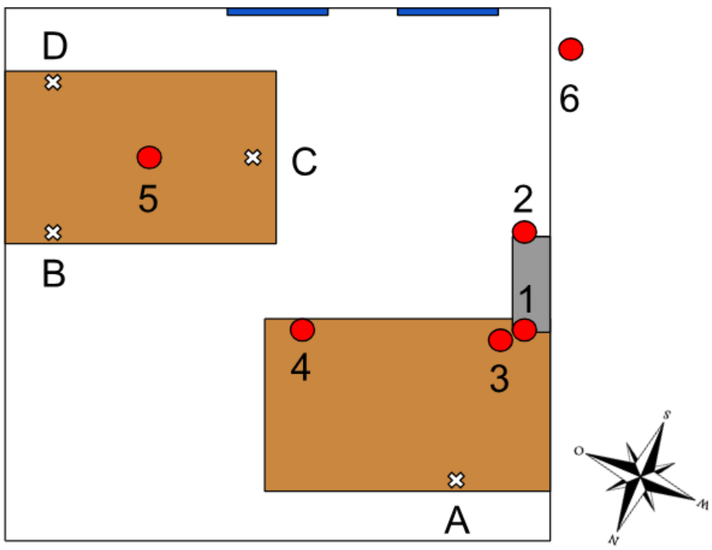

Figure 3.1 – Position of the sensors in the office

The measurements were conducted for each speed as 48 hours-analysis, starting at 8:00 and concluding at 7:55 of the following day. This process was repeated over two days. As previously stated in Chapter 2, five speeds were analysed, resulting in a total of 10 days of measurements. Data were recorded every five minutes, resulting in a total of 288 CO_2 concentration values recorded for each 24-hour interval. Furthermore, also the room occupancy was monitored in parallel every five minutes. The number of people can be used as an indicative factor to better understand and explain the CO_2 trend within the office: the greater the occupancy, the greater the internal production of carbon dioxide within the room. The other measured quantities (temperature and relative humidity) were also recorded by the sensors with the same time step, i.e. every five minutes. The PV28 sensor, which was used to measure the outdoor concentration, was the unique exception. It was able to record the concentration with a time step of one hour, which is a sufficient frequency for checking the daily profile of the outside air.

3.1.2 Flow rate measurements

The supply flow rate was calculated by measuring the air speed using the Testo 425 hot-wire anemometer (see Table A.4 in Appendix A for the technical datasheet). Each measurement was conducted in accordance with the following procedure: initially, a matrix of fifteen points was constructed. This matrix consisted of five horizontal lines, each comprising three points, with a distance of 3 cm between two adjacent horizontal lines and a distance of 1 cm between two points within the same line. The sensor was positioned at each point of the matrix for a period of three seconds, resulting in a total measurement time of 55 seconds. The average velocity value was calculated based on these 55 seconds. This procedure was repeated three times, resulting in three average velocity values. At this point, the mean of the three values was calculated, and from this average velocity, knowing the cross-sectional area, it was possible to obtain the air flow rate at the entrance of the room. The whole procedure was carried out both by measuring the velocity at the exit of the grille and by measuring the velocity after removing the grille (thus guarantee a rectangular section free of grilles and vents). Once the flow rates were determined, it was possible to calculate the air change rates guaranteed by each system speed simply dividing the flow rate by the total volume of the room. A further observation that can be made concerns the air flow rate: it can be divided by the number of persons giving the flow rate in l/s per person. This value can then be compared with the Standard [5] to get an idea of whether the air exchange can be suitable for a number of people or not.

These measurements were taken at the end of the CO_2 concentration measurements. Between the acquisition of one speed and the following one, at least 15 minutes were waited, in order to permit the system sufficient time to stabilise the new speed (and to avoid measuring an increasing/decreasing value instead of a stationary value).

3.2 Experimental data analysis

3.2.1 CO_2 distribution and standard deviation

In order to assess whether the ventilation system is able to guarantee good mixing inside the room, it's possible to observe the values measured by the three HOBO sensors: if the three values are close to each other, it means that the CO_2 concentration is homogeneous inside the room (in particular at desk height, a position of interest when focusing on offices). A suitable method for evaluating the internal uniformity is to calculate the standard deviation between the values recorded by the HOBO sensors and the mean value of the three measurements: a smaller standard deviation indicates a more effective ventilation system.

In particular, the standard deviation between the three sensors inside the office was calculated using the standard deviation function of Excel for each interval of five minutes. To better understand the impact of the result, it's expressed also as a percentage of the mean value of that specific time interval (e.g. for an interval of five minutes: HOBO 1 = 1134 ppm; HOBO 2 = 1092 ppm; HOBO 3 = 1077; standard deviation = 29.5; mean value = 1101; standard deviation in percentage respect to the mean value = 2.68%).

Another aspect to consider concerns the possible stratification of CO_2; therefore, a specific measurement was made with a HOBO sensor at 0.8 m (desk height) and another HOBO sensor at 2 m height. The measurement was carried out from 10:00 to 15:00, with the ventilation system set to velocity 2, with the aim of finding out whether height plays an important role in the distribution of CO_2.

3.2.2 IAQ and occupancy analysis

Another interesting aspect to analyse is the IAQ, in particular the share of time in which a class of IAQ is fulfilled. Furthermore, an examination of the occupancy distribution is required to complete this analysis, as the average concentration within the office is closely linked not only to the flow rate but also to the generation of carbon dioxide, and consequently to the occupancy. Therefore, the analysis is limited to working hours, defined as the period between 8:00 and 18:00. The objective of this calculation is to see, for each operating speed and therefore for each flow rate, the air quality and the category that can be guaranteed for the majority of hours, and the flow rate that may be required for a room of this size with the number of people varying within a given range. To achieve this result, the following steps were undertaken:

- Starting from Table 1.4 and remembering that the IAQ classes can be defined through the CO_2 concentration above the external value, the CO_2 threshold values that delineate the 3 different categories were calculated for each specific case, taking as the outdoor concentration the average concentration in the production hall during working hours (i.e. the concentrations obtained by adding 550 ppm and 800 ppm to the external one);

- Remembering that the concentration was calculated with a 5-minute time step, it was determined the percentage of time in which the level of CO_2 concentration in the room is included in each IAQ category (i.e. the percentage of time when the concentration was below the 550 ppm above the external value, between 550 and 800 ppm above the external value and greater than 800 ppm above the external concentration);
- The occupancy distribution from 8:00 to 18:00 was calculated and graphically represented and finally combined with the results obtained in the previous step.

3.2.3 Ventilation effectiveness

The ventilation effectiveness (ε_v) was calculated according to Equation 2, presented in the introduction chapter, section 1.4.

The different terms of the equation were measured by the different sensors in the following way:

- Exhaust concentration c_e was measured through the sensor Aranet 2;
- Supply concentration c_s was measured through the sensor Aranet 1;
- Room concentration c_i was taken as the average value between the measurements made by the three HOBO sensors.

As the CO_2 concentration is measured every five minutes, also ε_v is evaluated every five minutes.

The expanded uncertainty of the ventilation effectiveness was also calculated, and the error propagation formula used was as follows:

$$u(\varepsilon_v) = \sqrt{\left(\frac{\partial \varepsilon_v}{\partial c_e} * \sigma\right)^2 + \left(\frac{\partial \varepsilon_v}{\partial c_s} * \sigma\right)^2 + \left(\frac{\partial \varepsilon_v}{\partial c_i} * \sigma\right)^2} \qquad (11)$$

Where the different terms have the following meaning:

- $u(\varepsilon_v)$ is the ventilation effectiveness uncertainty;
- $\partial\varepsilon_v/\partial c_e$ is the partial derivative of the ventilation effectiveness respect to the exhaust concentration;
- $\partial\varepsilon_v/\partial c_s$ is the partial derivative of the ventilation effectiveness respect to the supply concentration;
- $\partial\varepsilon_v/\partial c_i$ is the partial derivative of the ventilation effectiveness respect to the room concentration;
- σ is the average of the standard deviation calculated during the calibration.

The uncertainty $u(\varepsilon_v)$ was calculated for each value of ε_v, then the value $2u(\varepsilon_v)$ was used to define the result interval with a 95% confidence level, representing the ventilation effectiveness as $\varepsilon_v \pm 2u(\varepsilon_v)$.

3.2.4 Air change rate from the CO_2 decay

The Equation 10 introduced in the Chapter 1 explains the relationship between the concentration in the room at time *t* and the air change rate *n*, in particular if the internal generation of CO_2 is null (i.e. there are no people in the office), the velocity of the decay of the CO_2 concentration depends only on the air change rate.

By constructing a graph with the trend of carbon dioxide concentration on the y-axis and time on the x-axis, considering the time interval since the office emptied until a concentration similar to that outside was obtained, it is possible to represent the relationship expressed in equation 10.

On the x-axis, time is expressed in hours, in this case the hours that have passed since the office emptied. On the y-axis, on the other hand, it is necessary to scale the average CO_2 with the outdoor value, in order to obtain an exponential decay curve of the CO_2 concentration above outdoor. At this point it is possible to create an exponential trend line that best represents the CO_2 concentration curve, and since this curve represents the relationship of equation 10, the term at the exponent of the curve equation represents the air change rate *n*.

A comparison of the latest calculated air change per hour with the one derived from the flow rate calculation represents an effective method to consolidate the result obtained from direct measurements and to compare the experimental flow rate measurement with the estimation obtained from the variation in concentration over time.

The value of air change rate obtained in the absence of mechanical ventilation represents the infiltration rate. When the ventilation system is switched off, there is no forced air exchange and the only ventilation that occurs is due to infiltration through the door and window frames. The CO_2 decay observed in this situation allows the calculation of how many air changes per hour the infiltrations into the office correspond to.

3.3 CFD analysis

The objective of the CFD analysis was to represent the experimental tests within CFD software, namely scFLOW (Cradle), in order to compare the results of the measurements with the results of the simulations (in terms of concentration and ventilation efficiency) and to understand whether the CFD model represents the real model accurately. To achieve this goal, periods of consistent occupancy were selected and delineated within the software. The subsequent paragraphs will provide a detailed description of the CFD analysis.

3.3.1 Description of the preprocessor

The initial step involved the upload of the 3D geometry of the room into the scFLOW preprocessor, with the objective of establishing an environment that closely resembles the actual one. This environment was then utilised for the execution of simulations. Figure 3.2 presents the top view of the model employed, maintaining the same orientation as the simplified drawing in Figure 3.1. Figures 3.3 and 3.4 offer side views: Figure 3.3 is from the long side opposite the ventilation machine's position, while Figure 3.4 is from the short side facing outwards.

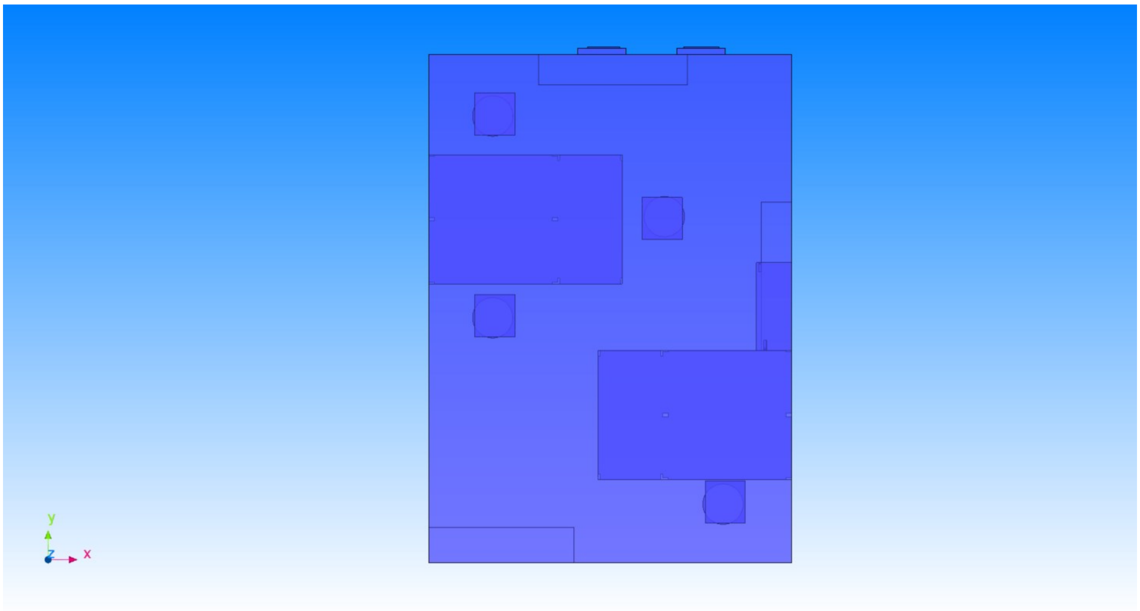

Figure 3.2 – 3D representation, top view

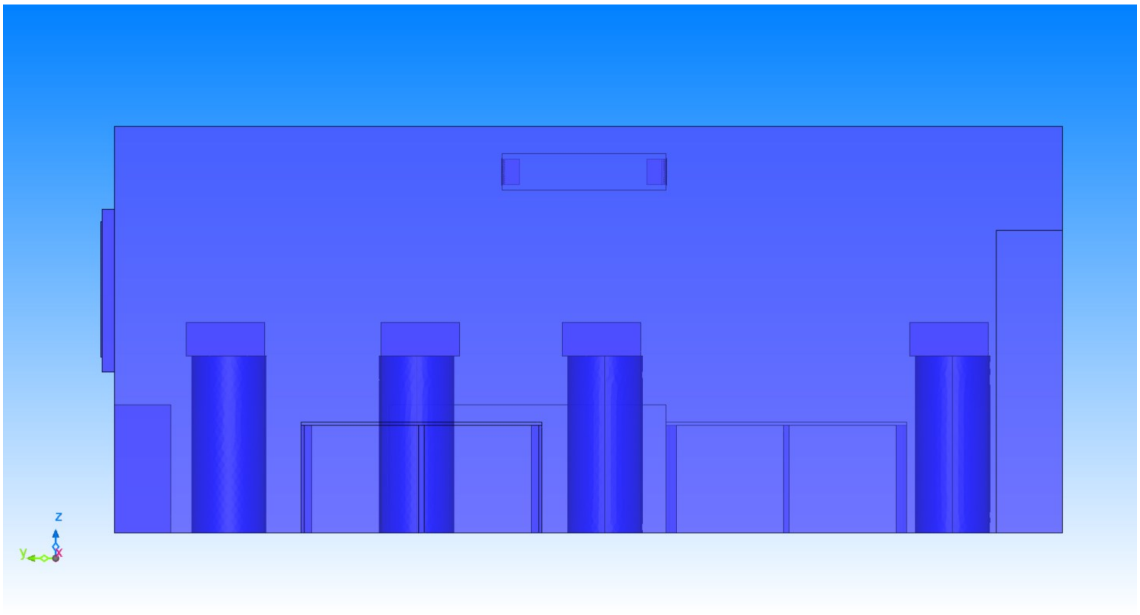

Figure 3.3 – 3D representation, long side view

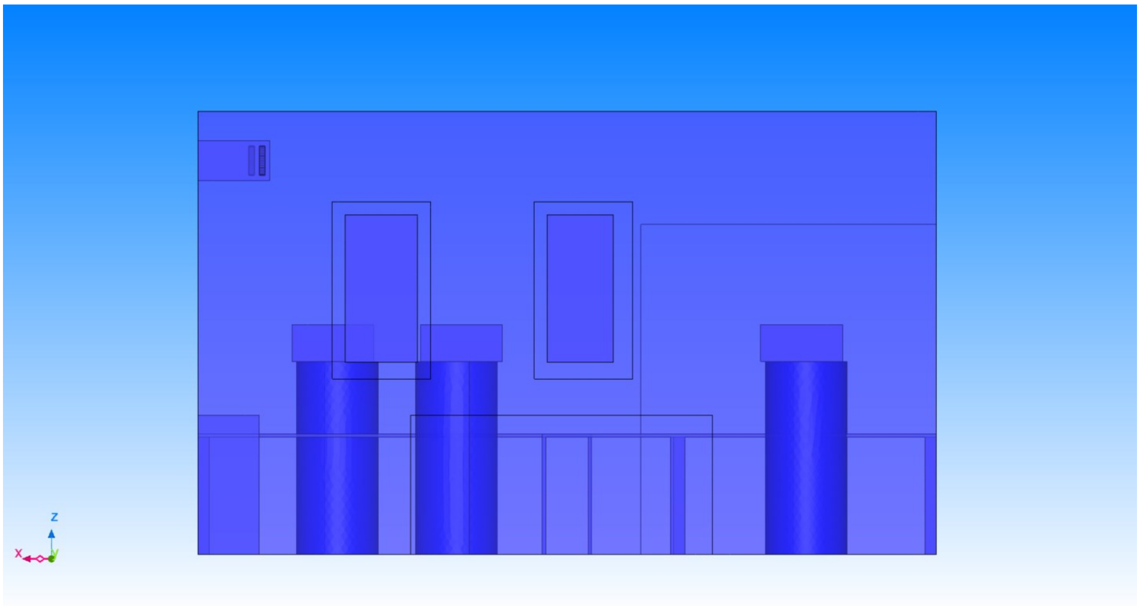

Figure 3.4 – 3D representation, short side view

The analyses were done in transient mode, with a time step of 30 seconds, i.e. with 2 cycles per minute, and the flow is set as turbulent flow.

The next step concerns the definition of the pollutant, i.e. CO_2. To do this, the *diffusive species* function was used, considering a diffusivity of $1.4*10^{-5}$ m^2/s [22].

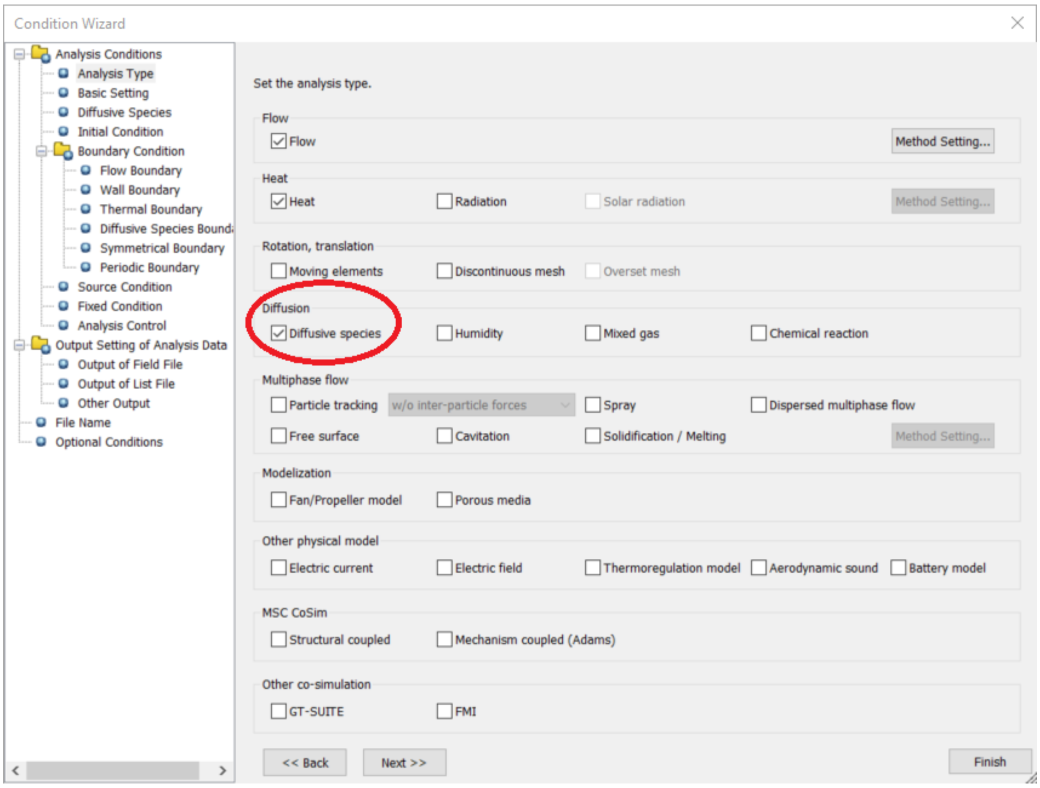

Figure 3.5 – Conditions window: diffusive species

The first challenge consisted of defining and including the generation of CO_2 emitted by the people in the room. As shown in the study by Persily and de Jonge [7], the CO_2 emitted by a person at rest, precisely with a met of 1.2, and in an age range of 20 to 50 years is 0.0046 l/s. Considering a CO_2 density at 0 °C of 1977 g/m^3 [23], the density at 20 °C was obtained using the following relationship:

$$\rho_{CO_2} = \frac{M_{m,CO_2} * p}{R * T} \tag{12}$$

Where the different terms have the following meaning:

- $M_{m,CO2}$ is the molar mass [kg/mol];
- p is the pressure in pascal [Pa];
- R is the universal gas constant, equal to 8.314 J/(mol * K);
- T is the temperature [K].

Given a molar mass of 0.044 kg/mol, the density at 20 °C is equal to 1829.65 g/m^3.

From this data, it is possible to obtain the CO_2 generation expressed in g/h starting from the value expressed in l/s (0.0046 l/s), resulting in a value of 30.3 g/h.

The subsequent stage of the process was to calculate the theoretical concentration of CO_2 in the room after a time *t* employing a mass balance. The equation 13 was used:

$$\mathrm{CO_2}(t) = CO_{2,int} + \left[CO_{2,gen} + Q_{supply} * CO_{2,ext} * \left(\frac{1-L}{100}\right) - Q_{exhaust} * CO_{2,int,vol}\right] * \frac{\Delta t}{60} \tag{13}$$

Where the different terms have the following meaning:

- $CO_2(t)$ is the concentration in the room at time t [g];
- $CO_{2,int}$ is the internal concentration [g];
- $CO_{2,gen}$ is the CO_2 generated inside the room [g/h];
- Q_{supply} is the supply flow rate [m^3/h];
- $CO_{2,ext}$ is the external concentration [g/m^3];
- L is the internal leakage, assumed to 3%;
- $Q_{exhaust}$ is the exhaust flow rate [m^3/h];
- $CO_{2,int,vol}$ is the CO_2 generated inside the room divided by the volume of the room [g/m^3];
- Δt is the time between two different steps [min].

Knowing the internal CO_2 in g, it's possible to obtain the concentration of carbon dioxide in ppm after a certain time *t*.

Through this relationship it was possible to calculate the concentration over time given the following boundary conditions: initial concentration, external concentration, supply flow rate and number of people (i.e. generation of CO_2).

In the software there is no option to specify the generation of CO_2 in the form of a flow rate from a specific surface, but a concentration is required as input, and to overcome this limitation the “source condition” option has been used. This option allows the user to define the generation of a species expressed in quantity/second, the choice of the unit of measurement of the quantity is free, but the unit of measurement used in the preprocessor is the same one that will be obtained later in the postprocessor. The aim was to obtain a concentration expressed in ppm in the postprocessor, so the difficulty was found in defining the CO_2 generated by a person in ppm/s. To obtain this value, test simulations were carried out in order to find the right value to be assigned to the *source condition* function, to obtain an average concentration over the entire volume of the room at time *t* in accordance with the concentration calculated theoretically using equation 11. Several attempts were made, and comparing the theoretical CO_2 concentration trend with the one obtained in the simulations, it was seen that the source value that provided the best match between the simulations and the theoretical calculation is 4 ppm/s per person, so it was assumed that each person inside the room emits this quantity of CO_2, and it was set as the source value in the preprocessor, as shown in Figure 3.6

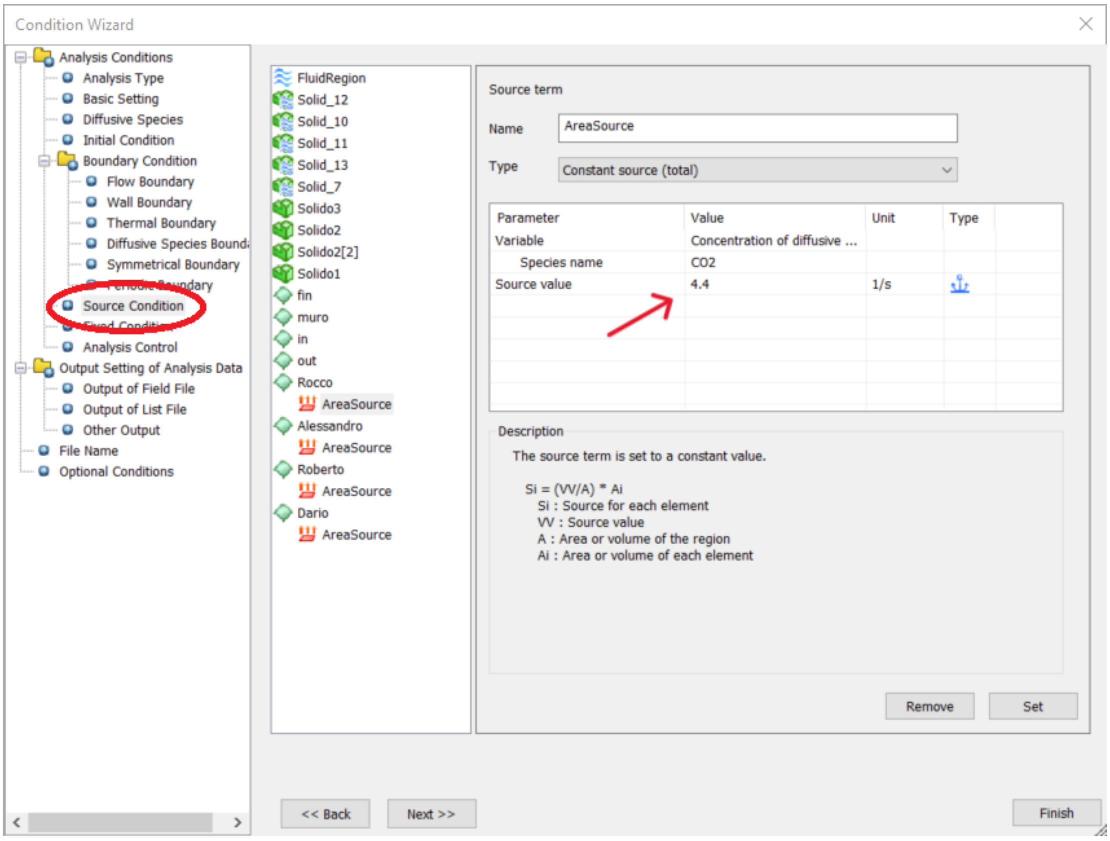

Figure 3.6 – Conditions window: source condition

Before proceeding with the simulation, several initial conditions must be defined. Firstly, the initial CO_2 concentration must be specified; i.e. the concentration measured in the room at the beginning of the analysed period. The value that was used corresponds to the average value between the measurements of the three HOBO sensors in the five minutes preceding the analysed period. Another parameter that must be defined is the CO_2 concentration in the supply air: in the results of the measurements, it was possible to see that this value was not constant over time, but underwent fluctuations. Within the scFLOW framework, it was necessary to indicate a constant concentration value for all the cycles of a single simulation. The value selected for this purpose is equivalent to the average of the concentrations measured at the inlet during the period under scrutiny. To elucidate the concept, a numerical example is provided. The values in the supply concentration column correspond to the value measured at the time indicated in the adjacent cell, the mean concentration value corresponds to the average of all these values and it is the number that was used as input in scFLOW.

Time	Supply concentration	Mean concentration
11:35	677	654.17
11:40	664	
11:45	676	
11:50	665	
11:55	651	
12:00	644	
12:05	652	
12:10	647	
12:15	640	
12:20	653	
12:25	644	
12:30	637	

Table 3.1 – Example of supply concentration used in scFLOW

The boundary conditions used in the analysis were the following:

- Initial condition: air at 20 °C for all the simulations, initial concentration of CO_2 different for each analysis;
- Flow boundary, supply: air at 20 °C, direction normal to the boundary, turbulence intensity of 5% and ratio of 100 for all the simulations. Volume flow rate and concentration of CO_2 different for each analysis;
- Flow boundary, extraction: static pressure (outflow), with a pressure of 0 Pa;

- Thermal boundary: adiabatic condition to the boundary with outside (condition automatically applied by the software).

In order to ensure the stability of the simulations and to avoid any potential divergences in the calculations, the "stability oriented" option was activated, as illustrated in Figures 3.7 and 3.8.

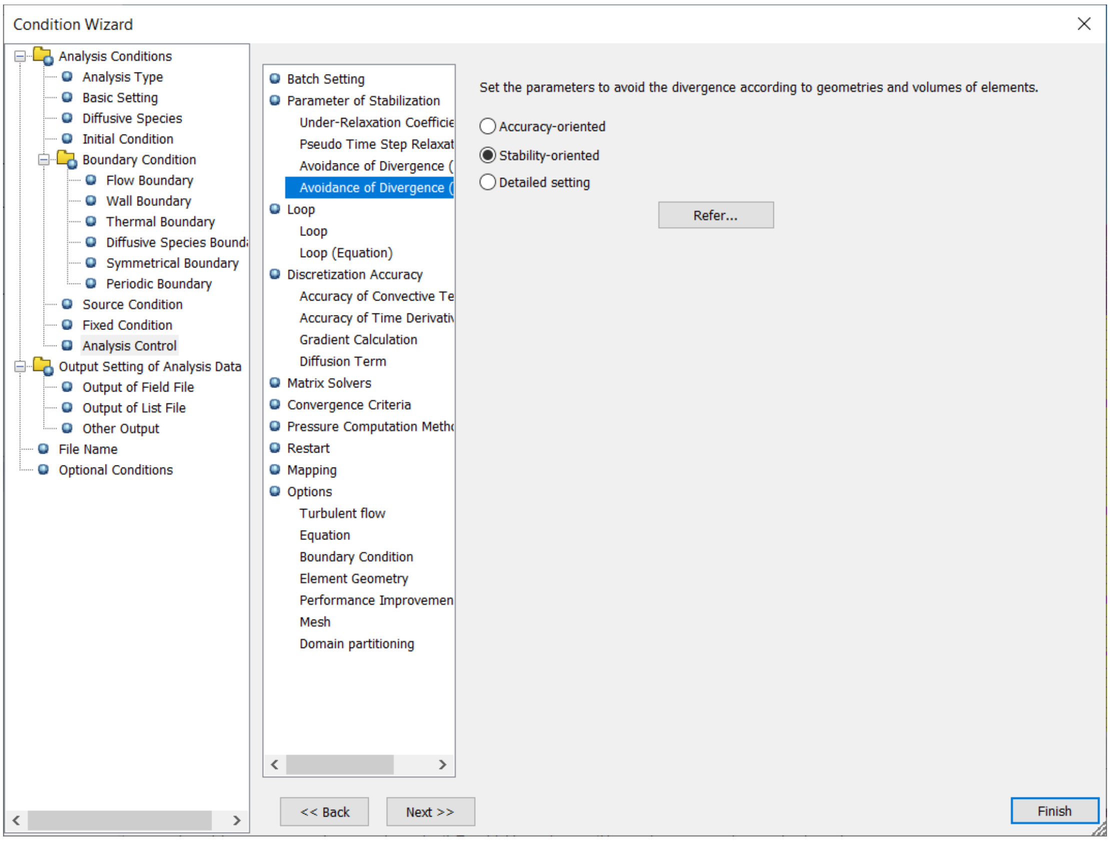

Figure 3.7 – Stability oriented option: avoidance of divergence

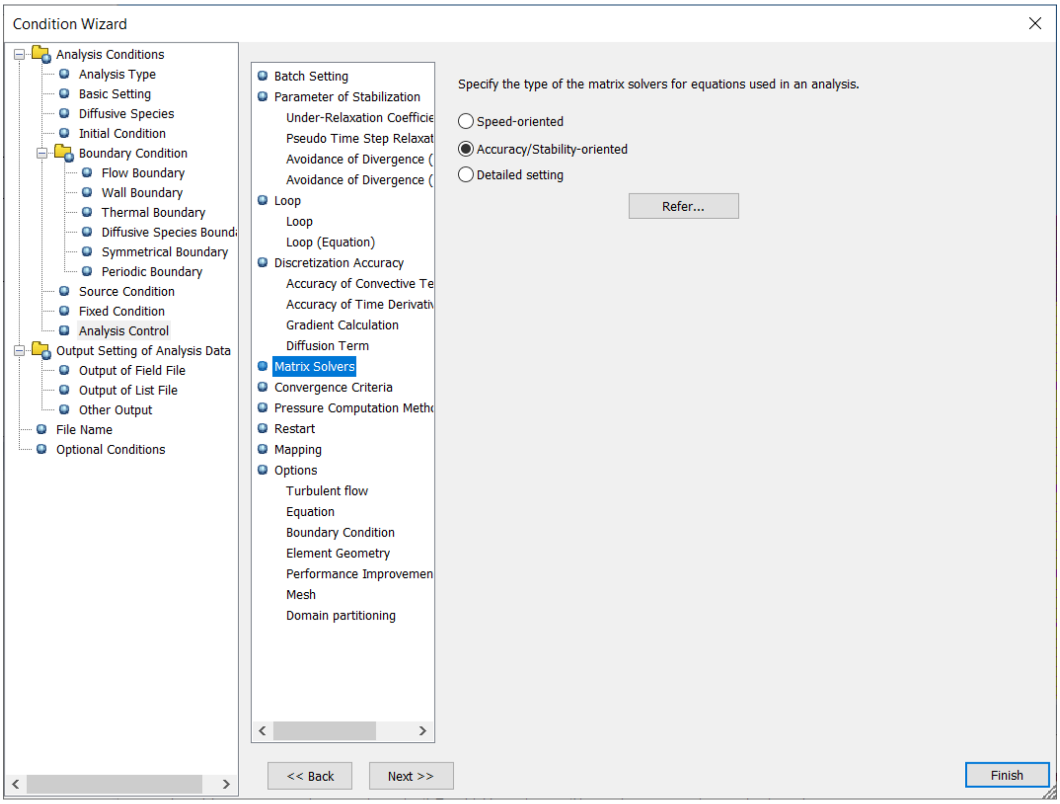

Figure 3.8 – Stability oriented option: matrix solvers

The next step concerns the creation of the octree and of the mesh, specifically the minimum and maximum size of the octree elements were limited to achieve greater precision, as can be seen in Figure 3.9. The mesh generation parameters are illustrated in Figure 3.10.

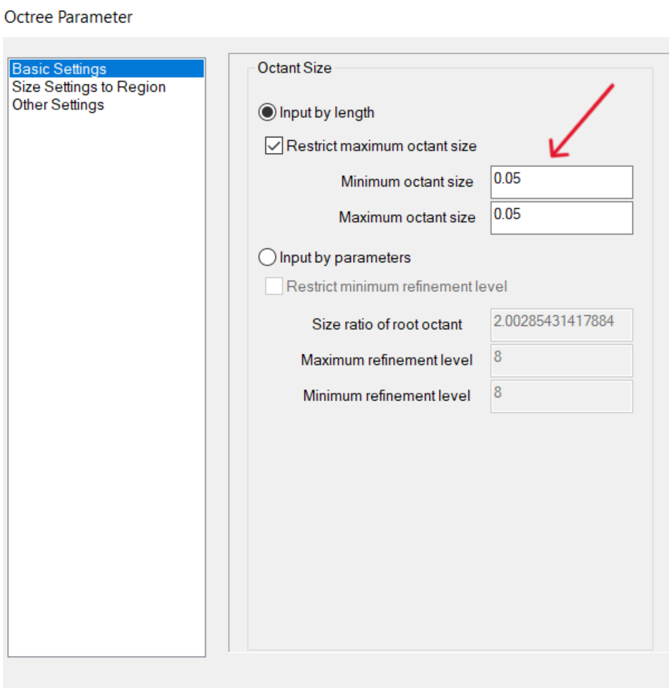

Figure 3.9 – Octree parameters: minimum and maximum octant size

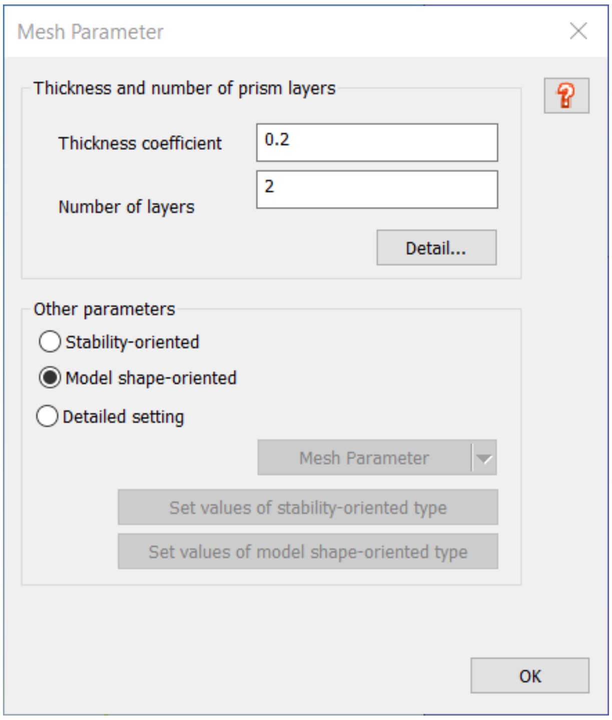

Figure 3.10 – Mesh parameters

3.3.2 Description of the solver

After entering the appropriate initial conditions in the preprocessor, the next step was to run the simulation using the scFLOW solver. Once the simulation was complete, the .fph file could be opened in the postprocessor to continue the analysis.

3.3.3 Description of the postprocessor

The goal of the postprocessor was to obtain the mean concentration values in the room and at the extraction as time elapsed (in particular every 5 minutes), to facilitate comparison with the measurements. In order to best represent the values measured by the three HOBO sensors, a horizontal plane was created at a height of 0.8 meters, passing through the three points where the sensors were positioned, and the average concentration was calculated (see Figure 3.11). Conversely, the extraction concentration was obtained by establishing a vertical surface placed near the extraction grille (in a similar position to that occupied by the sensor) and calculating the mean concentration on this plane (see Figure 3.12).

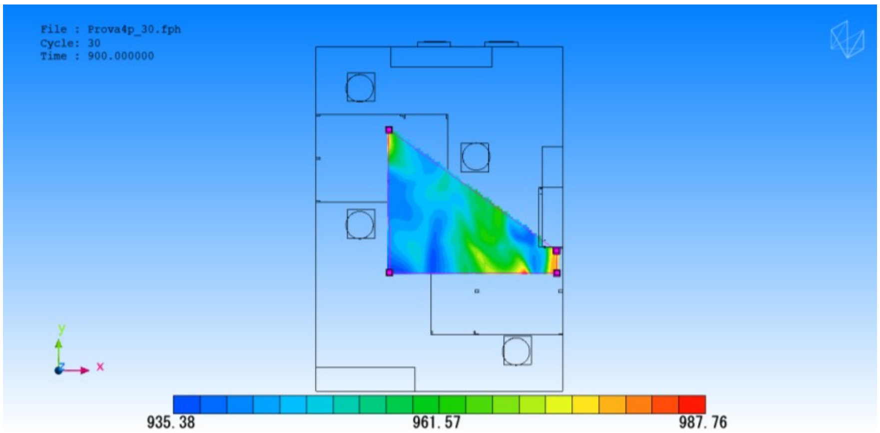

Figure 3.11 – Example of concentration distribution, horizontal plane

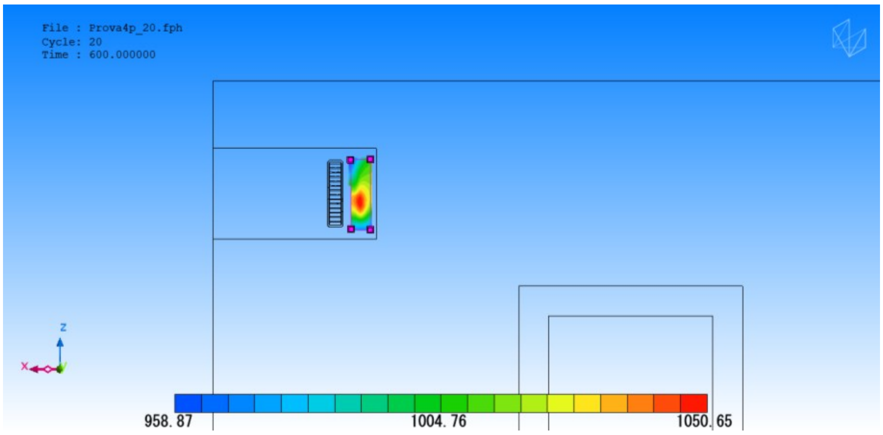

Figure 3.12 – Example of concentration distribution, surface at the extraction

The calculation of ventilation efficiency was undertaken by using the mean values in the horizontal plane and in the plane in proximity to the extraction, with the aim of comparing the efficiency obtained from measurements with that obtained from simulations. The supply concentration, which appears in the formula of ventilation effectiveness, was taken as the input value specified in the preprocessor, as detailed in Table 3.1

In the context of employing simulations to represent new case studies that have not been previously measured in experimental settings, the average concentration in the occupied volume [12] can be used as the internal concentration. In this case, with the aim of ensuring conditions as close as possible to those observed in the experimental measurements, it was decided to evaluate the average concentration in a plane passing through the 3 sensor points.

4. RESULTS

In this chapter, the results of the study are reported in full. These results begin with the measurements and indices and continue with the results of CFD simulations. Each result is accompanied by a commentary and analysis, with the aim of enhancing the comprehension of the numerical data.

The analysis of these results begins with the results of the data collection, i.e. CO_2 concentration (4.1.1) and flow rate measurements (4.1.2). This section is followed by the results of the analysis of the data, in particular the analysis of the CO_2 distribution (4.2.1) and of the IAQ and occupancy (4.2.2). Subsequent sections (4.2.3 and 4.2.4) present the results of the ventilation effectiveness and of the air change rate from the CO_2 decay, while the last part of the chapter is dedicated to the CFD results (4.3).

4.1 Results of experimental data collection

4.1.1 Measurements of CO_2 concentration

For each measurement, it is possible to see the CO_2 trend over time measured by the different sensors. For convenience, the location of the different sensors is shown below, facilitating the interpretation of the graphs:

- Aranet 1 → supply of fresh air;
- Aranet 2 → exhaust air;
- HOBOs → inside of the office;
- PV28 → external environment.

As explained in the previous chapters, a single measurement starts at 8:00 and ends at 7:55 the following day, the office is typically occupied from just before 8:00 until about 18:00 (the exit time can vary between 17:00 and 18:00, depending on the day), with the occupancy varying mostly unsteadily, except for the lunch break of about 1 hour and 15 minutes (from 12:45 to 14:00) when the office empties. As the main source of CO_2 generation is human respiration, from the time workers arrive at the office in the morning, the average CO_2 concentration starts to increase. Similarly, when people leave the office and carbon dioxide generation decreases, the average concentration measured by the three HOBO sensors also decreases. Another initial consideration that can be made is that for the same carbon dioxide generation, the greater the ventilation (i.e. the greater the flow rate of fresh air into the office), the lower the CO_2 concentration should be.

The graphs shown here analyse the CO_2 concentration from 8:00 to 19:00, i.e. from the daytime when the office is occupied until shortly after the last person has left the office. The CO_2 decay process and the related graphs will be analysed in detail in section 4.2.4, while the graphs concerning the night hours are not shown as they are not useful for the purpose of the study. It's represented also the occupancy trend, but the analysis of the occupancy is explained in the section 4.2.2.

As previously mentioned in the previous chapters, two measures have been conducted for each velocity, and the results are presented in the form of a graph for each velocity. The present chapter contains one graph for each flow rate, the second measure is documented in Appendix B.

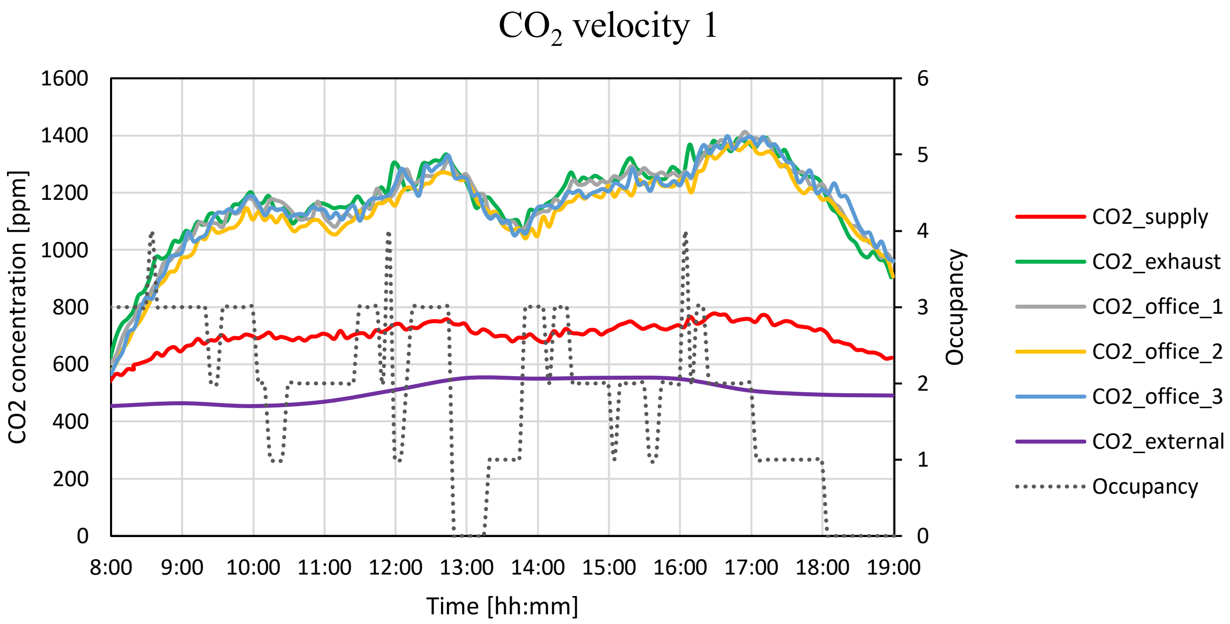

Figure 4.1 – CO_2 trend with velocity 1

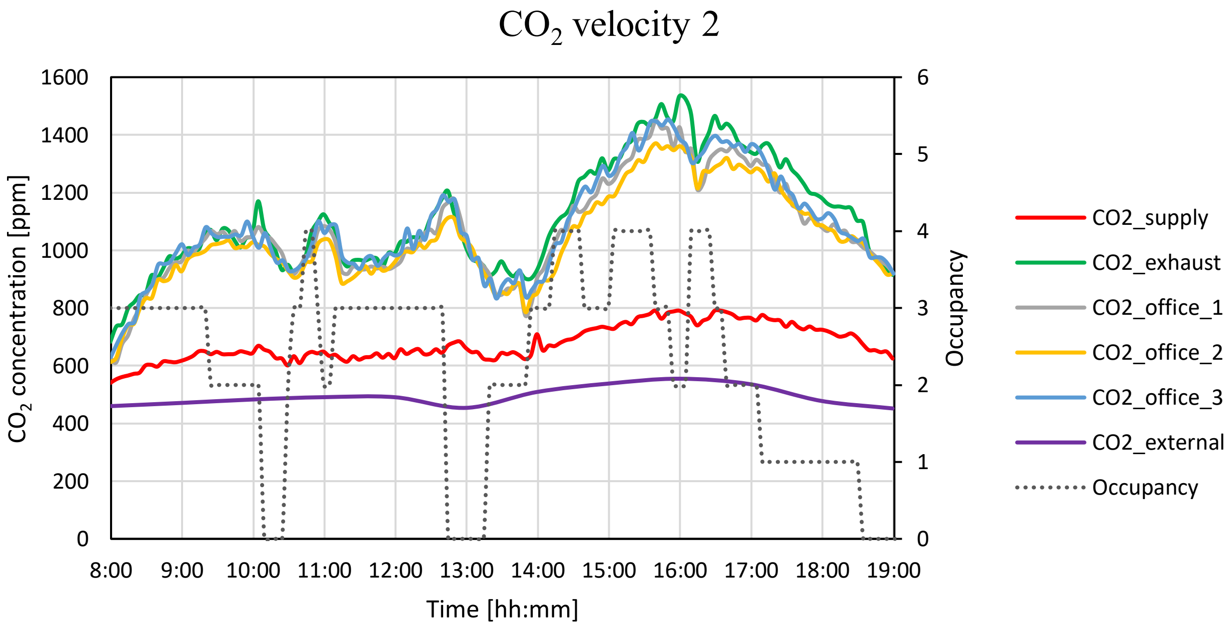

Figure 4.2 – CO_2 trend with velocity 2

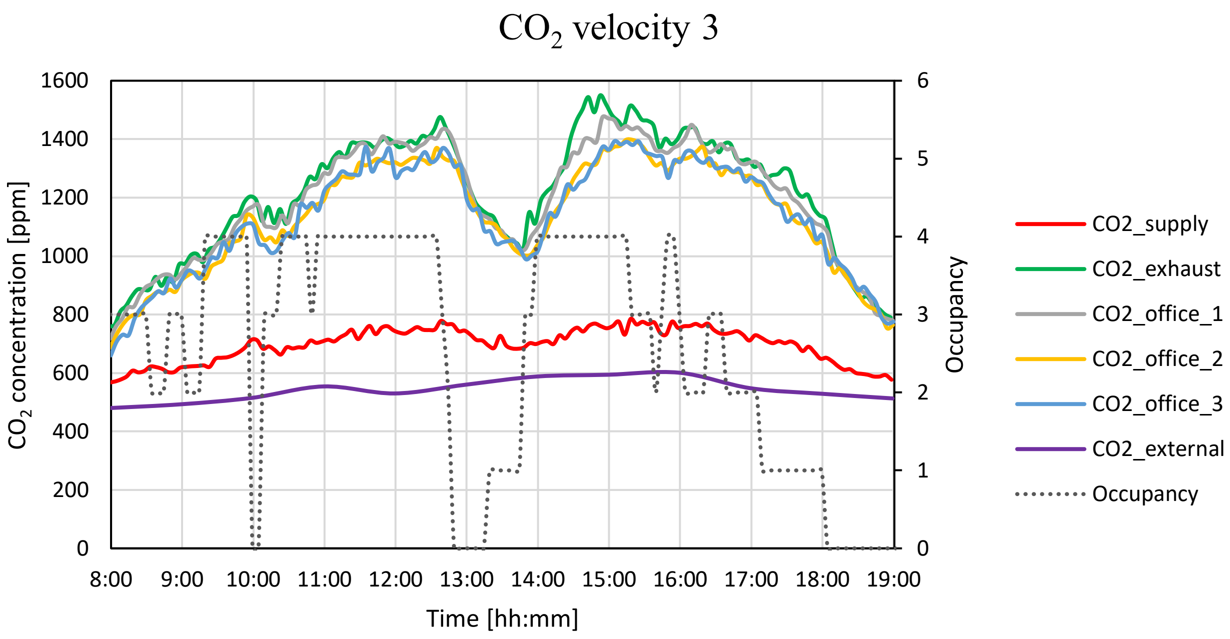

Figure 4.3 – CO_2 trend with velocity 3

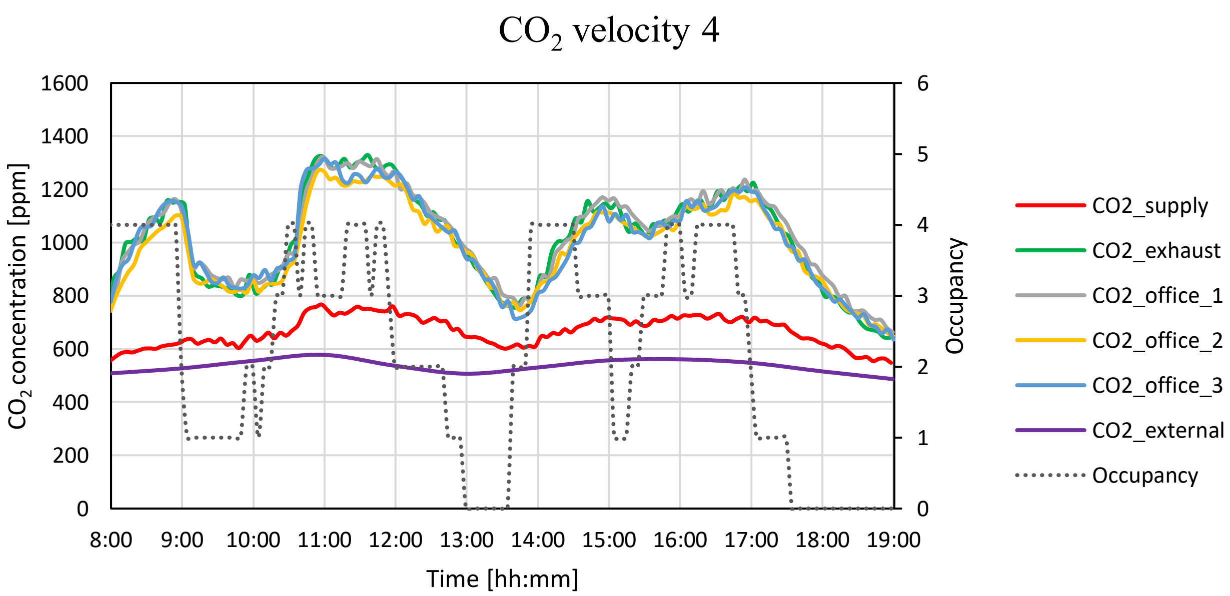

Figure 4.4 – CO_2 trend with velocity 4

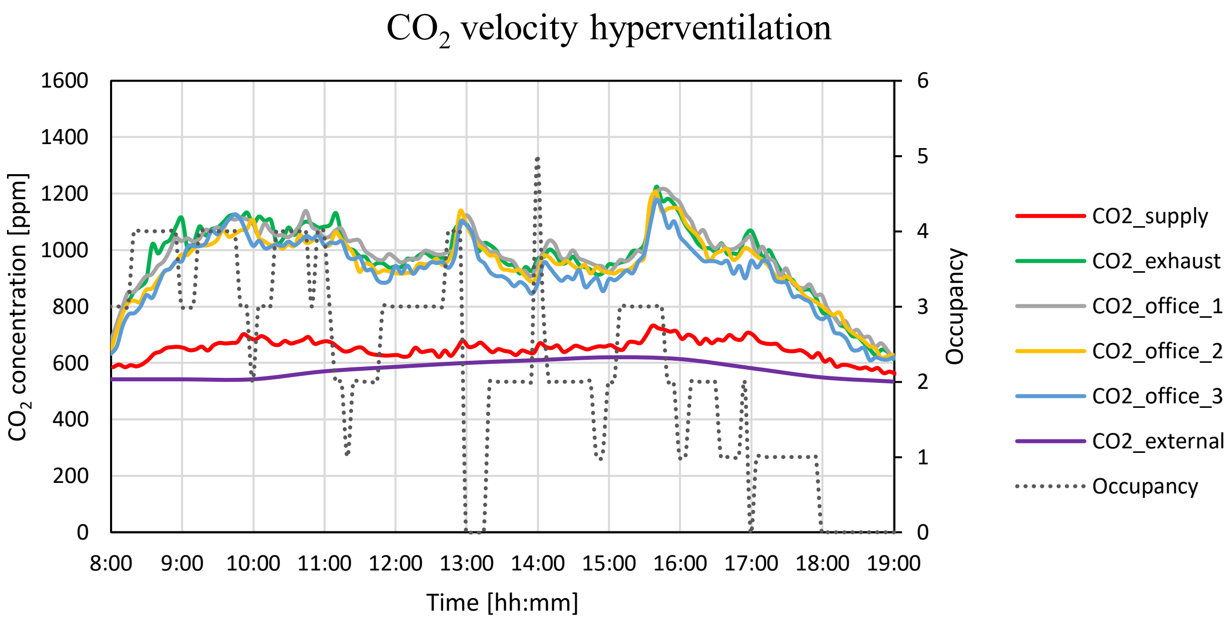

Figure 4.5 – CO_2 trend with velocity hyperventilation

In principle, the peak should be higher when the ventilation is lower; however, this consideration is only true when other conditions (especially occupancy, represented by dotted line in the graphs) are equal. Indeed, at velocities 2 and 3, higher peaks are attained than at velocity 1, despite greater ventilation; this is attributable to greater occupancy, which exerts a significant influence on the measured concentrations. It is also evident that with velocity 4 and hyperventilation there is a reduction in the magnitude of the peaks, which rarely exceeds 1200 ppm, values that were instead abundantly exceeded with the lower speeds.

It is interesting to observe the correlation between the trends in occupancy and the concentration within the office environment, as illustrated in Figure 4.3. During the morning hours, there is a consistent increase in both occupancy and the number of people in the office, except for the break at 10 o'clock, when the office empties and concentration drops. From 16:00, however, the occupancy rate started to fall, and at the same time the CO_2 concentration fell.

It is evident from the graphs that the values measured at the inlet are not constant throughout the day, but are influenced by the generation of CO_2 inside the office and the concentration trend in the outside environment. Theoretically this should not happen, but experimentally the results follow this observation for two main reasons: firstly, the inlet sensor was positioned a few cm outside the vent, which means that in addition to being affected by the fresh air it is also contaminated by the CO_2 present in the room. The second reason lies in the fact that the outdoor environment is not really an outdoor environment, with a concentration that fluctuates slightly during the course of the day.

Another common feature among all graphs is that the three HOBOs have similar, almost equal trends, while the value measured in the exhaust is almost always equal to or slightly higher than the trend of the three HOBOs that measure the concentration inside the office. This outcome is highly satisfactory, as it signifies that the ventilation efficiency is approximately unity and that the distribution of CO_2 across the three analysed points is nearly homogeneous.

These concepts will be addressed in more detail in the next paragraphs.

4.1.2 Results of air flow rate measurements

For each velocity there is a Table (i.e. Tables 4.1, 4.2, 4.3, 4.4 and 4.5), divided in two parts, which presents all the results. In the part *a)* there are the 3 results of the 3 different measurements conducted for each velocity, the average value between these measures, the correspondence flow rate and the resulting air change rate obtained with a certain flow rate. There are 2 rows: one referred to the measurement with the grille and one referred to the case without grille. In the part *b)* of each table the flow rate is reported both in m^3/h and in l/s. Furthermore, the flow rate in liters per second was divided by the number of people to obtain the amount of clean air per second that is delivered per person based on the number of people present (expressed in l/(s px)).

<table>
<tr><td rowspan="2">a)</td><td colspan="4">Average velocity [m/s]</td><td rowspan="2">Flow rate [m³/h]</td><td rowspan="2">Air change rate [h⁻¹]</td></tr>
<tr><td>Measure 1</td><td>Measure 2</td><td>Measure 3</td><td>Average value</td></tr>
<tr><td>With grille</td><td>2.1</td><td>2.1</td><td>2.2</td><td>2.1</td><td>44.0</td><td>0.55</td></tr>
<tr><td>Without grille</td><td>2.1</td><td>2.0</td><td>2.0</td><td>2.0</td><td>43.4</td><td>0.54</td></tr>
</table>

<table>
<tr><td rowspan="2">b)</td><td rowspan="2">Flow rate [m³/h]</td><td rowspan="2">Flow rate [l/s]</td><td colspan="5">Flow rate per person [l/(s px)]</td></tr>
<tr><td>1</td><td>2</td><td>3</td><td>4</td><td>5</td></tr>
<tr><td>With grille</td><td>44.0</td><td>12.2</td><td>12.2</td><td>6.1</td><td>4.1</td><td>3.1</td><td>2.4</td></tr>
<tr><td>Without grille</td><td>43.4</td><td>12.1</td><td>12.1</td><td>6.0</td><td>4.0</td><td>3.0</td><td>2.4</td></tr>
</table>

Table 4.1 – Flow rate measurement, velocity 1

a)	Average velocity [m/s]				**Flow rate [m³/h]**	Air change rate [h⁻¹]
	Measure 1	Measure 2	Measure 3	Average value		
With grille	3.3	3.2	3.2	3.2	**66.3**	0.83
Without grille	2.9	2.8	2.9	2.9	**61.1**	0.76

b)	Flow rate [m³/h]	Flow rate [l/s]	Flow rate per person [l/(s px)]				
			1	2	3	4	5
With grille	66.3	18.4	18.4	9.2	6.1	4.6	3.7
Without grille	61.1	17.0	17.0	8.5	5.7	4.2	3.4

Table 4.2 – Flow rate measurement, velocity 2

a)	Average velocity [m/s]				**Flow rate [m³/h]**	Air change rate [h⁻¹]
	Measure 1	Measure 2	Measure 3	Average value		
With grille	4.0	4.0	3.8	4.0	**81.2**	1.01
Without grille	3.5	3.5	3.5	3.5	**75.1**	0.93

b)	Flow rate [m³/h]	Flow rate [l/s]	Flow rate per person [l/(s px)]				
			1	2	3	4	5
With grille	81.2	22.6	22.6	11.3	7.5	5.6	4.5
Without grille	75.1	20.9	20.9	10.4	7.0	5.2	4.2

Table 4.3 – Flow rate measurement, velocity 3

a)	Average velocity [m/s]				**Flow rate [m^3/h]**	Air change rate [h^{-1}]
	Measure 1	Measure 2	Measure 3	Average value		
With grille	6.0	5.8	5.7	5.8	**118.9**	1.48
Without grille	5.3	5.2	5.1	5.2	**111.5**	1.39

b)	Flow rate [m^3/h]	Flow rate [l/s]	Flow rate per person [l/(s px)]				
			1	2	3	4	5
With grille	118.9	33.0	33.0	16.5	11.0	8.3	6.6
Without grille	111.5	31.0	31.0	15.5	10.3	7.7	6.2

Table 4.4 – Flow rate measurement, velocity 4

a)	Average velocity [m/s]				**Flow rate [m^3/h]**	Air change rate [h^{-1}]
	Measure 1	Measure 2	Measure 3	Average value		
With grille	6.9	6.5	6.6	6.6	**136.4**	1.70
Without grille	6.3	6.2	6.4	6.3	**134.7**	1.68

b)	Flow rate [m^3/h]	Flow rate [l/s]	Flow rate per person [l/(s px)]				
			1	2	3	4	5
With grille	136.4	37.9	37.9	19.0	12.6	9.5	7.6
Without grille	134.7	37.4	37.4	18.7	12.5	9.4	7.5

Table 4.5 – Flow rate measurement, velocity hyperventilation

It's evident that the operating range under scrutiny is wide, with measurements ranging from approximately 43 m^3/h in velocity 1 to over 130 m^3/h in hyperventilation mode. At velocity 1 the measured flow rate is 43 m^3/h both with and without grille, while at velocity 2 the flow rate is equal to 66 m^3/h considering the case with the grille and it's equal to 61 m^3/h without. A similar pattern is evident at speeds 3 and 4: at velocity 3 the flow rate is 81 m^3/h with the grille and 76 m^3/h without it, at velocity 4 the flow rate is 119 m^3/h with the grille and 112 m^3/h without. Conversely, in the hyperventilation mode, the two measured flow rates are very similar: 136 m^3/h and 135 m^3/h respectively.

As illustrated in the tables above, the number of air changes per hour for each flow rate is directly linked to the volume of the room, which is approximately 80 m^3. The range of values is from 0.55 h^{-1} at speed 1 to a maximum of approximately 1.7 h^{-1} with hyperventilation. The variation in flow rate between one speed and the next is relevant, particularly between speed 3 and speed 4 the largest delta is measured. Conversely, the least significant increase in flow rate is recorded between speeds 2 and 3.

The second table of each speed, on the other hand, is interesting to understand whether a given flow rate is suitable for a certain number of people. As explained in Table 1.4 in the introduction, to guarantee at least IAQ class II, a minimum of 7 l/s per person must be provided. Velocity 1 can only guarantee a flow rate of more than 7 l/s per person for an occupancy of one person, velocity 2 manages to do the same with an occupancy of 2 people, and so on: as one speed increases, the machine manages to cover the increase of one person.

The passage area is different between the case with a grid and the case without a grid. In the case with a grid, the thickness of the various fins present was subtracted to the total surface, in order to justify how large differences in velocity between the two cases result in smaller differences in terms of flow rate and air change rate.

The disparities in values observed among the three tests conducted at an equivalent velocity, and among the cases with and without the grille can be ascribed to the imperfect execution of the measurement process. Inaccuracies, for instance, may have occurred in the displacement of the sensor along the section, both in terms of duration and movement between the points of the matrix used as a reference

4.2 Results of experimental data analysis

4.2.1 CO_2 distribution and standard deviation

To study the homogeneity of the concentration within the room, the standard deviation between the values measured by the three HOBO sensors in each measurement was calculated. The standard deviation is presented in both numerical and percentage form in comparison to the mean value in each table, and the results of both measurements are provided for each velocity. The timeline analysed is related to the office occupation periods: namely from 8:00 to 12:45 and from 14:00 to 17:00. The results are presented in Table 4.6 and subsequent tables.

Standard deviation velocity 1				
Time	Average value measure 1		Average value measure 2	
	Numerical form	Percentage	Numerical form	Percentage
8:00-12:45	25.8	2.5%	32.6	2.5%
14:00-17:00	25.1	2.0%	42.6	3.7%
8:00-12:45; 14:00-17:00	25.5	2.3%	36.5	3.0%

Table 4.6 – Standard deviation, velocity 1

Standard deviation velocity 2				
Time	Average value measure 1		Average value measure 2	
	Numerical form	Percentage	Numerical form	Percentage
8:00-12:45	51.0	4.5%	25.3	2.6%
14:00-17:00	38.8	3.6%	42.6	3.5%
8:00-12:45; 14:00-17:00	46.3	4.1%	32.0	2.9%

Table 4.7 – Standard deviation, velocity 2

Standard deviation velocity 3				
Time	Average value measure 1		Average value measure 2	
	Numerical form	Percentage	Numerical form	Percentage
8:00-12:45	35.3	3.2%	22.7	2.7%
14:00-17:00	41.3	3.2%	19.5	2.1%
8:00-12:45; 14:00-17:00	37.6	3.2%	21.5	2.4%

Table 4.8 – Standard deviation, velocity 3

Standard deviation velocity 4				
Time	Average value measure 1		Average value measure 2	
	Numerical form	Percentage	Numerical form	Percentage
8:00-12:45	29.6	2.8%	26.7	2.8%
14:00-17:00	25.1	2.4%	28.6	2.9%
8:00-12:45; 14:00-17:00	27.9	2.7%	27.4	2.9%

Table 4.9 – Standard deviation, velocity 4

Standard deviation velocity hyperventilation				
Time	Average value measure 1		Average value measure 2	
	Numerical form	Percentage	Numerical form	Percentage
8:00-12:45	29.3	3.1%	32.2	3.2%
14:00-17:00	37.6	3.8%	25.6	2.6%
8:00-12:45; 14:00-17:00	32.5	3.3%	29.6	3.0%

Table 4.10 – Standard deviation velocity, hyperventilation

The mean value, expressed as a percentage, is consistently below 5%, which is a satisfactory outcome. This finding indicates that the three sensors are measuring values that are closely aligned, proving optimal mixing at the points of interest, i.e. the desks. This outcome is particularly encouraging, as it suggests that the installed machine in this office, operating under these specific conditions, guarantees a consistent air exchange between the various occupancy positions.

It is also interesting to note the absence of stratification in the CO_2 concentration. This is relevant because it means that the measured concentration values are not influenced by height (indicated by Z in Figure 4.6), and therefore there is no pollutant accumulation at the top of the room Therefore, the measured values at the extraction are only influenced by the ventilation, and not by the height. As demonstrated in Figure 4.6, the sensor positioned at 0.8 m and the one positioned at 2 m exhibited a similar trend during the occupancy periods, with no significant difference in concentration due to stratification.

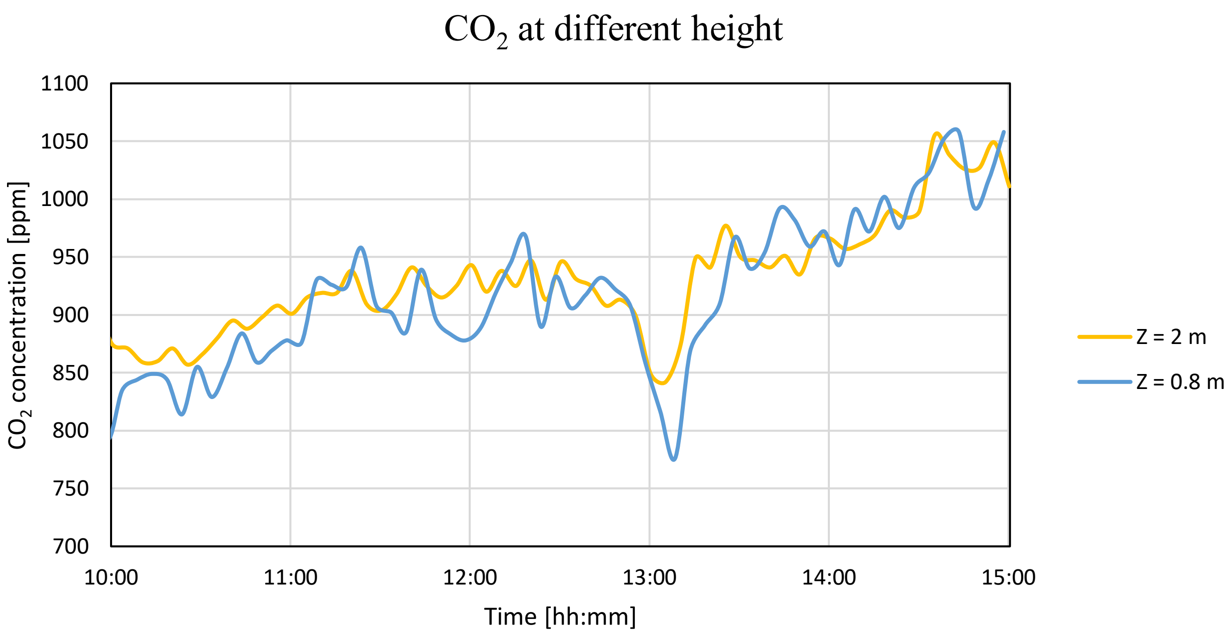

Figure 4.6 – CO_2 profiles at different height

4.2.2 IAQ and occupancy analysis

This paragraph provides a comprehensive overview of the temporal distribution of CO_2 levels and the occupancy levels across the various measurements.

In the Figure 4.7 *(a)*, the distribution of speeds across the various classes is evident. By examining each individual column, it is possible to ascertain the percentage of time that each speed has been allocated to a specific IAQ class. On the other hand, the Figure 4.7 *(b)* provides a comprehensive representation of the variability in occupancy levels across the various measurement periods, which allows for a greater understanding of the measurements and the results obtained.

Measure 1

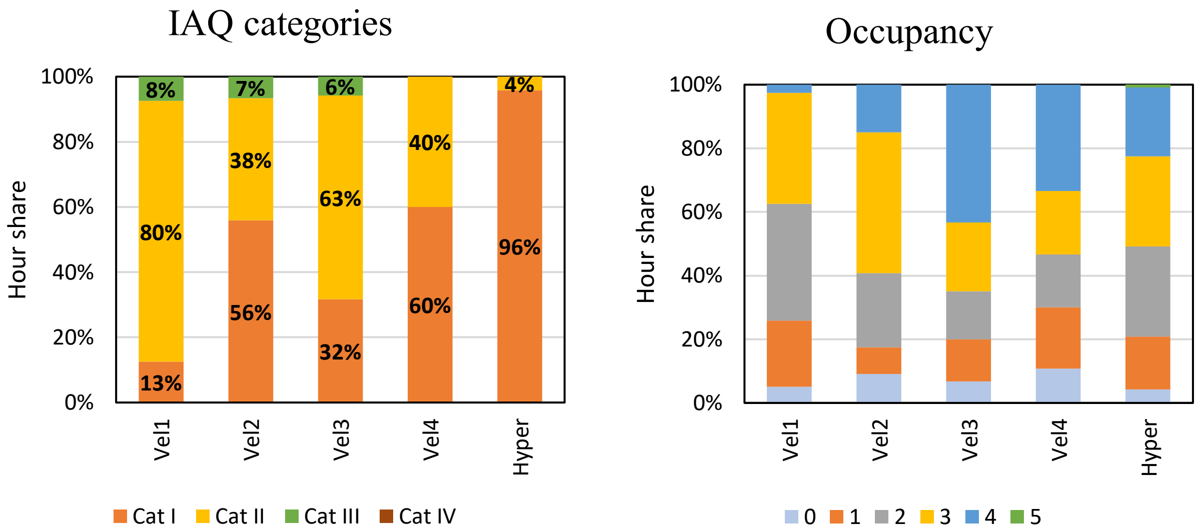

a) *b)*

Figure 4.7 – IAQ categories *(a)* and occupancy expressed in number of people *(b)*, measure 1

These results indicate that the machine is suitable for this office, and, more generally, for an office of a similar size and with an occupancy of up to four people. It is evident that, in most cases, the carbon dioxide concentration corresponds to class I or class II. A further aspect of this experimental test is that the presence of four individuals was observed to be infrequent at speeds 1 and 2, with a more stable occupancy between two and three persons, this justifies the low percentage of time at class III also at the lowest flow rates.

During the hyperventilation mode, despite the presence of 3 or 4 people in the room for approximately half of the time, the IAQ class I was ensured almost the entire time thanks to a significant supply of clean air.

Measure 2

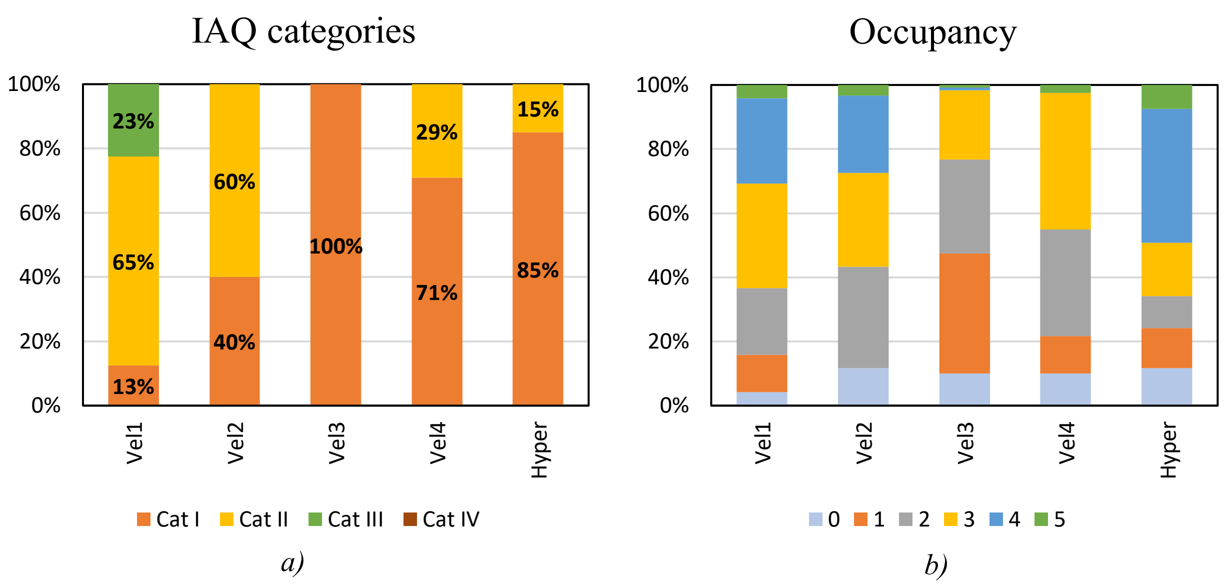

Figure 4.8 – IAQ categories *(a)* and occupancy expressed in number of people *(b)*, measure 2

In the second measurement, it is evident that at velocity 1, there was greater occupancy than in measurement 1, with a higher percentage of time involving four or five people. Consequently, Figure 4.8 demonstrates that at speed 1, there is an elevated proportion of class III, signifying that velocity 1 is inadequate when the number of people increases. A further distinction emerges at velocity 3, where the percentage of time spent with two and three people was higher than in trial 1, and periods with four people were even absent. Consequently, the data demonstrates that 100% of the time falls within class I, indicating a high level of control over the CO_2 concentration.

It is evident from the results that the machine's multiple speeds are well-suited to such levels of occupancy. The speed, which is easily adjustable, can be modified in accordance with the number of occupants present, ranging from speed 1 when there is only one person in the office to hyperventilation mode when the office is full. This capacity to modulate the ventilation rate facilitates the regulation of the CO_2 concentration, ensuring a comfortable environment for the occupants.

4.2.3 Results of ventilation effectiveness

The ventilation effectiveness is calculated over the course of the entire day; however, the period of interest for the study is during the office's occupancy period. The analysed timeline extends from 9:00 to 12:45 and from 14:00 to 17:00, with the lunch break spanning from 12:45 to 14:00. The office starts to fill up just before 8:00, but between 8:00 and 9:00 the differences in ppm concentration between the extraction value, the room average and the inlet value are small, so the efficiency has insignificant peaks which tend to flatten out soon after. At the end of the day, the office almost always empties between 17:00 and 18:00, however, to ensure uniformity in the results, the ventilation efficiency was calculated from 9:00 up to 17:00. This provides a consistent reference point, independent of individual cases. When the office is emptied, the three quantities in the formula (average concentration in the room, inlet concentration and exhaust concentration) take on values that are very close to each other, as in the early morning. This means that deviations of a few ppm can cause the ventilation efficiency to fluctuate between values of several units to even negative values. As a result, this parameter is of little use and interest. This is the reason behind the presentation of average values for the morning, afternoon, and entire working day (combining morning and afternoon) in this thesis.

Each speed is represented in two forms: firstly, as a graph (see Figures 4.9 – 4.13), and secondly, as a table (see Table 4.11 – 4.15). The graphs illustrate the efficiency trend during the day, while the tables present the average values at different times of the day and throughout the day. Each table presents the results of both measurements conducted for each speed, while the graphs illustrate only the trend of the first measurement. The graph of the second measurement can be found in the Appendix C.

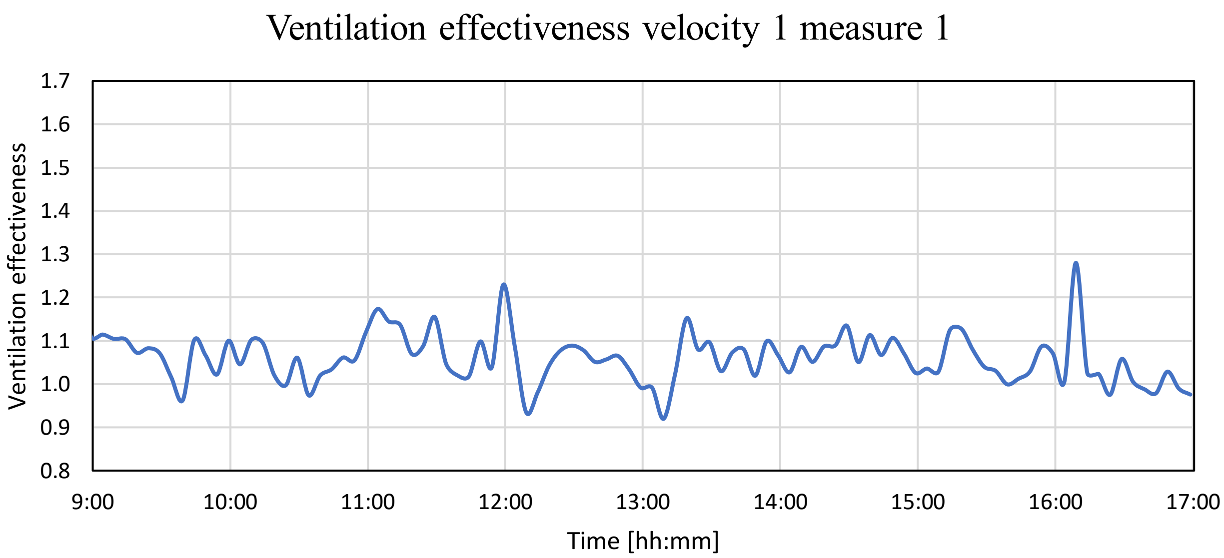

Figure 4.9 – Ventilation effectiveness, velocity 1

Ventilation effectiveness velocity 1		
Time	Average value measure 1	Average value measure 2
9:00-12:45	1.07 ± 0.13	1.02 ± 0.16
14:00-17:00	1.06 ± 0.13	1.08 ± 0.16
9:00-12:45; 14:00-17:00	1.06 ± 0.13	1.05 ± 0.16

Table 4.11 – Ventilation effectiveness with uncertainty, velocity 1

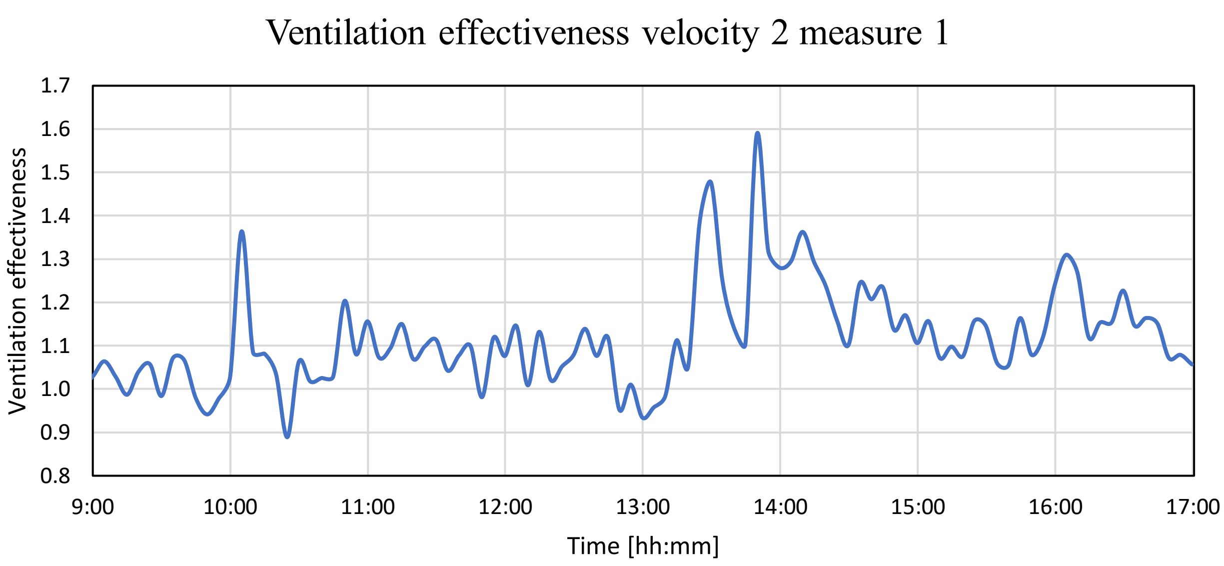

Figure 4.10 – Ventilation effectiveness, velocity 2

Ventilation effectiveness velocity 2		
Time	Average value measure 1	Average value measure 2
9:00-12:45	1.06 ± 0.15	1.14 ± 0.19
14:00-17:00	1.14 ± 0.15	1.18 ± 0.19
9:00-12:45; 14:00-17:00	1.10 ± 0.15	1.16 ± 0.19

Table 4.12 – Ventilation effectiveness with uncertainty, velocity 2

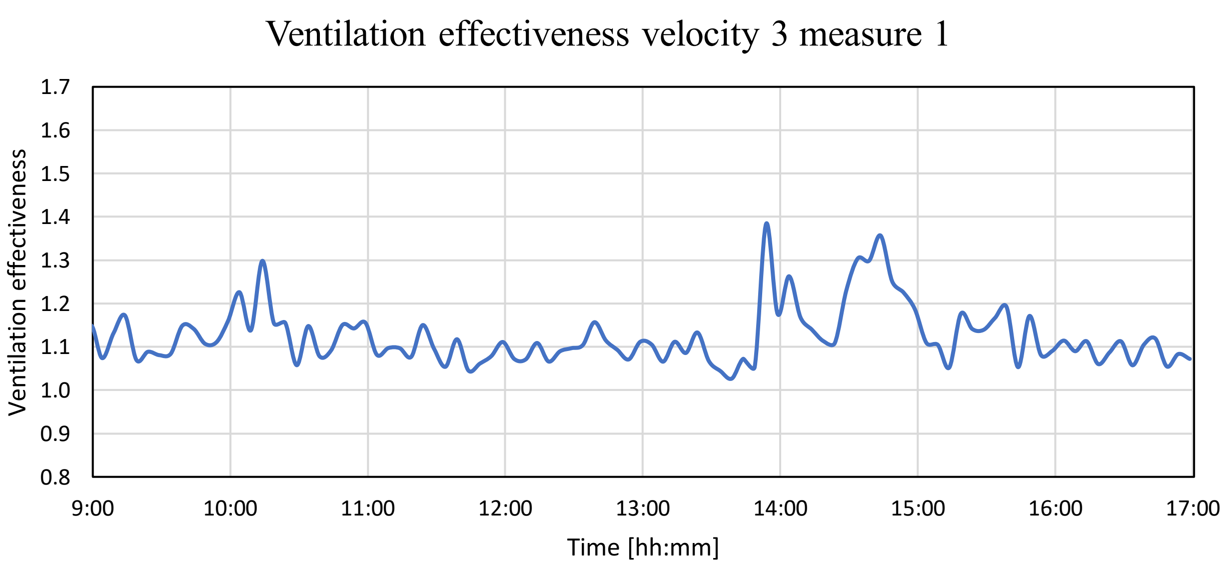

Figure 4.11 – Ventilation effectiveness, velocity 3

Ventilation effectiveness velocity 3		
Time	Average value measure 1	Average value measure 2
9:00-12:45	1.11 ± 0.13	1.07 ± 0.21
14:00-17:00	1.15 ± 0.13	1.12 ± 0.21
9:00-12:45; 14:00-17:00	1.12 ± 0.13	1.10 ± 0.21

Table 4.13 – Ventilation effectiveness with uncertainty, velocity 3

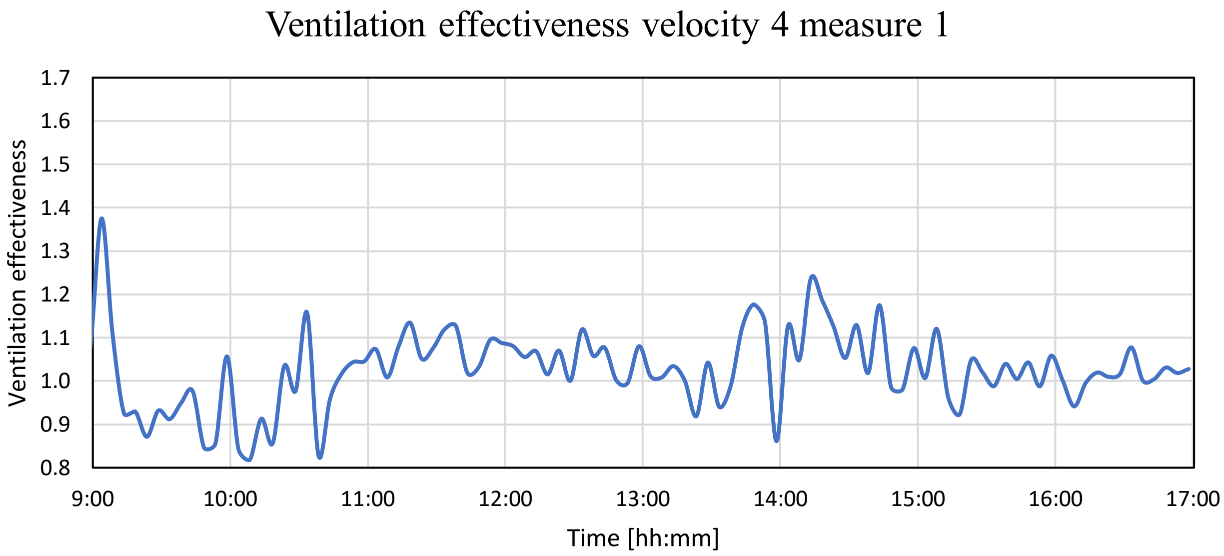

Figure 4.12 – Ventilation effectiveness, velocity 4

Ventilation effectiveness velocity 4		
Time	Average value measure 1	Average value measure 2
9:00-12:45	1.02 ± 0.19	1.00 ± 0.21
14:00-17:00	1.04 ± 0.19	1.04 ± 0.21
9:00-12:45; 14:00-17:00	1.03 ± 0.19	1.02 ± 0.21

Table 4.14 – Ventilation effectiveness with uncertainty, velocity 4

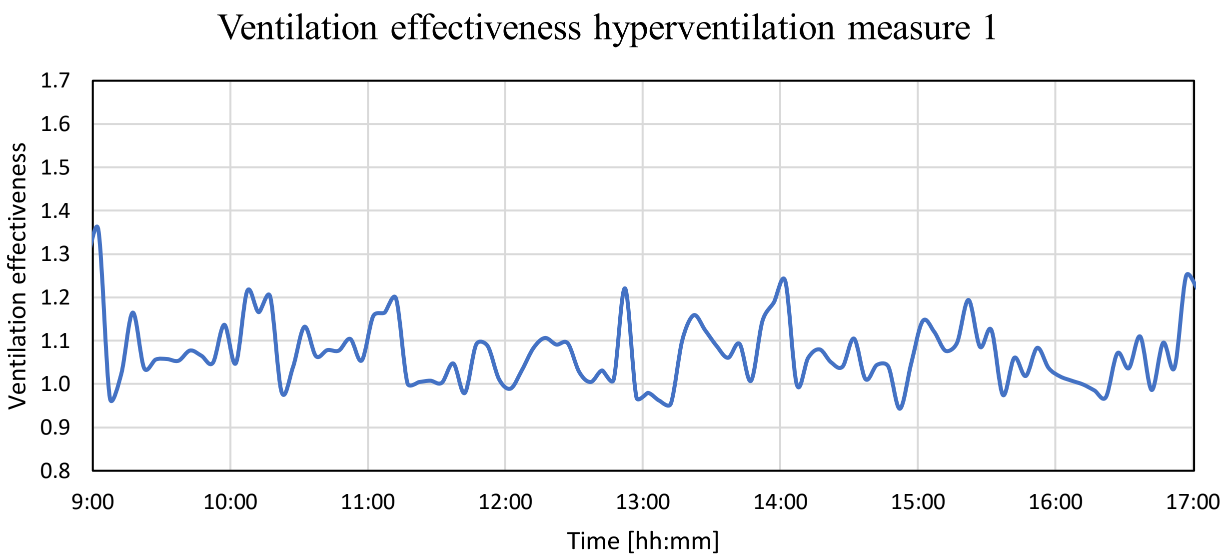

Figure 4.13 – Ventilation effectiveness, velocity hyperventilation

Ventilation effectiveness hyperventilation		
Time	Average value measure 1	Average value measure 2
9:00-12:45	1.08 ± 0.21	1.11 ± 0.21
14:00-17:00	1.06 ± 0.21	1.11 ± 0.21
9:00-12:45; 14:00-17:00	1.07 ± 0.21	1.11 ± 0.21

Table 4.15 – Ventilation effectiveness with uncertainty, velocity hyperventilation

As demonstrated in figures and tables above, the ventilation efficiency is consistently close to 1, with mean values frequently exceeding unity. This efficiency is equivalent to 1 in the context of perfect mixing, where the concentration at all points in the room is uniform, particularly the CO_2 concentration at the outlet is equivalent to the mean concentration within the room. However, when the value exceeds 1, it indicates that the outlet concentration exceeds the three HOBO measurements. This outcome validates the efficacy of this decentralized ventilation system. A key critique of decentralized ventilation systems with inlet and outlet in close proximity pertains to the inability to ensure homogeneous mixing within the room. In this experimental test, however, the results demonstrate that this particular machine, under these specific conditions, exhibits excellent performance, ensuring that the concentration at extraction is consistently greater than or equal to the room's average concentration.

One potential cause of the fluctuations is the non-constant occupancy levels, which result in variations in the number of people present and, consequently, in the CO_2 generation. For instance, a slight peak may be observed shortly after a person has exited a room, leading to a decrease in CO_2 generation and, consequently, a decline in the concentration measured by the HOBO sensors before a subsequent decrease in the exhaust.

The value used to consider the indoor concentration is the average of the three HOBO sensors, but even if the value of a single sensor had been used, the results would change slightly, because the values measured by the three sensors are often close to each other, as can be seen in section 4.2.1 regarding standard deviation.

It is also crucial to highlight that the experimental findings reveal that the ventilation efficiency remains unaffected by the machine's operational speed, as the results obtained are consistent across all conditions.

4.2.4 Air change rate from the CO_2 decay

The subsequent graphs illustrate the trend of CO_2 from the moment the office was vacated until the point at which the concentration stabilised and approached the external level. Graphically, this is evident from the curve, which closely approaches the x-axis. This analysis facilitates the appreciation of how the behaviour of carbon dioxide is influenced by the supply flow rate, and consequently how varying velocities result in different decay rates. An exponential trend line (with line equation attached) can also be seen in the graph, which best represents the behaviour of the curve; the term at the exponent represents the air change rate guaranteed by that particular flow rate. In addition to the figures a table is provided, comparing the value of the air changes per hour obtained from the exponential trend with the value obtained from the calculation of the flow rates (values taken from the results in section 4.1.2). This table facilitates a comparison of the two results and serves to confirm the quality and consistency of the work undertaken.

In addition to the 5-speed graphs, the CO_2 decay trend with the ventilation off is also visible (Figures 4.14-4.19). It is evident that CO_2 decay is more protracted in the absence of ventilation, with infiltration constituting the sole source of air exchange. The air change rate at the exponent of the curve equation, in this case, represents the air exchange due to infiltrations into the room (e.g. from doors and windows separating the office from other rooms) and it's equal to 0.14 h^{-1}, it's a fairly significant value and the reason may be either infiltrations or an exponential curve that does not perfectly represent the CO_2 curve.

For the understanding the figures, the time on the x-axis corresponds to the hours passed since the office was emptied (e.g. the value 1 corresponds to 1 hour that has passed since the office was emptied and therefore since the start of the measurement).

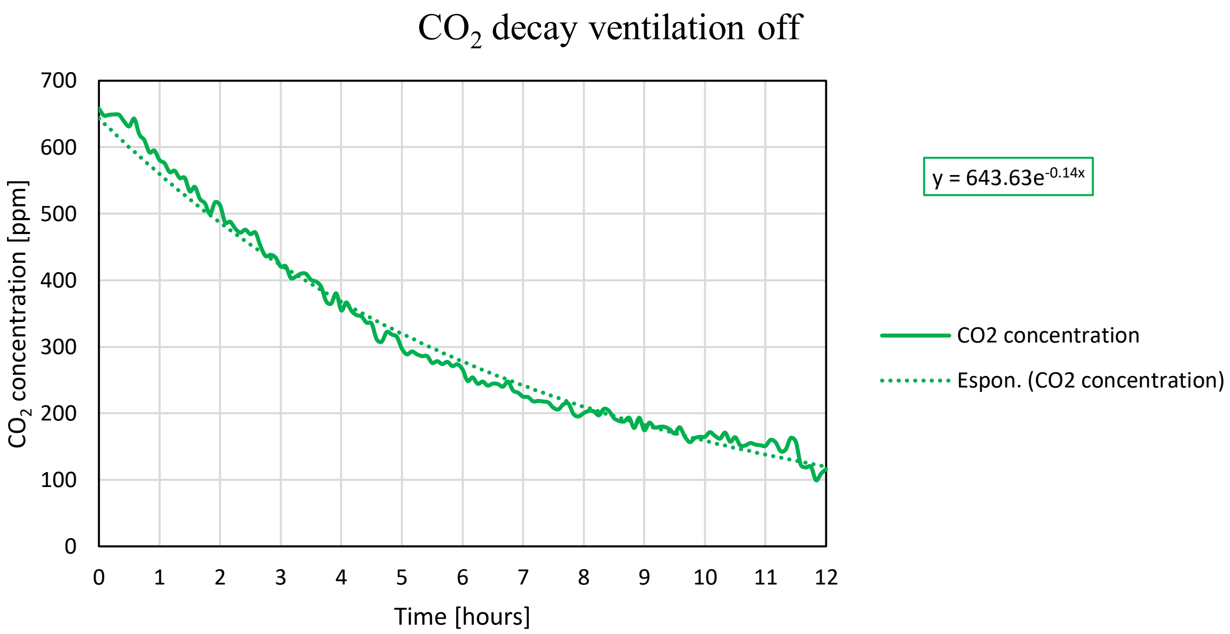

Figure 4.14 – CO_2 decay, ventilation off

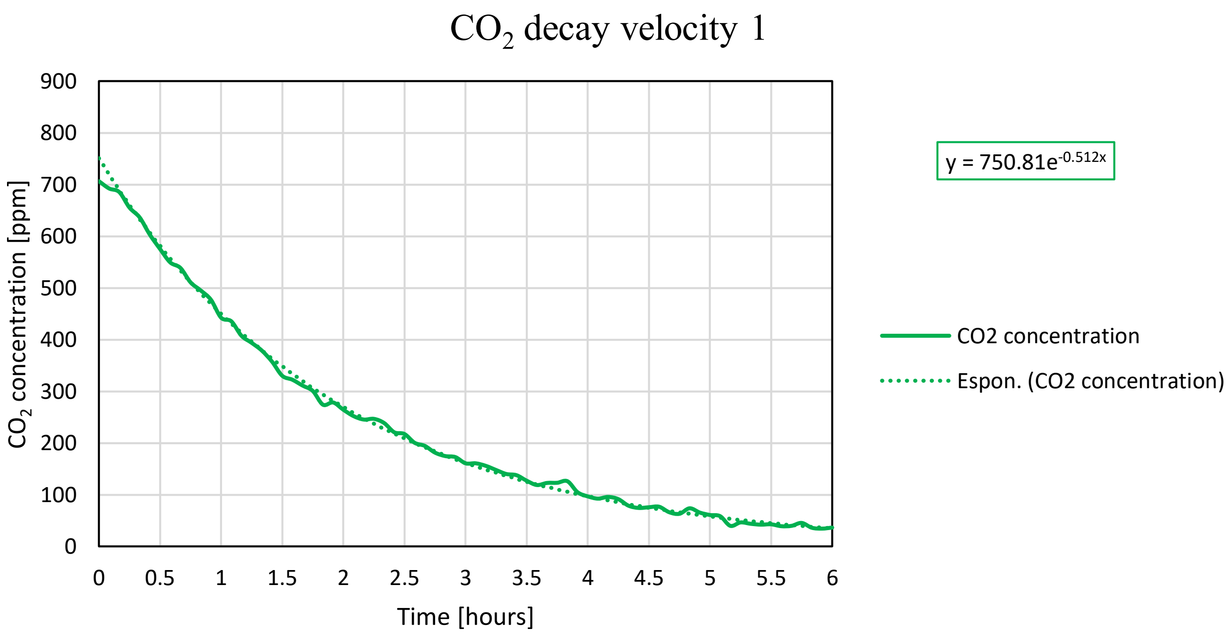

Figure 4.15 – CO_2 decay, velocity 1

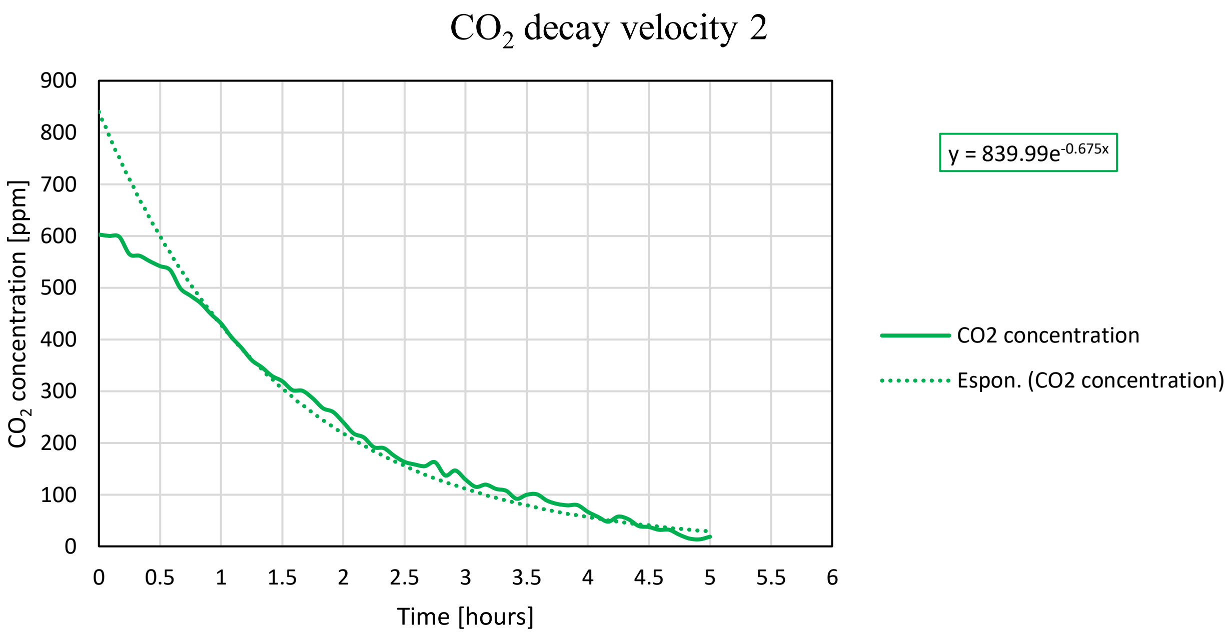

Figure 4.16 – CO_2 decay, velocity 2

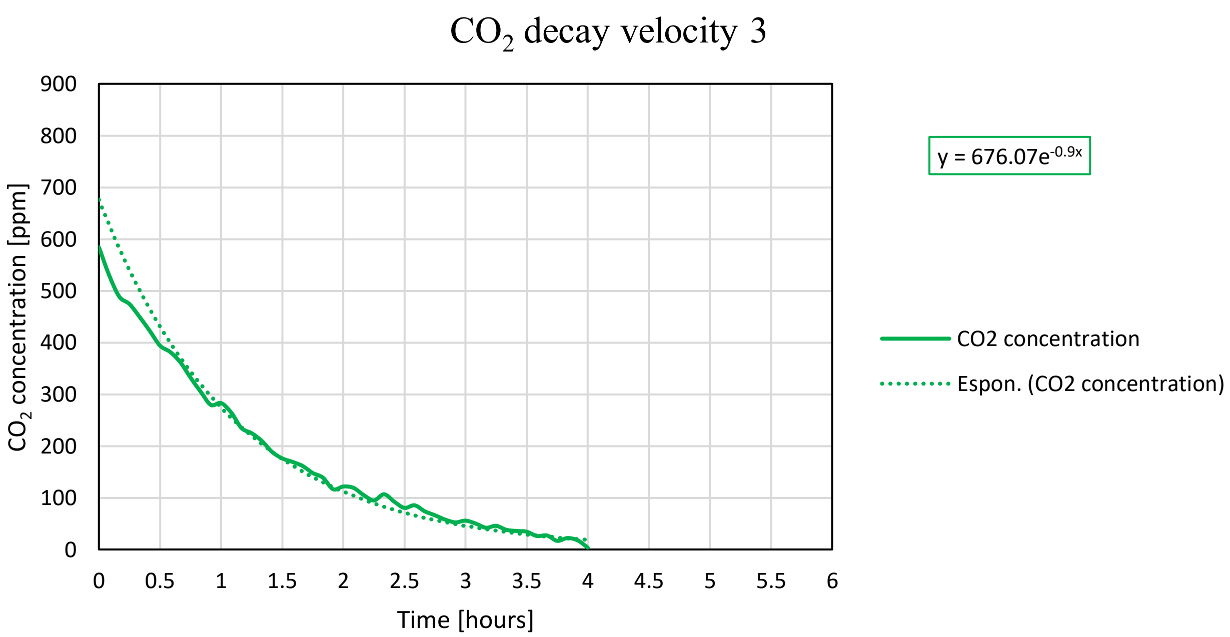

Figure 4.17 – CO_2 decay, velocity 3

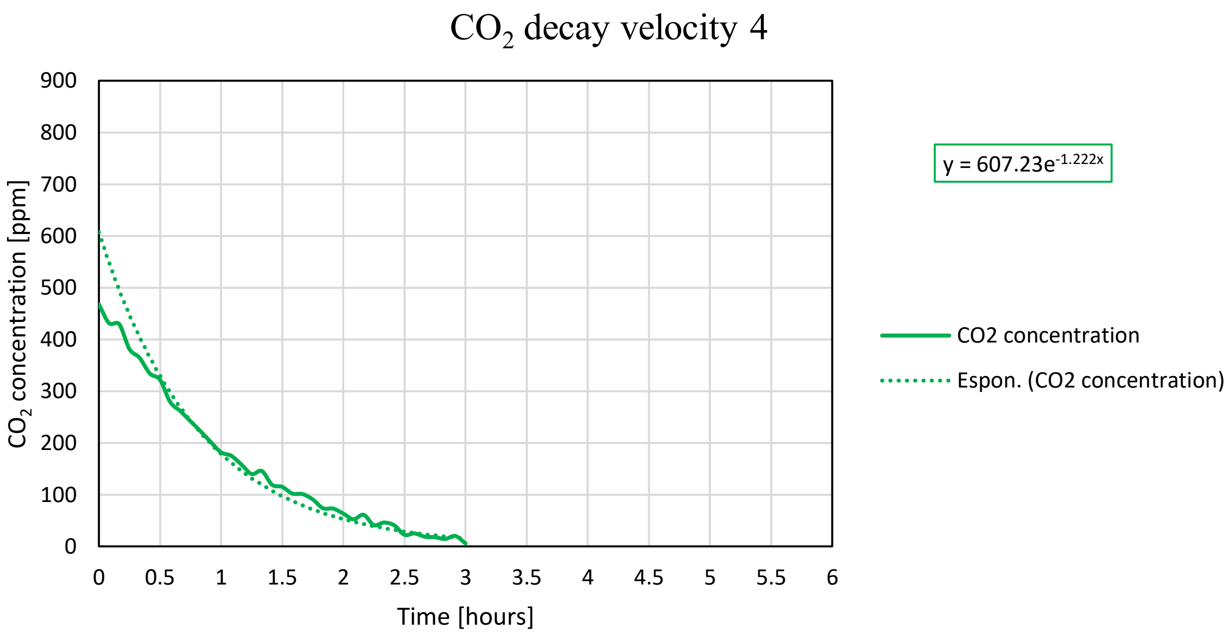

Figure 4.18 – CO_2 decay, velocity 4

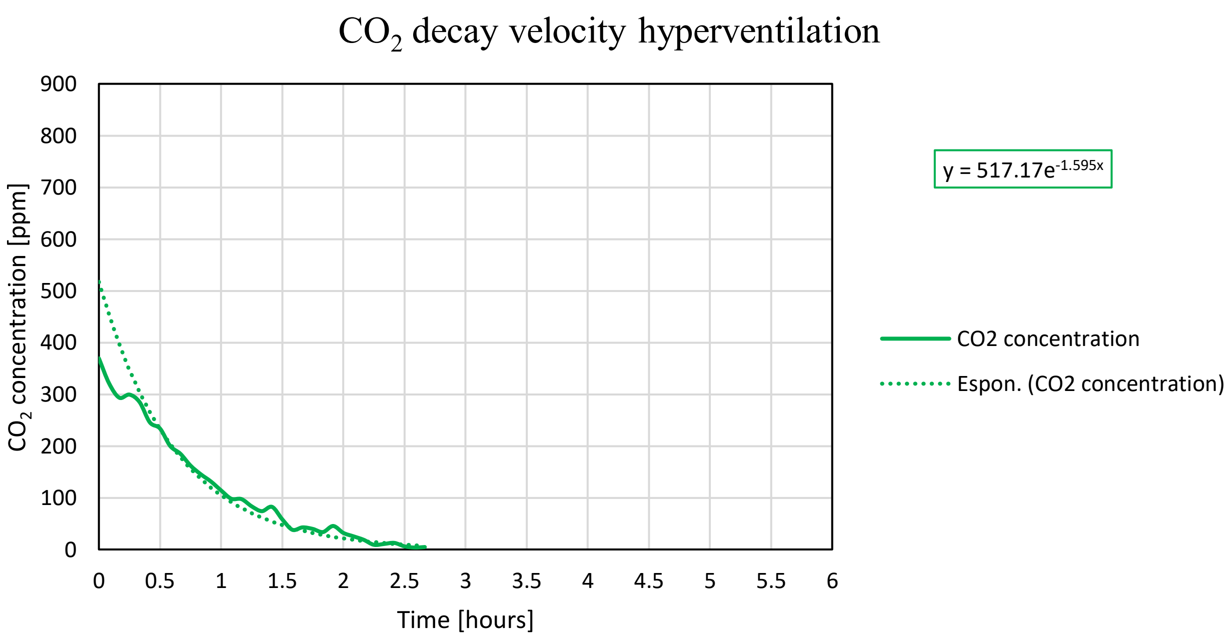

Figure 4.19 – CO_2 decay, velocity hyperventilation

	Air change rate n		
Velocity	From measured flow rates (grille)	From measured flow rates (no grille)	From exponential trend
Velocity 1	0.55	0.54	0.51
Velocity 2	0.83	0.76	0.68
Velocity 3	1.01	0.93	0.90
Velocity 4	1.48	1.39	1.22
Hyperventilation	1.70	1.68	1.60

Table 4.16 – Comparison between measured and calculated flow rates

The correlation between the air change rate values obtained from the flow rate measurements and those obtained from the CO_2 exponential decreasing trend has been observed, in particular the flow rates without the grille exhibit a strong correlation with the calculated values. This outcome serves to confirm the good results of the flow rate measurements.

4.3 Results of CFD analysis

In this section, the results of CFD simulations will be analysed, with a comparison between these results and the results of the measurements.

4.3.1 Assessment of CO_2 emission per person

As previously mentioned, the source condition value that was selected corresponds to 4 ppm/s per person. Figure 4.20 and 4.21 illustrate a comparison between the trend obtained from the theoretical model (based on Equation 12, "theoretical value" in the figures, dotted line) and that obtained from the simulations ("room simulation", continuous line). The x-axis of the graph represents the time in minutes that has elapsed since the start of the simulation, while the y-axis is calibrated to represent the concentration in ppm. Regarding the simulation, the value employed corresponds to the average concentration in the entire volume of the room.

Example 1

Boundary conditions				
Supply flow rate [m3/h]	External concentration [ppm]	Initial concentration [ppm]	Number of people	Time analysed [minutes]
43	697	1104	2	50

Table 4.17 – Boundary conditions, example 1

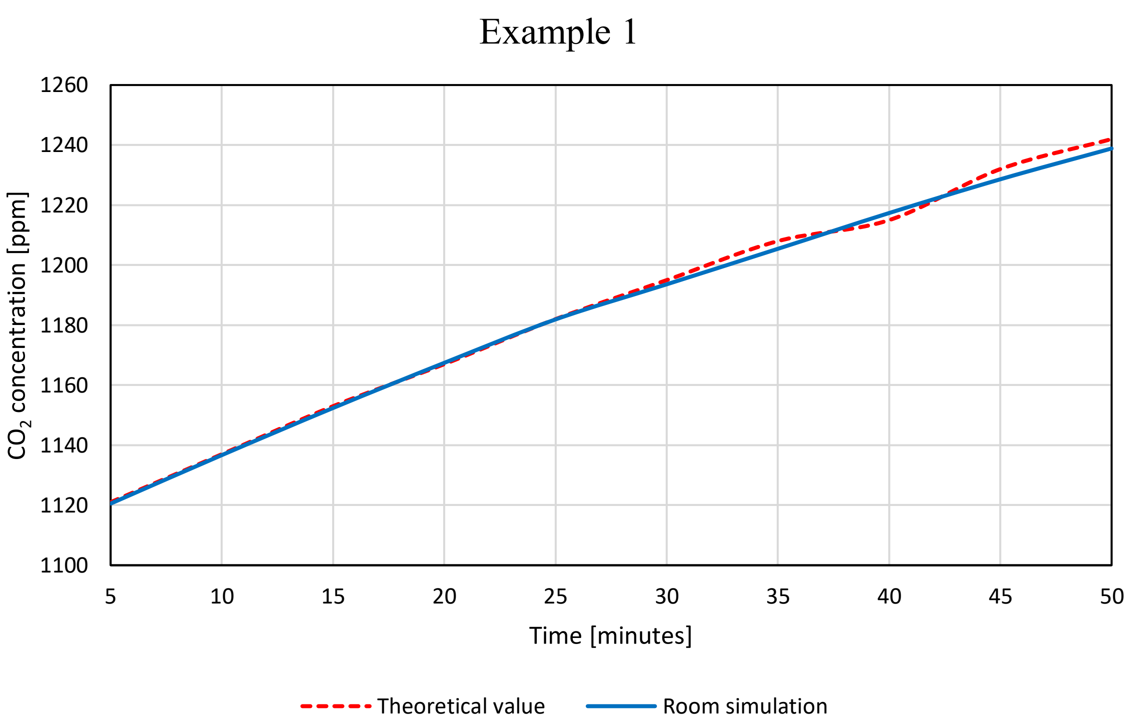

Figure 4.20 – Comparison between theoretical model and simulation, example 1

Example 2

Boundary conditions				
Supply flow rate [m3/h]	External concentration [ppm]	Initial concentration [ppm]	Number of people	Time analysed [minutes]
81	654	104	1	60

Table 4.18 – Boundary conditions, example 2

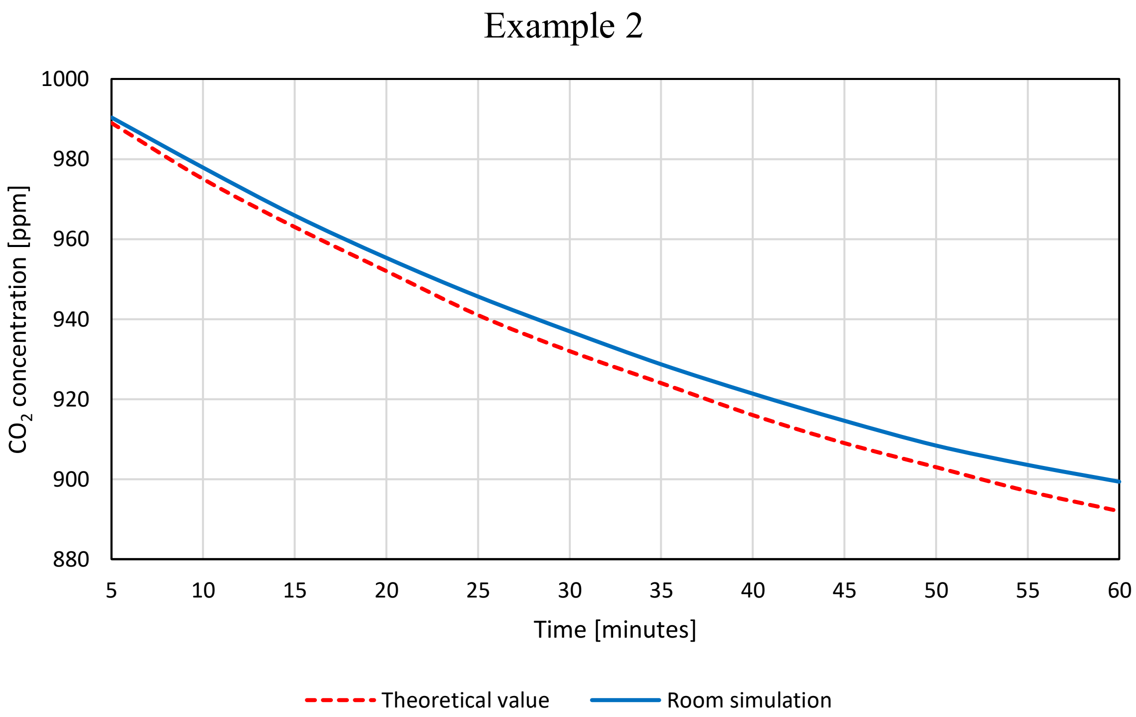

Figure 4.21 – Comparison between theoretical model and simulation, example 2

As is evident, the two curves in both cases are practically overlapping, with negligible deviation. This demonstrates that utilising 4 ppm/s within the preprocessor was an accurate decision. In the subsequent graphs, a comparison between simulation and measurement will be conducted without further analysing the comparison with the theoretical model.

4.3.2 Comparison between simulations and measurements

To compare measurements and simulations, periods with a constant occupancy over the 10 measurement days were identified, with the aim of being able to analyse a broad spectrum of case histories, including all speeds and occupancy levels, to obtain a sufficiently extensive result.

The velocities and relative occupancies that were analysed and then compared with the measurements are reported in Table 4.19. In addition, for each simulation, the velocity of the ventilation system and the number of people present in the room are reported.

Simulation number	Velocity	Number of people
1	1	1
2	1	2
3	2	2
4	2	3
5	3	1
6	3	4
7	4	1
8	4	3
9	Hyper	4

Table 4.19 – Characteristics of analysed periods in scFLOW

For each simulation, a graph is plotted comparing the trend of the average concentration measured in the room ("Room measurement") and the one measured at extraction ("Extraction measurement") with the average value obtained in scFLOW in the horizontal plane at 0.8 m ("Horizontal plane simulation") and in the surface positioned close to the extraction ("Extraction simulation"), as explained in Chapter 3, Figures 3.11 and 3.12. The x-axis shows the time in minutes, while the y-axis shows the concentration in ppm.

Regarding the analysis of ventilation effectiveness, the mean value of the effectiveness measured during the analysed period ("Measurement ventilation effectiveness" in Tables 4.21, 4.23, 4.25, 4.27, 4.29, 4.31, 4.33, 4.35 and 4.37) is compared with the mean effectiveness calculated from the simulation ("Simulation ventilation effectiveness").

Simulation 1

Boundary conditions				
Supply flow rate [m3/h]	External concentration [ppm]	Initial concentration [ppm]	Number of people	Time analysed [minutes]
43	745	1370	1	55

Table 4.20 – Boundary conditions, simulation 1

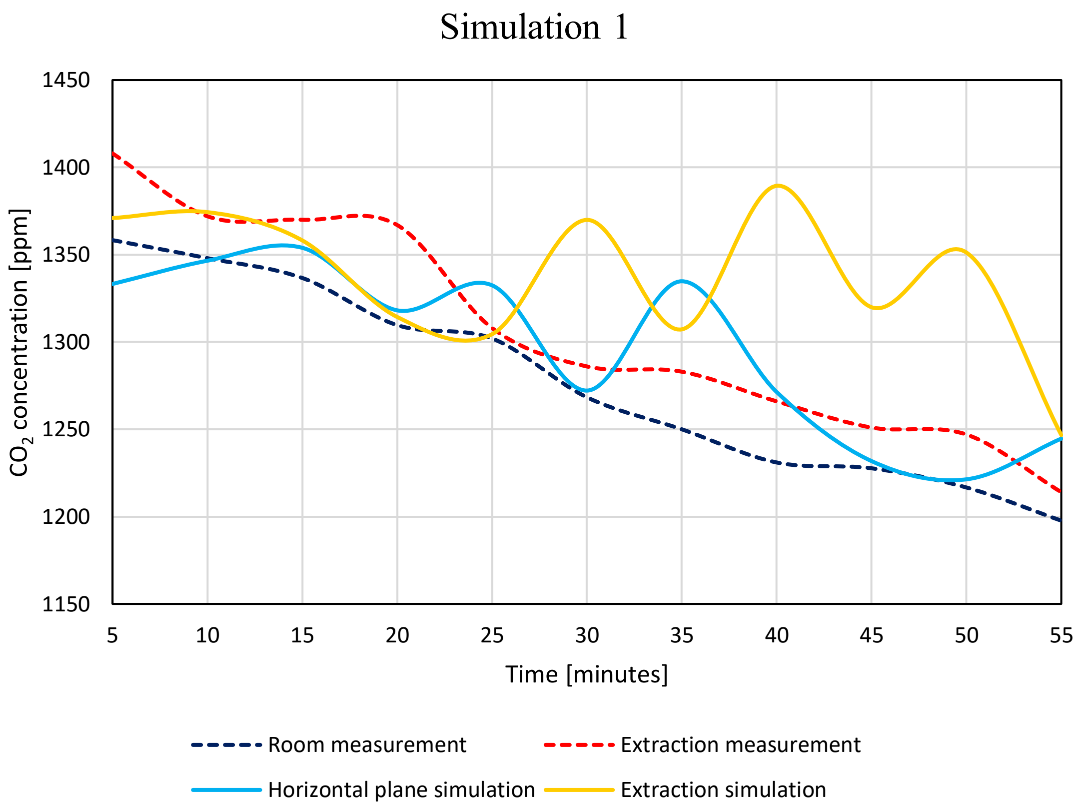

Figure 4.22 – Comparison of CO_2 concentration trend, simulation 1

Measurement ventilation effectiveness	Simulation ventilation effectiveness
1.06	1.08

Table 4.21 – Ventilation effectiveness, simulation 1

Simulation 2

Boundary conditions				
Supply flow rate [m3/h]	External concentration [ppm]	Initial concentration [ppm]	Number of people	Time analysed [minutes]
43	723	1204	2	60

Table 4.22 – Boundary conditions, simulation 2

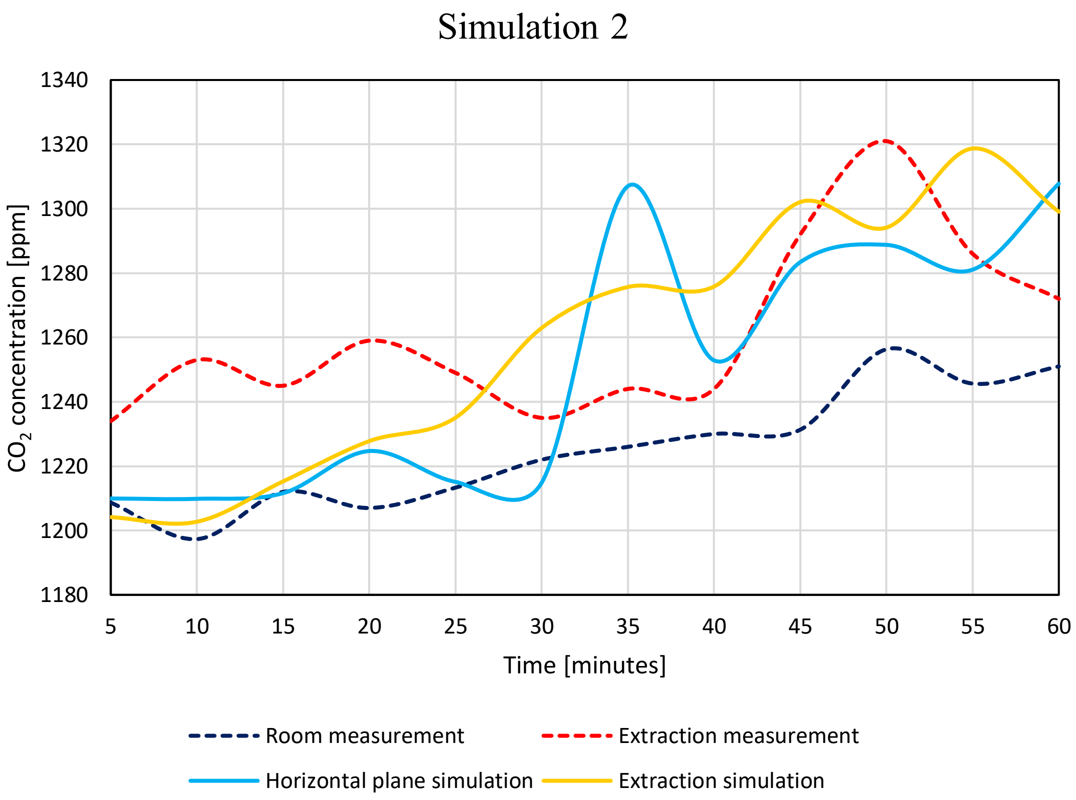

Figure 4.23 – Comparison of CO_2 concentration trend, simulation 2

Measurement ventilation effectiveness	Simulation ventilation effectiveness
1.07	1.02

Table 4.23 – Ventilation effectiveness, simulation 2

Simulation 3

Boundary conditions				
Supply flow rate [m3/h]	External concentration [ppm]	Initial concentration [ppm]	Number of people	Time analysed [minutes]
66	686	1181	2	50

Table 4.24 – Boundary conditions, simulation 3

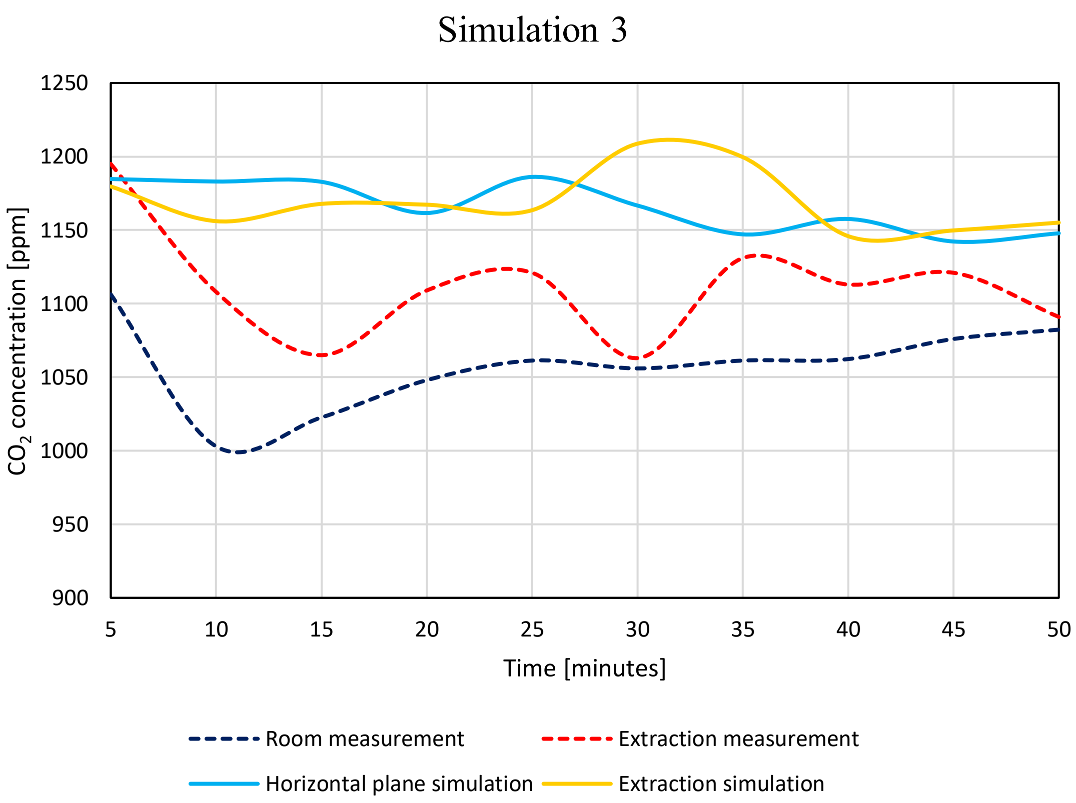

Figure 4.24 – Comparison of CO_2 concentration trend, simulation 3

Measurement ventilation effectiveness	Simulation ventilation effectiveness
1.15	1.01

Table 4.25 – Ventilation effectiveness, simulation 3

Simulation 4

Boundary conditions				
Supply flow rate [m3/h]	External concentration [ppm]	Initial concentration [ppm]	Number of people	Time analysed [minutes]
66	622	865	3	45

Table 4.26 – Boundary conditions, simulation 4

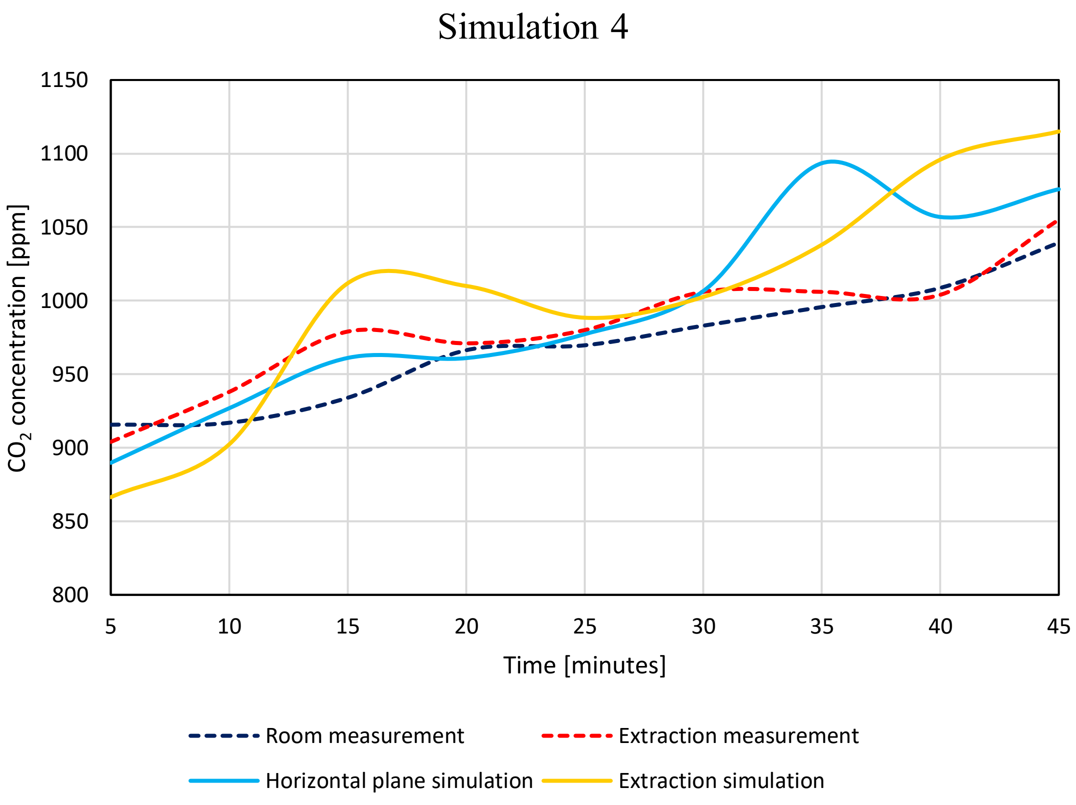

Figure 4.25 – Comparison of CO_2 concentration trend, simulation 4

Measurement ventilation effectiveness	Simulation ventilation effectiveness
1.04	1.02

Table 4.27 – Ventilation effectiveness, simulation 4

Simulation 5

Boundary conditions				
Supply flow rate [m3/h]	External concentration [ppm]	Initial concentration [ppm]	Number of people	Time analysed [minutes]
81	654	1004	1	60

Table 4.28 – Boundary conditions, simulation 5

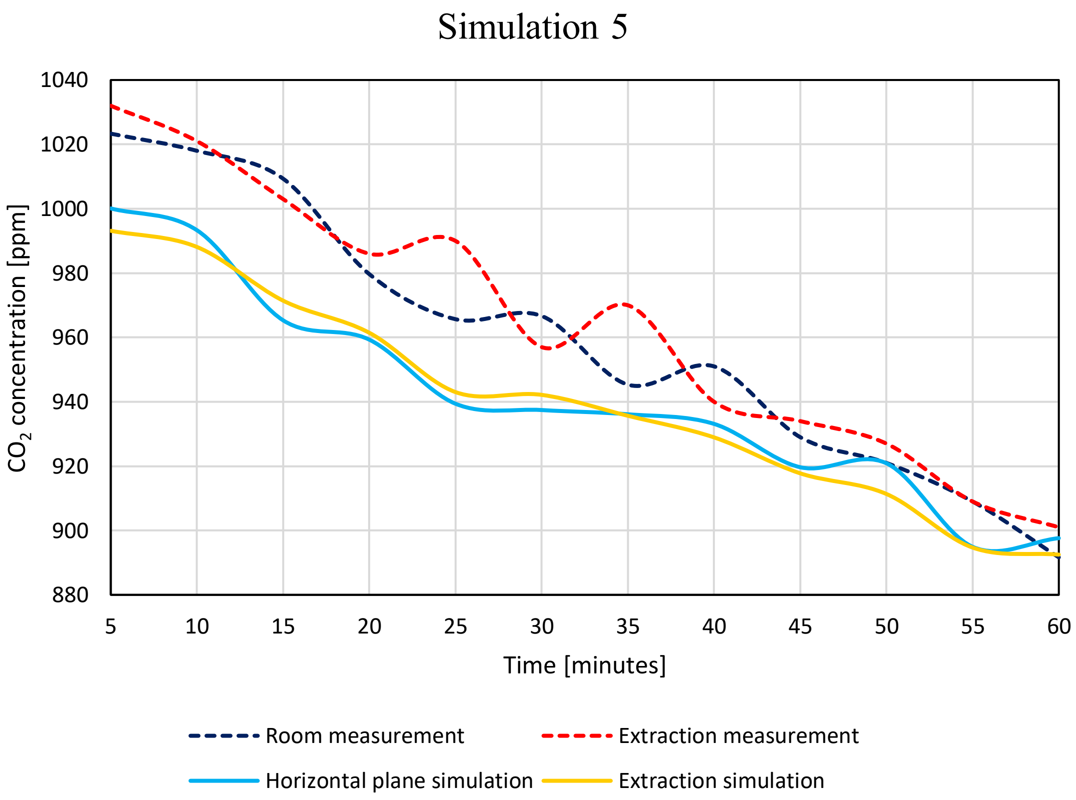

Figure 4.26 – Comparison of CO_2 concentration trend, simulation 5

Measurement ventilation effectiveness	Simulation ventilation effectiveness
1.02	0.99

Table 4.29 – Ventilation effectiveness, simulation 5

Simulation 6

Boundary conditions				
Supply flow rate [m3/h]	External concentration [ppm]	Initial concentration [ppm]	Number of people	Time analysed [minutes]
81	745	1328	4	65

Table 4.30 – Boundary conditions, simulation 6

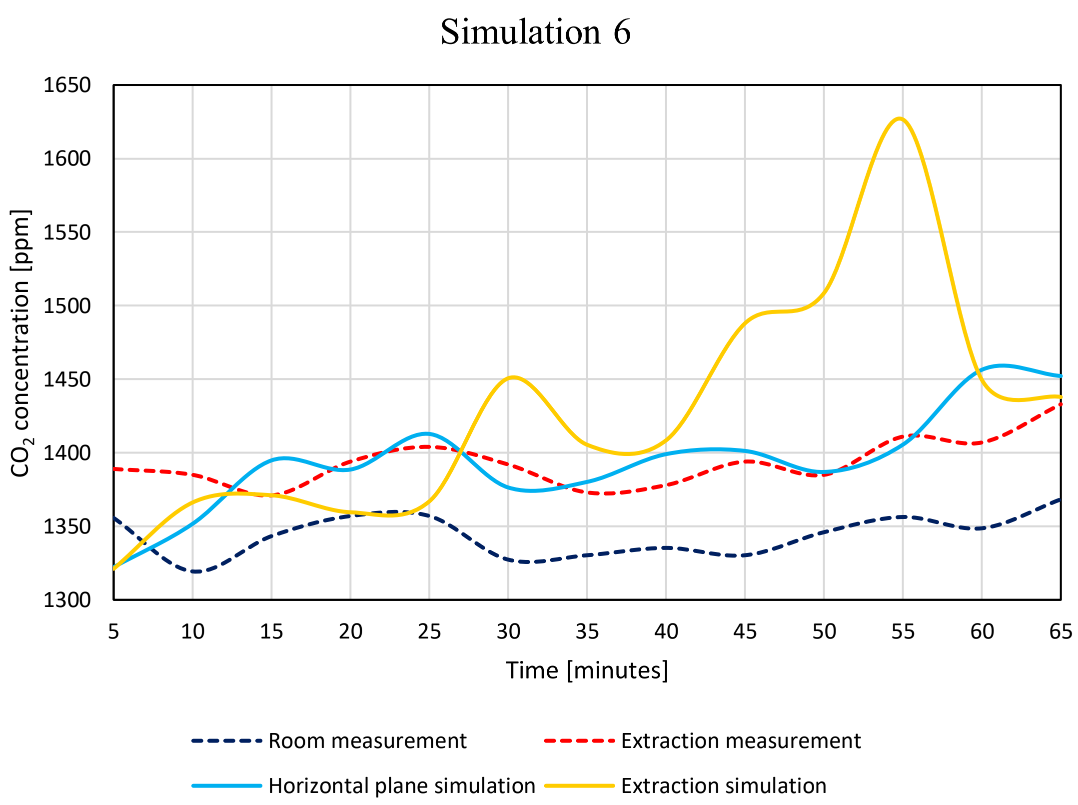

Figure 4.27 – Comparison of CO_2 concentration trend, simulation 6

Measurement ventilation effectiveness	Simulation ventilation effectiveness
1.08	1.05

Table 4.31 – Ventilation effectiveness, simulation 6

Simulation 7

Boundary conditions				
Supply flow rate [m3/h]	External concentration [ppm]	Initial concentration [ppm]	Number of people	Time analysed [minutes]
118	625	895	1	40

Table 4.32 – Boundary conditions, simulation 7

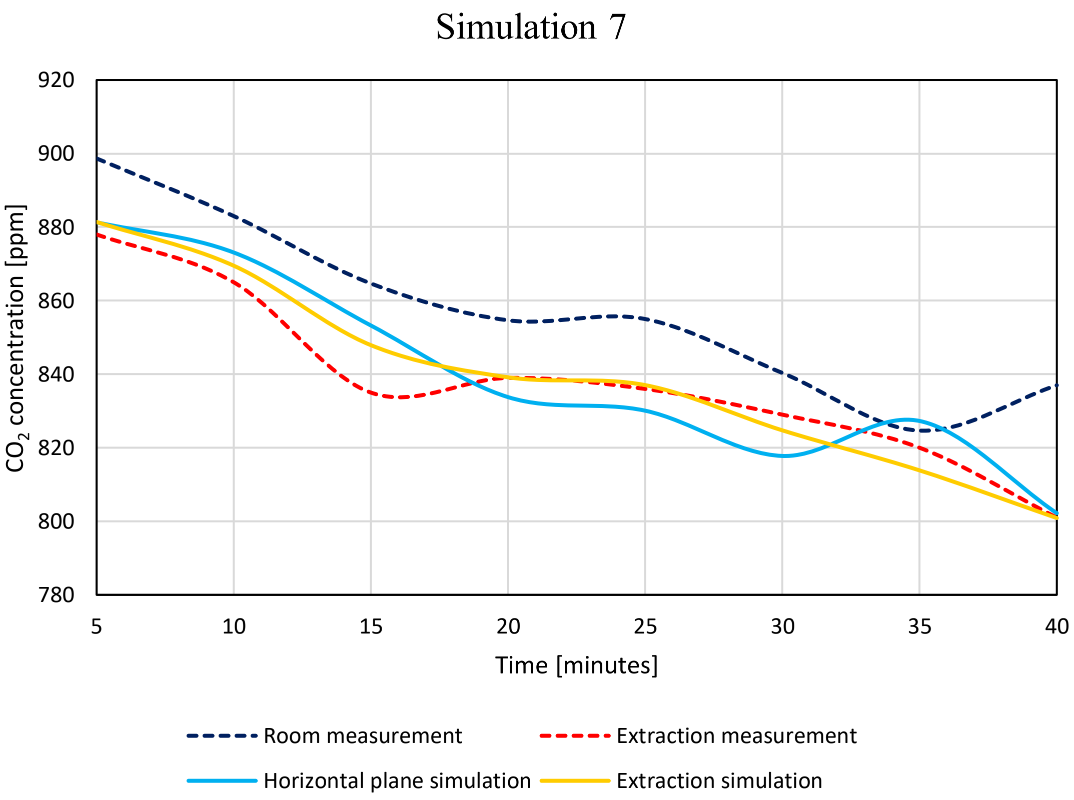

Figure 4.28 – Comparison of CO_2 concentration trend, simulation 7

Measurement ventilation effectiveness	Simulation ventilation effectiveness
0.92	1.00

Table 4.33 – Ventilation effectiveness, simulation 7

Simulation 8

Boundary conditions				
Supply flow rate [m3/h]	External concentration [ppm]	Initial concentration [ppm]	Number of people	Time analysed [minutes]
118	670	1043	3	100

Table 4.34 – Boundary conditions, simulation 8

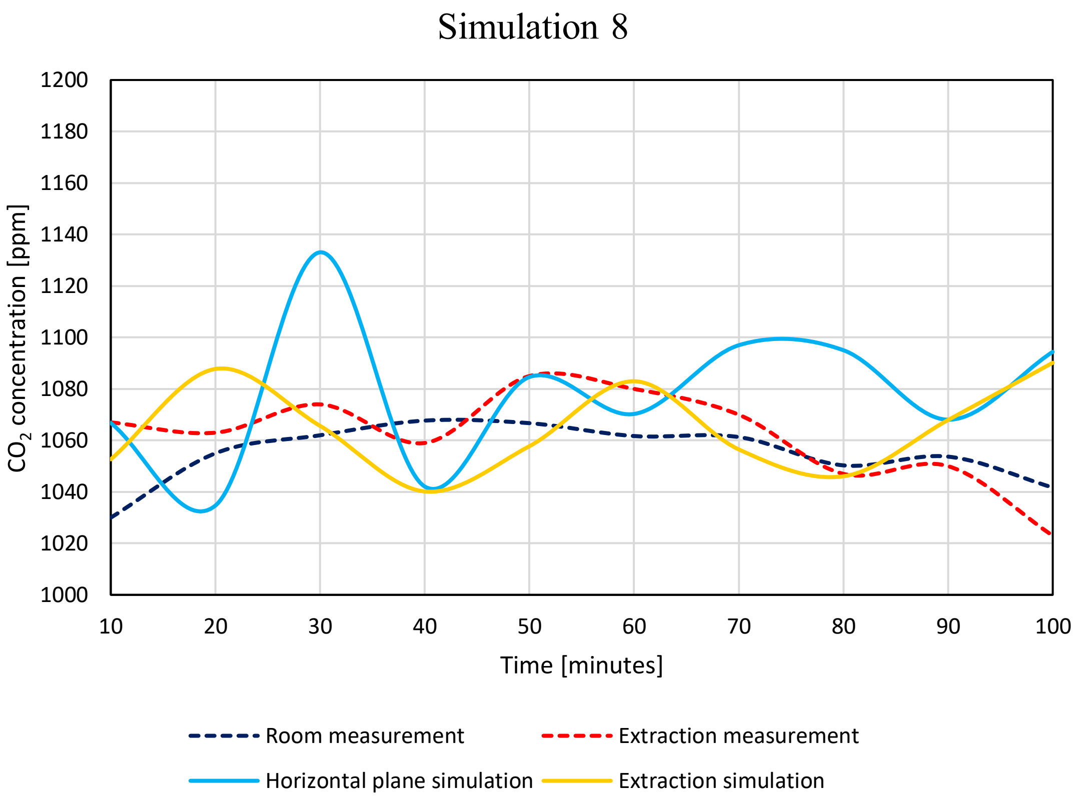

Figure 4.29 – Comparison of CO_2 concentration trend, simulation 8

Measurement ventilation effectiveness	Simulation ventilation effectiveness
1.02	0.97

Table 4.35 – Ventilation effectiveness, simulation 8

Simulation 9

Boundary conditions				
Supply flow rate [m3/h]	External concentration [ppm]	Initial concentration [ppm]	Number of people	Time analysed [minutes]
136	664	904	4	55

Table 4.36 – Boundary conditions, simulation 9

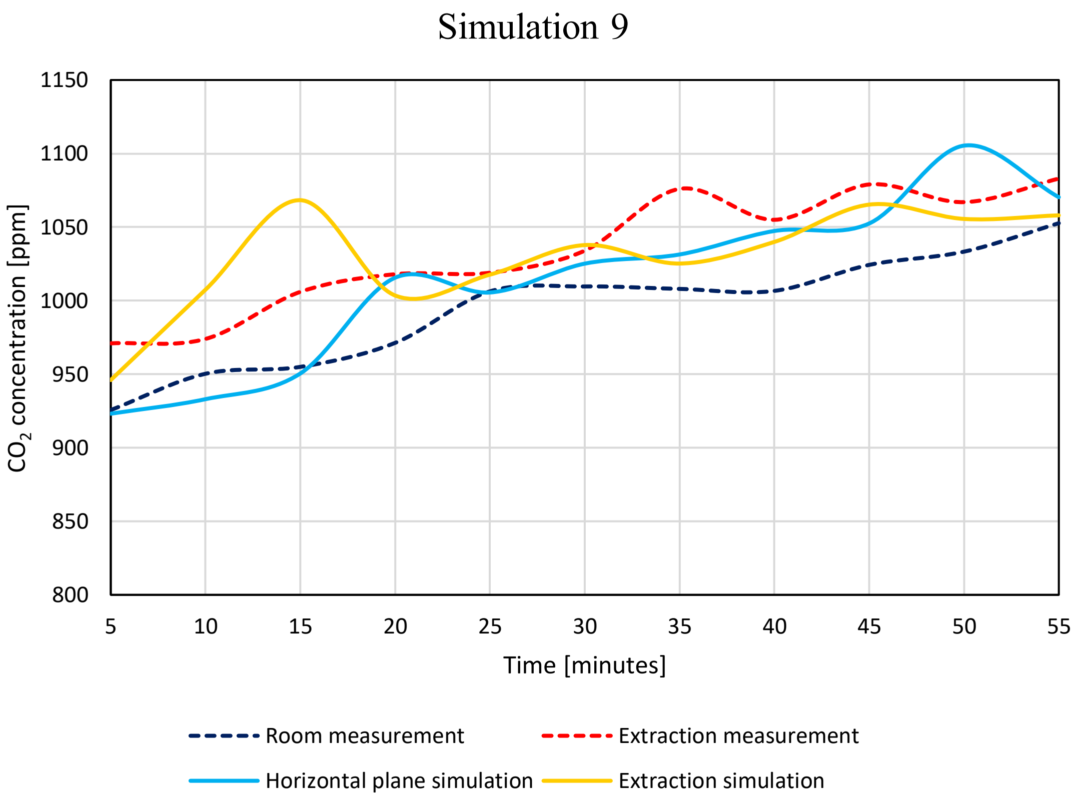

Figure 4.30 – Comparison of CO_2 concentration trend, simulation 9

Measurement ventilation effectiveness	Simulation ventilation effectiveness
1.12	1.06

Table 4.37 – Ventilation effectiveness, simulation 9

With regard to the comparison of carbon dioxide trends between measurement and simulation (see Figures 4.22 - 4.30), the initial observation pertains to the presence of certain peaks in the majority of cases (e.g. after 55 minutes in simulation 6, Figure 4.27 and after 30 minutes in simulation 8, Figure 4.29). The presence of these peaks can be attributed to the calculation of the mean value in a specifically created surface on scFLOW, whereas in the simulations, the value is taken as the precise position of the sensor. For instance, if there is a high concentration of CO_2 in a specific area of the horizontal plane at 0.8, such as in the proximity of a person emitting CO_2, the mean value increases and a peak is formed. It is evident that comparisons between an average value calculated over an area and a point-measured value inevitably involve simplifications. Consequently, it is more interesting to observe the course of the curve with respect to a single point. When observing the trend of the curve, it becomes evident that the simulations reflect the measured values with a high degree of detail. For instance, in both simulation 5 (Figure 4.26) and simulation 7 (Figure 4.28), a very good level of correspondence can be observed in the analysis.

It is interesting to note that in most cases, the measured concentrations are lower than the simulated ones, especially when considering the concentration inside the room. This discrepancy can be attributed to the fact that in the simulations, the only air supply is provided by the ventilation system, which has been given a flow rate equal to that measured experimentally. In reality, the airflow rate is influenced by additional factors, such as infiltration, which results in an increased exchange of clean air and, consequently, a slightly lower average concentration.

When analysing the results of the ventilation efficiency, it is important to note that, as was also done previously, the mean value was observed. In this case, the average value of the measurement over the specific period of time was compared with the mean value of the simulation. The values were taken every 5 minutes (just as in the measurements) and then averaged also in the simulation procedure. The outcomes of this study are highly satisfactory, as evidenced by the fact that, in simulations 1, 2, 4, 5, 6 and 8, the discrepancy between the mean measured value and the simulated value is less than or equal to 0.05, conforming with the confidence interval stipulated by the uncertainty calculation method employed in the preceding chapters.

5. CONCLUSIONS

The main objectives of the thesis are:

- Conduct a literature review to find out what the state of the art is about ventilation effectiveness, to understand which are the different indices that can be used for defining the performance of a ventilation system and to understand how to calculate the ventilation effectiveness of a system.
- Perform a measurement campaign to calculate the ventilation effectiveness of the decentralized system by measuring the distribution of the CO_2 concentration in the room under different flow rate and different occupancy conditions.
- Development of a CFD simulation model that is representative of the real case and may also be useful for other analyses in the future.

First of all, the concept of ventilation efficiency was defined, a notion that proved useful and central in analysing the system's ability to ensure adequate and homogeneous ventilation in the environment.

Measurements and analyses of the experimental data were then carried out, both regarding the carbon dioxide concentration and the flow rates that the analysed machine was able to guarantee. The different velocities of the system are well suited to the different occupancy levels, providing a comfortable environment for up to five people. In particular, it has been observed that the flow rate range goes from velocity 1, which guarantees an air change rate of 0.55 h^{-1} and a flow rate of 12 l/(s px) with an occupancy of one person, to hyperventilation mode, which guarantees an air change rate of 1.7 h^{-1} and a flow rate of more than 7 l/(s px) with an occupancy of five people.

The distribution of carbon dioxide in the room was found to be homogeneous, in particular the standard deviation between the measurements of the three sensors placed in the occupied zone is always less than 5 %. Another significant result is that the concentration measured in the proximity of the exhaust was almost always equal to or higher than the average concentration measured in the occupied zone, therefore the ventilation effectiveness derived from the measurements is equal to or slightly higher than 1.

The last section of the thesis concerns CFD simulations. Measurement periods with a stable occupancy were chosen and represented on scFLOW environment, with the aim of comparing both the CO_2 distribution and especially the ventilation efficiency with the measurement results. The ventilation effectiveness obtained from simulations was very close to the one obtained from measurements, with differences in the majority of cases less than or equal to 0.05.

A first limitation of the study, within which the results of the analysis are valid, is that measurements and simulations were carried out with both heating and cooling systems switched off. Therefore, a possible future work to extend the results of this thesis is to analyse the CO_2 distribution with heating and cooling on, and then compare the results with those obtained in this work, with the aim of determining whether heating and cooling systems have an effect on ventilation effectiveness.

Another possible extension would be to run new simulations with a higher level of detail, e.g. including electronic equipment in the office as heat sources, or including the contribution of solar radiation from windows.

APPENDIX

Appendix A

Technical datasheets of the measuring instruments used

Aranet

Model	Aranet4 HOME
CO_2 concentration	
Range	0 – 9999 ppm
Resolution	1 ppm
Accuracy	± (30 ppm + 3 % of reading)
Long term drift	Not available
Time constant τ	100 s
Temperature	
Range	0 – 50 °C
Resolution	0.1 °C
Accuracy	± 0.3 °C
Long term drift	0.03 °C/year
Time constant τ	10 min
Relative humidity	
Range	0 – 85 %
Resolution	1 %
Accuracy	± 3 %
Long term drift	0.5 %/year
Time constant τ	6 min
Atmospheric pressure	
Range	600 – 1100 hPa
Resolution	1 hPa
Accuracy	+3 hPa / -2 hPa
Long term drift	1 hPa/year
Time constant τ	0 s (instantaneous)
General specifications	
Dimensions	71 x 71 x 24 mm
Weight (incl. batteries)	104 g
Enclosure material	Polycarbonate

Table A.1 – Datasheet of Aranet

HOBO

Model	HOBO MX CO_2 Logger MX1102A
CO_2 concentration	
Range	0 – 5000 ppm
Resolution	1 ppm
Accuracy	± 50 ppm ± 5% of reading
Warm up time	15 seconds
Temperature	
Range	0 – 50 °C
Resolution	0.024 °C at 25 °C
Accuracy	± 0.21 °C from 0 °C to 50 °C
Long term drift	< 0.1 °C/year
Relative humidity	
Range	1 – 90 %
Resolution	0.01 %
Accuracy	± 2 % from 20 % to 80 %, ± 6 % below 20 % and above 80 %
Long term drift	< 0.1 °C/year
General specifications	
Dimensions	7.62 x 12.95 x 4.78 cm
Weight	267.4 g

Table A.2 – Datasheet of HOBO

PV28-AW

Model	PV28-AW
CO_2 concentration	
Range	400 – 5000 ppm
Resolution	1 ppm
Accuracy	± (50 ppm + 5% of reading)
Temperature	
Range	0 – 50 °C
Resolution	1 °C
Accuracy	± 1 °C
Relative humidity	
Range	0 – 99 %
Resolution	1 %
Accuracy	± 5 %
General specifications	
Dimensions	70 x 84 x 35 mm

Table A.3 – Datasheet of PV28-AW

Testo 425 hot wire anemometer

Model	Testo 425
Air velocity	
Range	0 – 20 m/s
Resolution	0.01 m/s
Accuracy	± 0.03 m/s + 5%
Temperature	
Range	- 20 + 70 °C
Resolution	0.1 °C
Accuracy	± 0.5 °C

Table A.4 – Datasheet of Testo 425

Appendix B

Results of CO_2 measurements

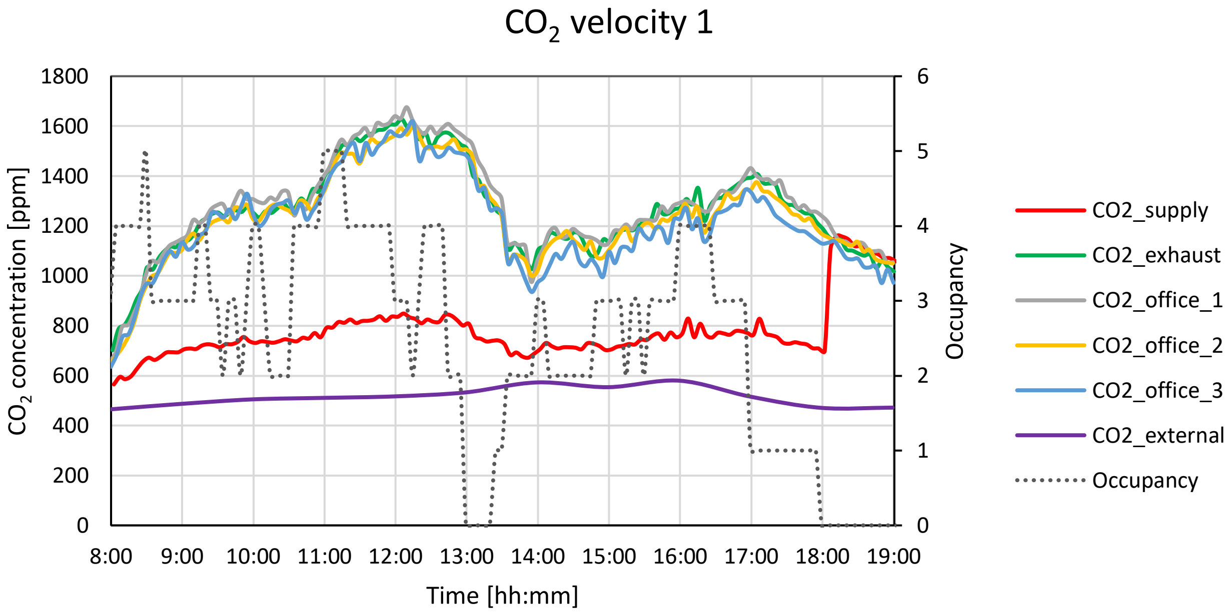

Figure B.1 – CO_2 trend with velocity 1 measure 2

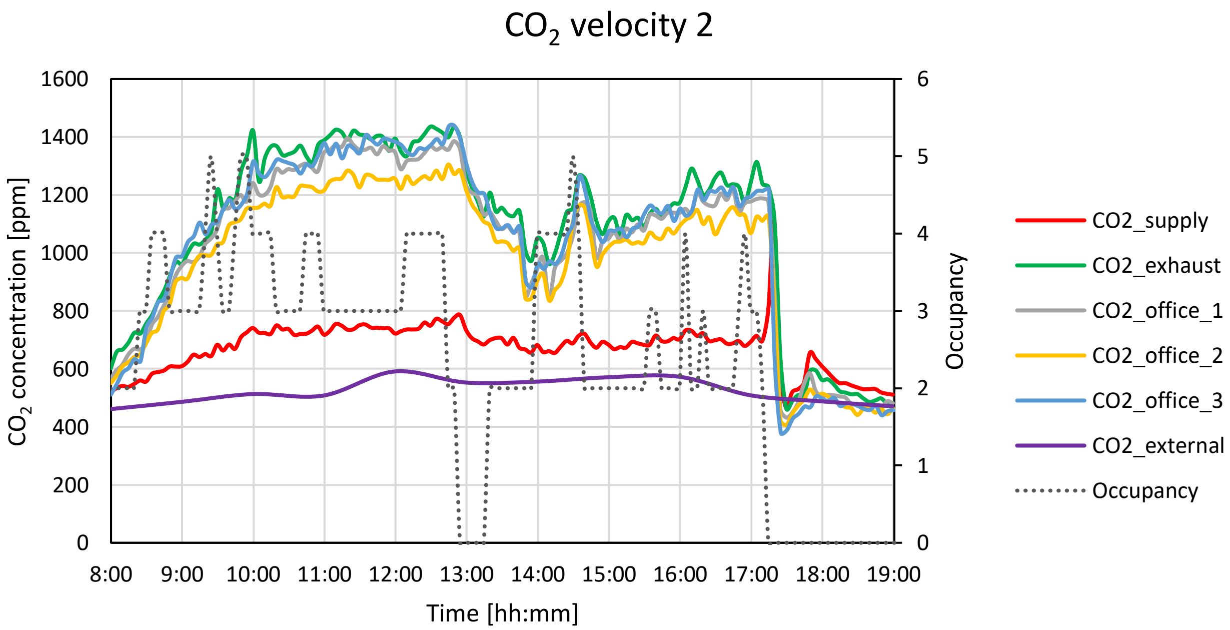

Figure B.2 – CO_2 trend with velocity 2 measure 2

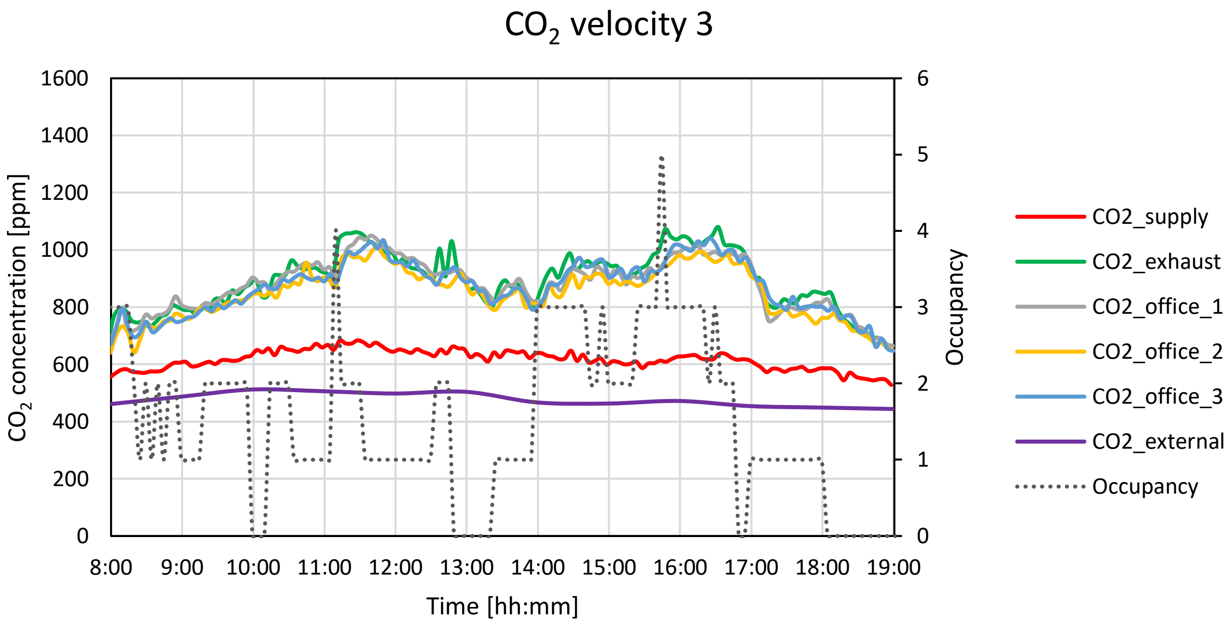

Figure B.3 – CO_2 trend with velocity 3 measure 2

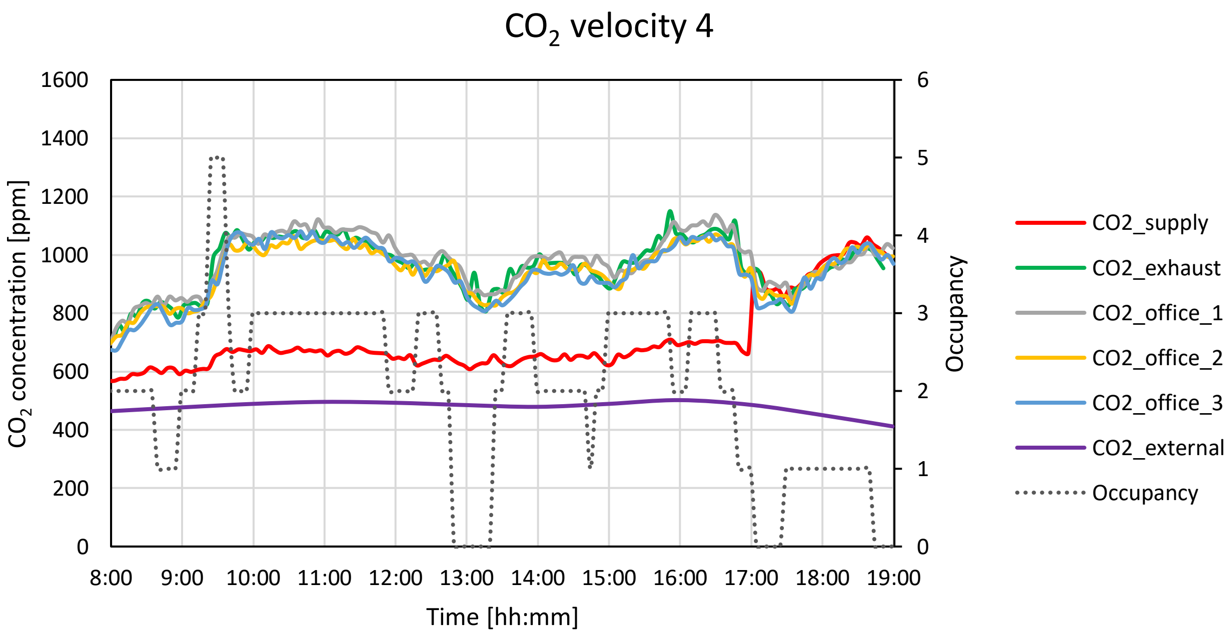

Figure B.4 – CO_2 trend with velocity 4 measure 2

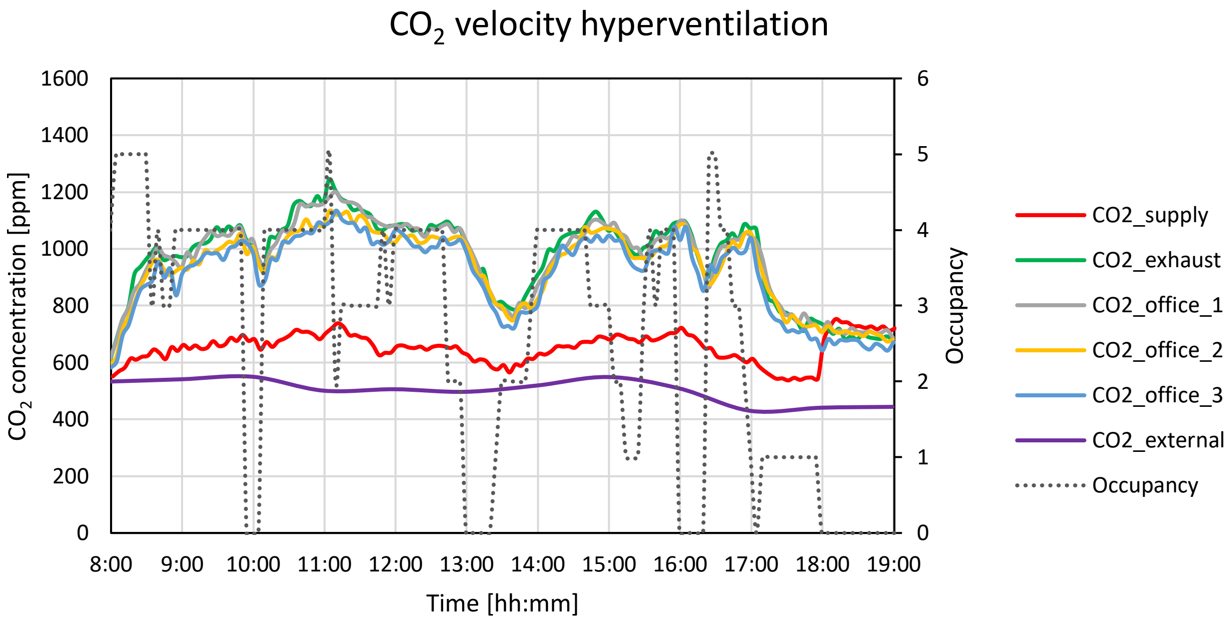

Figure B.5 – CO_2 trend with velocity hyperventilation measure 2

Appendix C

Results of ventilation effectiveness

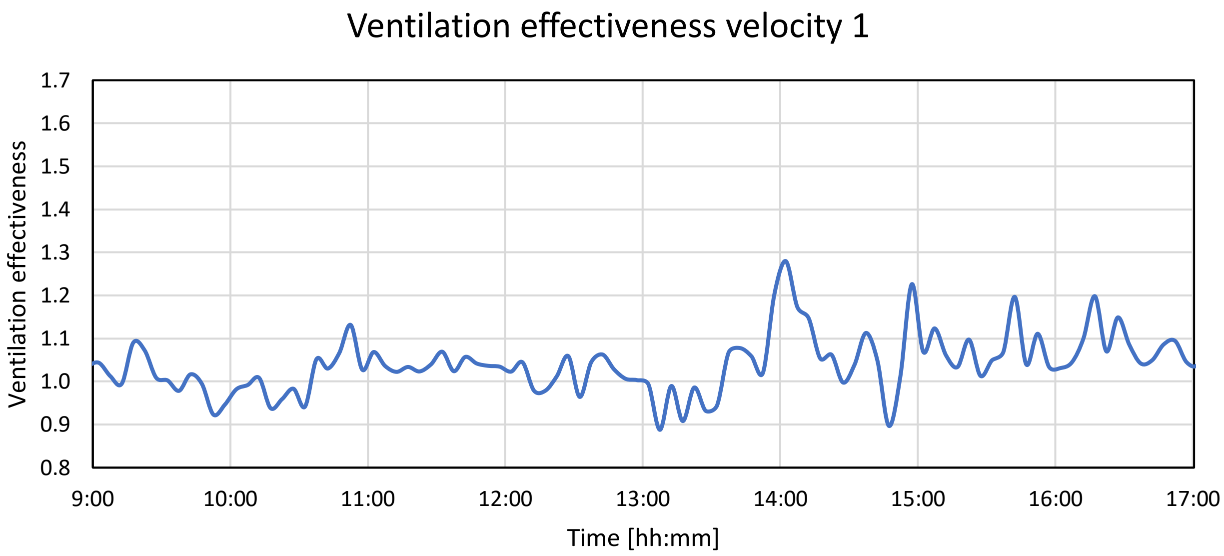

Figure C.1 – ventilation effectiveness with velocity 1, measure 2

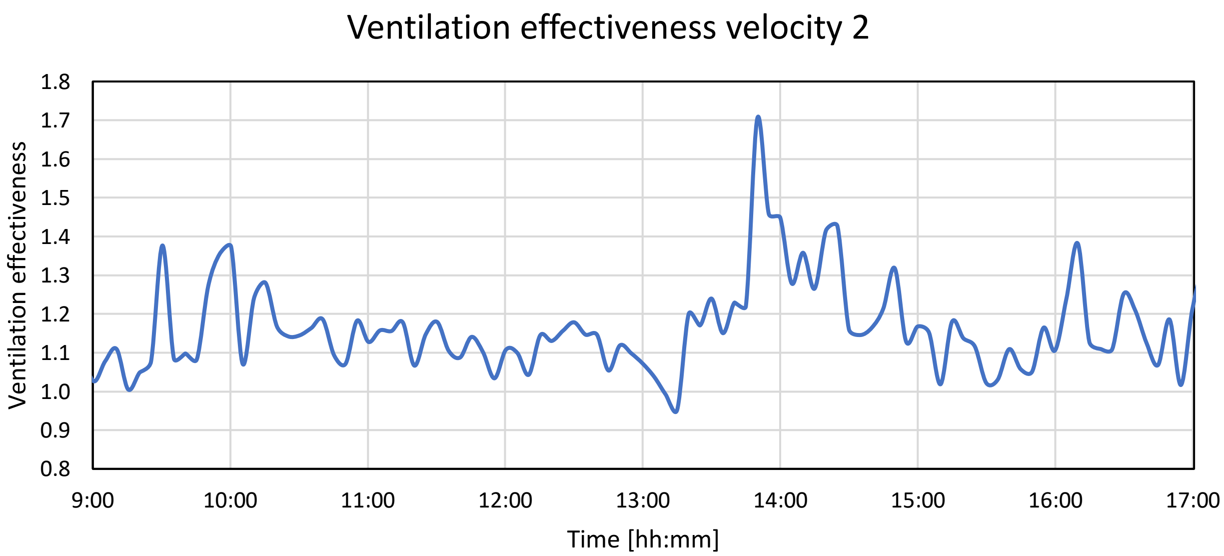

Figure C.2 – ventilation effectiveness with velocity 2, measure 2

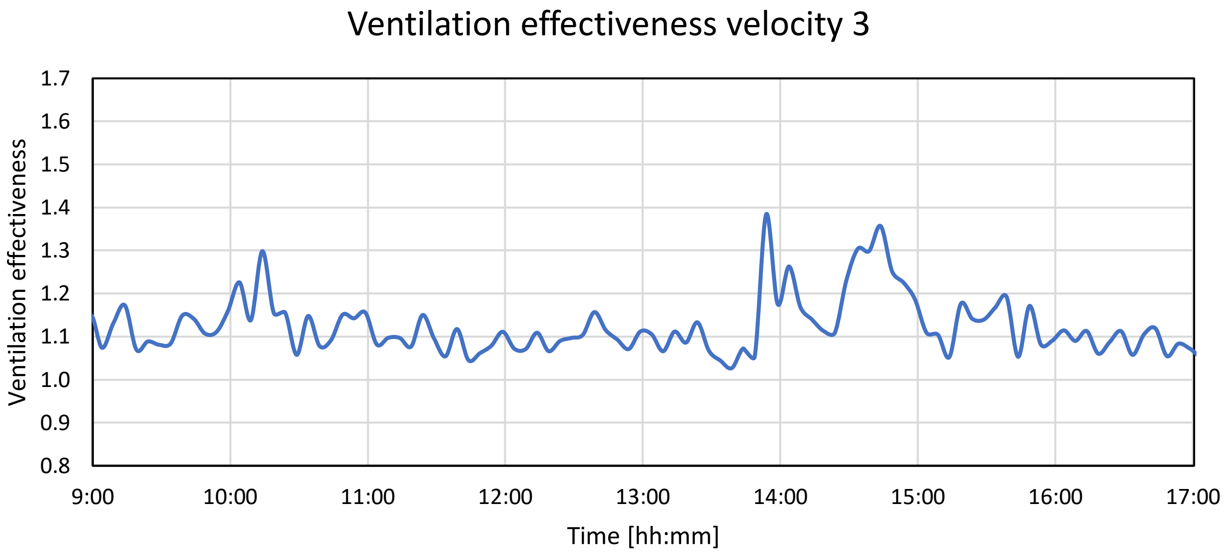

Figure C.3 – ventilation effectiveness with velocity 3, measure 2

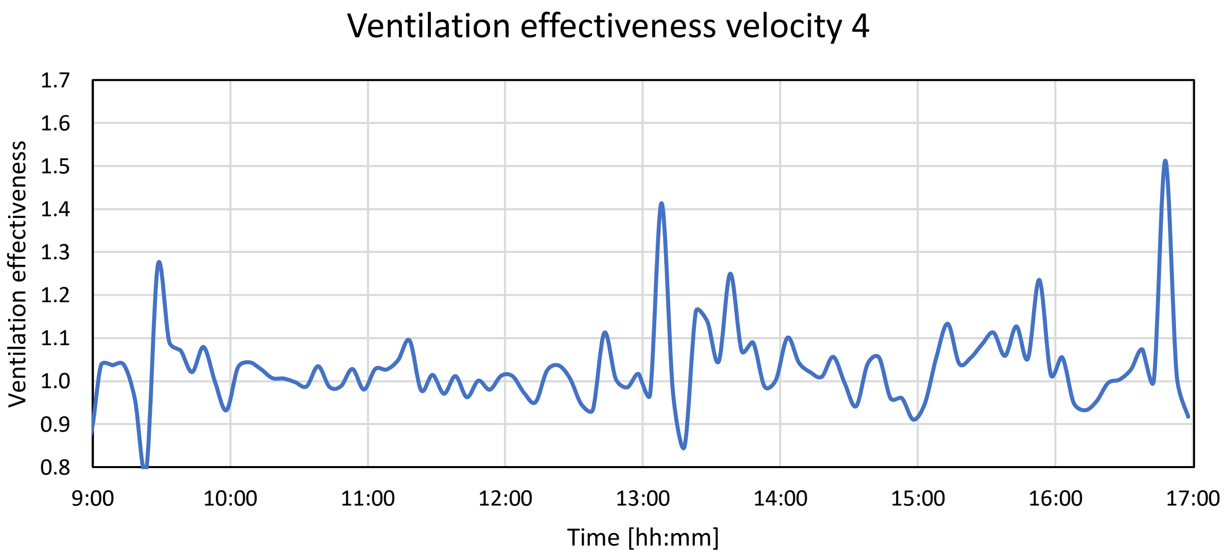

Figure C.4 – ventilation effectiveness with velocity 4, measure 2

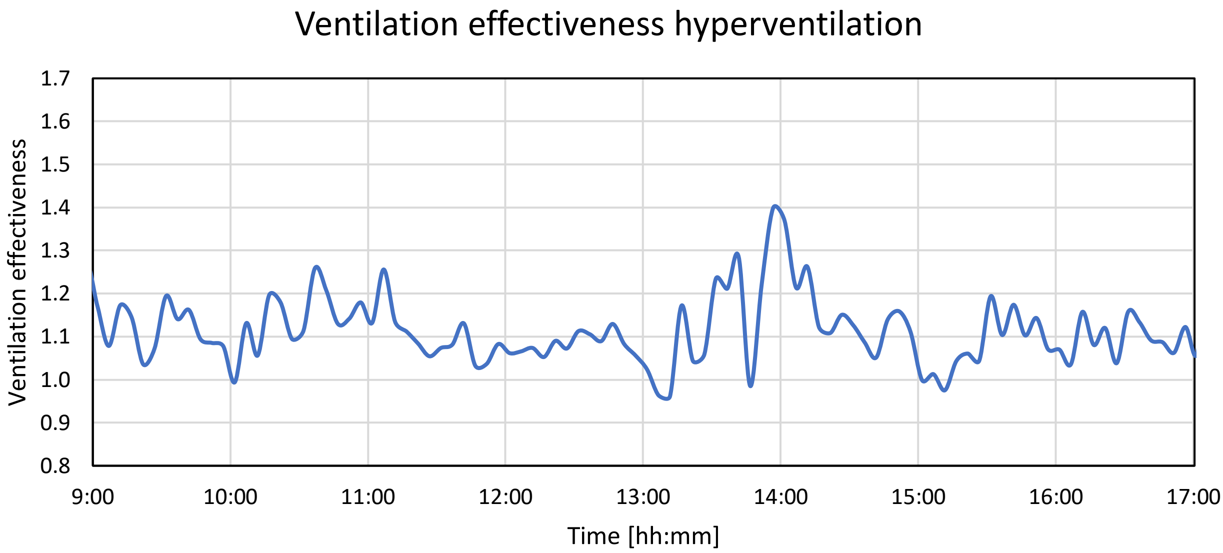

Figure C.5 – ventilation effectiveness with velocity hyperventilation, measure 2

References

[1] ASHRAE, Standard ASHRAE 62.1, 2010.

[2] H. B. Awbi, Ventilation of buildings, second edition, 2003.

[3] ASHRAE, Standard ASHRAE 55, 2017.

[4] EN 16798-1, 2019.

[5] EN ISO 7730, 2005.

[6] M. De Carli, Notes of HVAC, Università degli Studi di Padova.

[7] A. Persily and L. d. Jonge, “Carbon dioxide generation rates for building occupants,” 2017.

[8] “inquinamento,” [Online]. Available: https://www.inquinamento.org/radon.html.

[9] A. Lombardia, “Arpa Lombardia,” [Online]. Available: https://www.arpalombardia.it/temi-ambientali/radioattivita/il-radon/livelli-di-riferimento/.

[10] WHO, Linee guida globali OMS sulla qualità dell’aria, 2022.

[11] M. Sanbderg, “What is Ventilation Efficiency?,” *Building and Environment,* vol. 16, no. 2, pp. 123-135, 1981.

[12] EN 16798-3, 2017.

[13] E. Mundt, H. M. Mathisen, P. V. Mielsen and A. Moser, Ventilation effectiveness, REHVA Guidebook.

[14] N. Monarkin, “Reversible decentralized ventilation: experimental determination of efficiency by carbon dioxide level”.

[15] T. van Hooff e B. Blocken, Full scale measurements of indoor environmental conditions and natural ventilation in a large semi-enclosed stadium: possibilities and limitations for CFD validation, 2012.

[16] T. van Hooff and B. Blocken, “CFD evaluation of natural ventilation of indoor environments by the concentration decay method: CO2 gas dispersion from a semi-enclosed stadium,” 2013.

[17] S. Iskra, M. Detelin e M. Sergey, «Numerical investigation of metabolic CO2 distribution in an occupied ventilated classroom,» 2016.

[18] M. Arsen e M. Detelin, «Validity of CO2 based ventilation design,» 2019.

[19] S. Iskra, M. Detelin, M. Sergey e A. Radostina, «The effect of metabolic CO2 source distribution in a mechanically ventilated classroom on the CO2 concentration in the breathing zone,» 2021.

[20] K. Martin, M. Alo, V. Karl-Villem, S. Raimo e K. Jarek, «Ventilation effectiveness and incomplete mixing in air distribution design for airborne transmission,» 2025.

[21] S. Sheng, Y. Toshio, K. Tomohiro e N. Chou, «Ventilation efficiency and improvements for displacement ventilation systems during heating: a case study of a ward with vertical induction units,» 2024.

[22] W. J. Massman, «A review of the molecular diffusivities of H20, CO2, CH4, CO, O3, SO2, NH3, N20, N0, and NO2 in air, O2 and N2 near STP,» 1998.

[23] W. Braker e A. Mossman, Matheson gas data book 6th ed, 1980.

Acknowledgments

Desidero esprimere la mia profonda gratitudine al professor De Carli per avermi dato la possibilità di approfondire un tema interessante e stimolante tramite questo studio.

Ringrazio con sincera riconoscenza Marco Marigo per la costante disponibilità e i confronti continui e indispensabili, che hanno contribuito significativamente allo sviluppo di questo lavoro.

Infine, rivolgo un sentito ringraziamento a Helty, in particolar modo a Dario, Roberto, Rocco, Francesco e Matteo, per avermi dato l'opportunità di collaborare a questo progetto, per avermi accolto con stima e fiducia da subito e per il supporto che non è mai mancato.